CATALYSIS OF THE ELECTROREDUCTION OF DIOXYGEN BY MONOMERIC AND DIMERIC COBALT PORPHYRINS

Thesis by

Richard Raymond Durand, Jr.

In Partial Fulfillment of the Requirements

for the Degree of

Doctor of Philosophy

California Institute of Technology

Pasadena, California

1984

(Submitted June 28, 1983)

To Mom and Dad,

Kevin, Donna and Claire

ACKNOWLEDGEMENTS

I would like to express my graditude to the many people who have contributed to my efforts prior to graduate school. I have been fortunate to always have the generous and loving support of my family. I have also been able to be associated with many outstanding individuals in high school and during my undergraduate years at WPI.

At Caltech, the interactions with my advisor, Fred Anson, have contributed greatly to my development as a scientist. He has always been a source of encouragement and enthusiasm. I will always appreciate the opportunity I have had to be associated with him. I would also like to acknowledge the interactions I have had with Bob Gagné and his group during the early part of my stay here.

I would also like to acknowledge the interactions I have had with Professors James Collman and Henry Taube and their research groups at Stanford. The collaborative efforts have been a fruitful source of stimulation.

There have been many members of the Anson group past and present who have made the day to day life at the south end of the 3rd floor Noyes so enjoyable. I have been lucky to be exposed to a wide variety of interesting cultures and personalities in the forms of:
Dr. Kiyotaka Shigehara, Dr. Takeo Ohsaka, Dr. Seizo Miyata, Dr. Roger Mortimer, Dr. Pat Martigny, Dr. Piotr Wrona, Dr. Jim McQuillan, Dr. Hsue-Yang Liu, Dr. Tin-Wu Tang,

Dr. Carl Murray, Dr. Ron McHatton, Dr. Mark Bowers, Brian Willet, Mark Paffett, Roger Baar, Dan Buttry, Chi-Woo Lee, Yu-Min Tsou, Steve Gipson, Ching-Long Ni, Denice Ball, Deidre Askew. Each and every one has had his own particular impact on my days.

I would further like to acknowledge a few of the close personal friendships within and outside the group. First of all, Dan Buttry has been a great labmate and friend. The many hours we have spent sharing failures and successes and the countless times when we were so inspired by a joint idea (whether dealing with chemistry or otherwise) to act upon it will be sorely missed. Dan and his wife, Kathie, have been close friends for my entire stay here and it has been much appreciated.

My housemates of the last three years, Pete Felker and our recurring summer roommate, Patti Chaifetz, have helped me to weather (no pun intended) the ups and downs of living in a true architectural wonder. Mark and Terri Bowers have become really close friends to me since our meeting. They have been kind enough to share many a fine outing with me. Mark's spontaneity has really made life enjoyable. I would like to generally acknowledge the many other friends I have made while at Caltech. They have all contributed to a more pleasant stay.

Dr. Oliver Wulf has been a source of inspiration. The many enjoyable conversations we have had have reflected

his enthusiasm for life and learning. His strong pride in our common alma mater (although 60 years apart) will always be remembered.

I would like to thank the Institute for support in the form of assistantships during my tenure.

Finally, Mrs. Nancy O'Connor is thanked for the fine job done in typing this thesis.

ABSTRACT

Mechanistic aspects of the catalytic electroreduction of dioxygen by monomeric and dimeric cobalt porphyrins were investigated. The catalysts were examined while either adsorbed to graphite electrodes or dissolved in concentrated acids.

Monomeric cobalt(II) porphyrins adsorbed to graphite electrodes were found to reduce dioxygen to hydrogen peroxide. Cyclic and rotating disk voltammetry were used to examine the kinetics and mechanism of the catalyzed reactions. These monomeric catalysts exhibited behavior atypical of simple redox catalysis.

The mechanisms by which the reduction of dioxygen at graphite electrodes is catalyzed by cofacial dicobalt and related porphyrins has been investigated. The products of the reductions, the electrode potential where the reduction proceeds and the mechanistic role of protons were among the topics examined. A comparison of the behavior of several new cofacial metalloporphyrins has led to a more detailed proposal for the mechanisms by which they operate.

Monomeric and dimeric cobalt porphyrins have been dissolved in trifluoromethanesulfonic acid (5.6 M) and concentrated phosphoric acid without demetalation. The electrocatalytic reduction of dioxygen by solutions of the catalysts was examined by rotating disk and ring-disk

voltammetry. The dissolved metalloporphyrins provide improved stability to the catalysts.

The reaction of a cobalt(II) complex with superoxide was examined electrochemically in a non-aqueous electrolyte. The affinity of superoxide for cobalt(II) has been demonstrated by cyclic voltammetry. The results of this study were related to mechanisms of dioxygen reduction in aqueous media.

TABLE OF CONTENTS

Chapter 1

Introduction

Modified electrode surfaces have become of great interest for their possible use in catalyzing oxidation-reduction reactions.[1-3] Electrode modification can be carried out by; (a) simple adsorption of catalysts; (b) casting of polymer films which have incorporated sites; or (c) covalent attachment of a catalyst to the electrode surface. A wide variety of modified surfaces have been examined for electrocatalytic properties toward various substrates.

A particularly important electrochemical reaction which has stimulated the modified electrode field is the reduction of dioxygen directly to water. This reaction takes place at an air cathode in a fuel cell. A fuel cell is a galvanic electrochemical cell in which a fuel (e.g., hydrogen or methanol) is oxidized at the anode, while an oxidant (e.g., a very convenient and cheap source is oxygen from air) is reduced at the cathode.[4] The direct conversion of chemical energy to electrical energy is carried out. Such an isothermal process has many advantages over combustion generated electrical energy (i.e., higher efficiency, lower pollution, and less maintenance). The fuel cell is by no means a recent innovation. A H_2/O_2 electrochemical cell was first constructed by Grove in 1839.[5] The virtues of such a cell were recognized in the ensuing fifty years. However, until recently a fuel cell has not been considered as an attractive energy alternative. This stems from the

fact that the commercial viability of such cells has been limited by the supply and cost of electrode catalysts. Platinum metal is the most efficient catalyst known for the direct reduction of oxygen to water. Platinum is not ideal even if it were to be cost effective. There is a significant overvoltage associated with O_2 to H_2O conversion which limits the efficiency of the cell. Many efforts are currently being made to replace or improve upon platinum metal catalysts.

The typical electrolytes for fuel cell operation have been strong acids or bases at high temperatures. High temperatures are necessary to drive off the products of anodic and cathodic reactions (i.e., CO_2 from methanol and H_2O from oxygen) preventing buildup in the cell. Acidic electrolytes are particularly desirable for soluble hydrocarbon based fuels since the product CO_2 will not accumulate in the form of carbonate as would happen in basic electrolytes. The thermodynamic constraints on the principal pathways to the four electron reduction of oxygen in acidic media are the following:[6]

$$O_2 + 2H^+ + 2e^- \rightleftharpoons H_2O_2 \qquad E_1 = +0.68V \quad (1)$$

$$H_2O_2 + 2H^+ + 2e^- \rightleftharpoons 2H_2O \qquad E_2 = +1.77V \quad (2)$$

$$O_2 + 4H^+ + 4e^- \rightleftharpoons 2H_2O \qquad E_3 = +1.23V \quad (3)$$

(These potentials are the reversible thermodynamic potentials in 1M acid versus a normal hydrogen electrode.) The scheme above denotes two pathways to produce an overall

four electron reduction of dioxygen. The O_2 reduction can be accomplished by the sequential reduction by two electron steps via hydrogen peroxide as an intermediate or directly by four electrons without H_2O_2 formation. The direct four electron reduction can proceed at the thermodynamic potential of +1.23V. The consecutive two electron transfers through H_2O_2 will have a potential governed by the first step, +0.68V. The further reduction of H_2O_2 occurs but the potential cannot exceed the thermodynamic value for its formation. In terms of operating an electrochemical fuel cell, there could be a loss of more than 0.5V in output by producing H_2O_2 as an intermediate. Therefore it is highly desirable to reduce oxygen directly to water.

Many different types of materials have been examined as potential electrocatalysts. Metal oxides, chalcogenides, and a variety of organometallic complexes have been investigated.[7-9] The organometallic catalysts have typically been macrocyclic moieties which contain metals capable of interacting with oxygen. Many of these complexes have been found to be well suited to adsorbing to graphite electrodes. The possible development of a catalytically active modified graphite electrode has been an especially attractive area of research.

The first report of a metal macrocyclic complex as an oxygen reduction catalyst was made by Jasinki in 1964.[10] He observed that a cobalt phthalocyanine complex dispersed

on graphite was an effective catalyst in alkaline solution. Since that time, a wide variety of macrocyclic complexes have been studied.[11] Cobalt and iron derivatives have attracted the greatest attention. These catalysts have been observed to reduce O_2 to H_2O_2 and H_2O. In all known examples of monomeric catalysts, H_2O_2 is either the product or an intermediate. The direct four electron reduction has only been observed for a dimeric dicobalt cofacial porphyrin.[12-15] This catalyst reduces oxygen at very positive potentials without H_2O_2 formation. A great deal of the earlier efforts in this field have focused on examining and comparing catalysts without much attention to unifying mechanistic understandings of the relationship between various catalysts.

The efforts described in this thesis have been part of a larger effort by Anson and co-workers to understand mechanistic aspects of the electrocatalytic reduction of dioxygen by homogeneous and heterogeneous catalysts.[16-19] These studies have involved many different approaches to produce catalytically active electrodes. It would be of great interest to understand essential mechanistic features of the catalysis, so that criteria for the design of new more active molecular catalysts are available.

Chapter 2 describes a mechanistic study of a monomeric cobalt porphyrin catalyst adsorbed on a graphite electrode as an oxygen reduction catalyst.[20] This catalyst is

typical of previously investigated cobalt porphyrins. In this study, a careful examination has been made of (1) the relationship between the metal reduction potential and the catalytic reduction potential; (2) the pH dependence of the catalysis; (3) whether there is kinetic control of the catalysis under well-defined mass transport conditions. This monomeric species was found to exhibit several properties not previously noted in other studies. A wide variety of other cobalt porphyrins has been examined and compared to the results of this study. A general mechanism for oxygen reduction catalyzed by cobalt porphyrins has been established.

Chapter 3 describes the mechanistic study of cofacial dimeric metalloporphyrins.[21] The products of reaction, electrode potential where reaction proceeds and mechanistic role of protons were among the topics examined. The best known catalyst has been examined in greater detail than was previously possible. The electrochemical response for the best dicobalt catalyst has been clearly observed and the relationship between the catalysis and metal electrochemistry established. A variety of new heterobinuclear cofacial species and derivatives with varied bridging groups has also been investigated. A comparison of the behavior of these various catalysts has led to a more detailed proposal for the mechanisms by which they may operate in catalyzing the electro-reduction of dioxygen.

Chapter 4 describes observations on solubilizing monomeric and dimeric cobalt porphyrins in strong or concentrated acids.[22] The stability of the metal complex has been found to be a function of the nature of the acid and its strength. In 5.6M trifluoromethanesulfonic acid and concentrated phosphoric acid, the cobalt porphyrins appear to be stable. The catalytic responses of these solubilized complexes have been examined. The monomeric cobalt porphyrin was able to reduce oxygen to water under these conditions. The stability of the dimeric cobalt porphyrins was improved if some catalyst resided in the electrolyte.

Chapter 5 describes the study of the reaction of electrochemically generated superoxide with a tetra-aza cobalt(II) macrocycle by cyclic voltammetry. The reaction produces a cobalt(II)-superoxide adduct. The adduct is stable on the electrochemical timescales and can be reoxidized to cobalt(II) and dioxygen at more positive potentials than those where it is formed.

REFERENCES AND NOTES

1. K. D. Snell and A. G. Keenan, Chem. Soc. Rev., 8, 259 (1979).

2. R. W. Murray, Acc. Chem. Res., 13, 135 (1980).

3. W. J. Albery and A. R. Hillman, Annual Reports C, Royal Society of London, 377 (1981).

4. K. R. Williams, "An Introduction to Fuel Cells," Elsevier, Amsterdam (1966).

5. W. R. Grove, Phil. Mag., 14, 127 (1839).

6. W. M. Latimer, "Oxidation Potentials," Prentice-Hall, New York (1952).

7. E. Yeager in "Electrocatalysis on Non-Metallic Surfaces," NBS Special Publication No. 455, p. 203 (1976).

8. F. van den Brink, E. Barendrecht, and W. Visscher, J. R. Neth. Chem. Soc., 99, 253 (1980).

9. P. N. Ross, Jr. and F. T. Wagner, Report to Los Alamos National Laboratory (Contract No. CRI-7090W-1), March 1982.

10. R. Jasinski, Nature, 201, 1212 (1964).

11. H. Jahnke, M. Schöborn, and G. Zimmerman, Topics in Current Chemistry, 61, 133 (1976).

12. J. P. Collman, C. M. Elliott, T. R. Halbert, and B. S. Tovros, Proc. Natl. Acad. Sci. USA, 74, 18

13. J. P. Collman, M. Marrocco, P. Denisevich, C. Koval, and F. C. Anson, J. Electroanal. Chem., 101, 117 (1979)

REFERENCES AND NOTES

14. J. P. Collman, P. Denisevich, Y. Konai, M. Marrocco, C. Koval, and F. C. Anson, J. Am. Chem. Soc., 102, 6027 (1980).

15. J. P. Collman, F. C. Anson, S. Bencosme, A. Chong, T. Collins, P. Denisevich, E. Evitt, T. Geiger, J. Ibers, G. Jameson, Y. Konai, C. Koval, K. Meier, R. Oakley, R. Pettman, E. Schmittou, and J. Sessler, in "Organic Synthesis, Today and Tomorrow," B. M. Trost and C. R. Hutchison, eds., Pergamon Press, New York, p. 29, (1981).

16. T. Geiger and F. C. Anson, J. Am. Chem. Soc., 103, 7489 (1981).

17. K. Shigehara and F. C. Anson, J. Electroanal. Chem., 132, 107 (1982).

18. P. Martiguy and F. C. Anson, J. Electroanal. Chem., 139, 383 (1982).

19. K. Shigehara and F. C. Anson, J. Phys. Chem., 86, 2776 (1982).

20. Parts of this chapter have been published; R. R. Durand, Jr. and F. C. Anson, J. Electroanal. Chem., 134, 273 (1982).

21. This chapter has been modified from a recent publication; R. R. Durand, Jr., C. S. Bencosme, J. P. Collman, and F. C. Anson, J. Am. Chem. Soc., 105, 2710 (1983).

REFERENCES AND NOTES

22. A preliminary note has recently been prepared on aspects of this chapter; R. R. Durand, Jr., J. P. Collman, and F. C. Anson, J. Electroanal. Chem., submitted.

Chapter 2

Catalysis of Dioxygen Reduction at Graphite Electrodes by Adsorbed Cobalt(II) Porphyrins

INTRODUCTION

The cobalt porphyrin, I, shown in Figure 1 is one of the monomeric precursors employed in the synthesis of the cofacial porphyrin catalysts (see Chapter 3).[1-3] An examination of the electrochemistry of I adsorbed on a graphite electrode as a function of pH of the electrolyte and absence and presence of dioxygen and hydrogen peroxide has been carried out. One of the interesting properties exhibited by graphite electrodes coated with I is the notable potency toward the catalytic oxidation of hydrogen peroxide at all pH values culminating in a nearly nernstian response for the O_2/O_2H^- couple at high pH. A clear separation in potential between the cobalt centered redox electrochemistry and the catalytic dioxygen reduction was observed at all pH values. A mechanism is proposed to account for the above observations.

Figure 1. The cobalt porphyrin catalyst employed in this study.

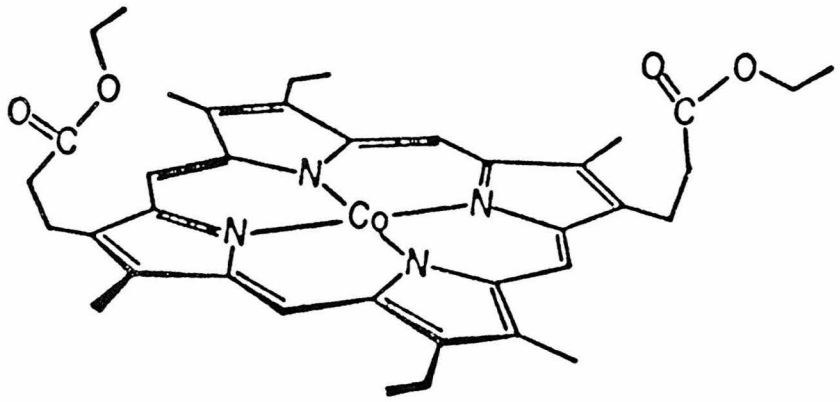

I

EXPERIMENTAL

The cobalt porphyrin, I, synthesized as described in Reference 2, was a gift from Professor J. P. Collman as were the substituted derivatives of this porphyrin. Cobalt tetraphenylporphyrin (CoTPP) and cobalt octaethylporphyrin (CoOEP) were also received from Professor Collman. The free ligands for the cobalt complexes of tetra-(p-sulfonato) phyenylporphyrin (TSTPP), tetra (p-methoxy)-phenylporphyrin (TMeOPP), tetrapyridylporphyrin (TPyP), and tetra-N-methyl-pyridylporphyrin (TMPyP) were obtained from Mid-Century Chemical Co. (Posen, Illinois) as was a cobalt tetrapyridylporphyrin (CoTPyP) sample. CoTPyP was recrystallized from water and chromatographed prior to use. CoTMPyP was prepared by method analogous to that described previously for the corresponding iron complex.[4] CoTMeOPP was prepared by refluxing the free ligand and cobaltous acetate in dimethylformamide for one hour. The resultant solid was chromatographed on silica gel. The incorporation of cobalt into these ligands was verified by visible spectroscopy on a HP 8450 UV-visible spectrometer. All other reagents employed were analytical grade and were used without further purification. Solutions were prepared from distilled water that was further purified by passage through a Barnstead Nanopure purification train. Buffer solutions had the following compositions:

pH 0.3	0.5 M Trifluoroacetic acid
pH 2	0.05 M KCl + 0.01 MHCl
pH 3-5	0.05 M KH phthalate + HCl or NaOH
pH 6-7	0.05 M KH_2PO_4 + NaOH
pH 8-10.8	0.02 M $Na_2B_4O_7$ + HCl or NaOH
pH 12-13	0.05 M KCl + NaOH
pH 14	1.0 M NaOH

A conventional two-compartment electrochemical cell was used. All potentials were quoted versus a standard saturated calomel reference electrode (SCE). PAR Model 174, 175, 173 and 179 electrochemical instruments were used to obtain cyclic voltammograms that were recorded directly with an x-y recorder at scan rates up to 500 mV s^{-1} or after acquisition by a digital oscilloscope (Tektronix Model 5223) at higher scan rates. Rotating disk and ring-disk voltammograms were obtained with the apparatus and procedures previously described.[2,5] In calculating the Levich limiting currents at rotating disk electrodes, the following parameters were used: Kinematic viscosity of water: 0.01 cm s^{-1}; diffusion coefficient for dioxygen: 1.7×10^{-5} cm^2 s^{-1}; solubility of dioxygen in 1 M NaOH: 1.0 mM. The electrodes were edge plane polyolefin tubing and were polished to a rough finish with No. 600 SiC paper (3M Co., Minneapolis, Minnesota). The cobalt porphyrins were applied to the electrode by transferring a measured volume of a standard solution of the porphyrin in 1,2-dichloroethane to the electrode surface and allowing the

Figure 2. Cyclic voltammograms of I adsorbed on pyrolytic graphite electrodes in supporting electrolytes of various pH.

A) under argon. B) under dioxygen.

Scan rate; 83 mV s^{-1}.

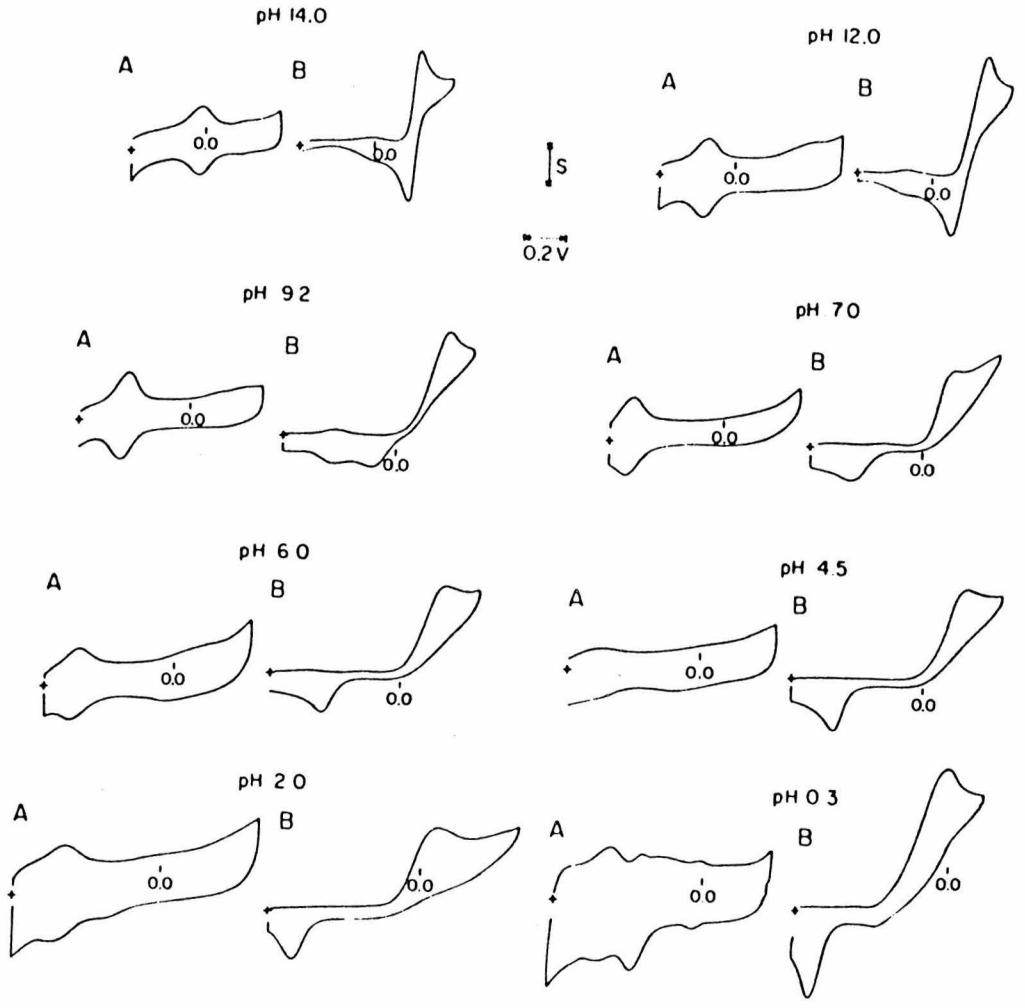
pH 14.0
A
B
0.0
0.0
5
0.2 V
pH 12.0
A
B
0.0
0.0
pH 9.2
A
B
0.0
0.0
pH 7.0
A
B
0.0
0.0
pH 6.0
A
B
0.0
0.0
pH 4.5
A
B
0.0
0.0
pH 2.0
A
B
0.0
0.0
pH 0.3
A
B
0.0
0.0

solvent to evaporate. The concentration of the porphyrin in the dichloroethane solution was determined spectrophotometrically (ε = 1.9 x 10^5 M^{-1} cm^{-1} at λ_{max} = 393 nm). The water soluble porphyrins could also be adsorbed spontaneously by soaking in an aqueous solution of the complex.

RESULTS

Voltammetry of the Adsorbed Porphyrins in the Absence of Dioxygen

The cobalt porphyrin, I, adsorbed on the surface of a pyrolytic graphite electrode exhibits prominent oxidation and reduction waves as shown in Figure 2A for a series of supporting electrolytes having pH values from 0.3 to 14. The peak currents increase linearly with the potential scan rate and the anodic and cathodic peak potentials are very nearly equal as expected for reactants attached to electrode surfaces.[6,7]

The quantities of electroactive I present on the electrode were obtained by measuring the areas under the cyclic voltammograms recorded in 1 M NaOH. As the concentration of porphyrin was increased in the aliquots of dichloroethane deposited on the electrode surface, the areas of the voltammograms increased but only until a coverage corresponding to about one monolayer was reached. Further increases in the porphyrin concentration produced only small changes in the magnitudes of the electrochemical responses. This could have resulted from the physical loss

of all but the first monolayer of the adsorbed porphyrin when the electrode was immersed in the aqueous solution of NaOH. Alternatively, only a single layer of multi-layer deposits might retain its electroactivity. A clear distinction between these two explanations was not possible. In any case, all electrodes were coated by exposing them to more than monolayer quantities of I dissolved in dichloroethane. The quantity of electro-active I present in the resulting coating was 4×10^{-10} mole cm^{-2}.

It is clear from Figure 2A, the peak current of the voltammograms for the adsorbed I are significantly smaller at pH values below 6 than at pH 14. This does not result from stripping of the porphyrin from the surface by the acidic electrolytes because an electrode that exhibits the response shown for pH 2 will immediately yield the larger response shown for pH 14 when it is transferred to 1 M NaOH. The difference in the magnitude of the peak currents appears at about the same pH where the peak potentials become independent of pH (vide infra) and it might reflect a more sluggish electrode reaction rate for the aquo than for the hydroxy form of the cobalt(III) center. But, whatever their origin, the larger and sharper voltammograms obtained in 1 M NaOH were used to measure the quantities of I adsorbed on the electrodes.

The peak potentials shift to more positive values as the pH decreases. A plot of the average of the cathodic

and anodic peak potentials (i.e., the formal potential) vs. pH is linear between pH 6 and 14 with a slope of 65 mV/pH unit (Figure 3). Below pH 6 the peak potentials become essentially independent of further changes in pH. This behavior is consistent with assignment of the surface wave to reactions (1) and (2), where L represents the porphyrin ligand:

$$LCo^{III}OH + H^+ + e \rightleftharpoons LCo^{II}OH_2 \qquad (1)$$

$$LCo^{III}OH_2 + e \rightleftharpoons LCo^{II}OH_2 \qquad (2)$$

At pH values above 6, reaction 1 is predominant while reaction 2 represents the electrode reaction at lower pH values.

This interpretation is supported by the response of the peak potentials to the addition to the supporting electrolyte of imidazole, a base known to coordinate to the axial positions of metalloporphyrins. Figure 4 shows the surface waves for the adsorbed porphyrin in the presence and absence of imidazole. The shift of the peak to more negative potentials is in the direction expected for stronger binding of the imidazole by the Co(III) porphyrin. Similar shifts in reduction potentials are seen when axial bases are coordinated to many metallporphyrins.[8,9] It is also noteworthy that the magnitude of the shift in peak potential caused by imidazole is independent of pH in the same range where the peak potentials exhibit a pH

Figure 3. pH dependence of the potential for the Co(III/II) couple of porphyrin I.

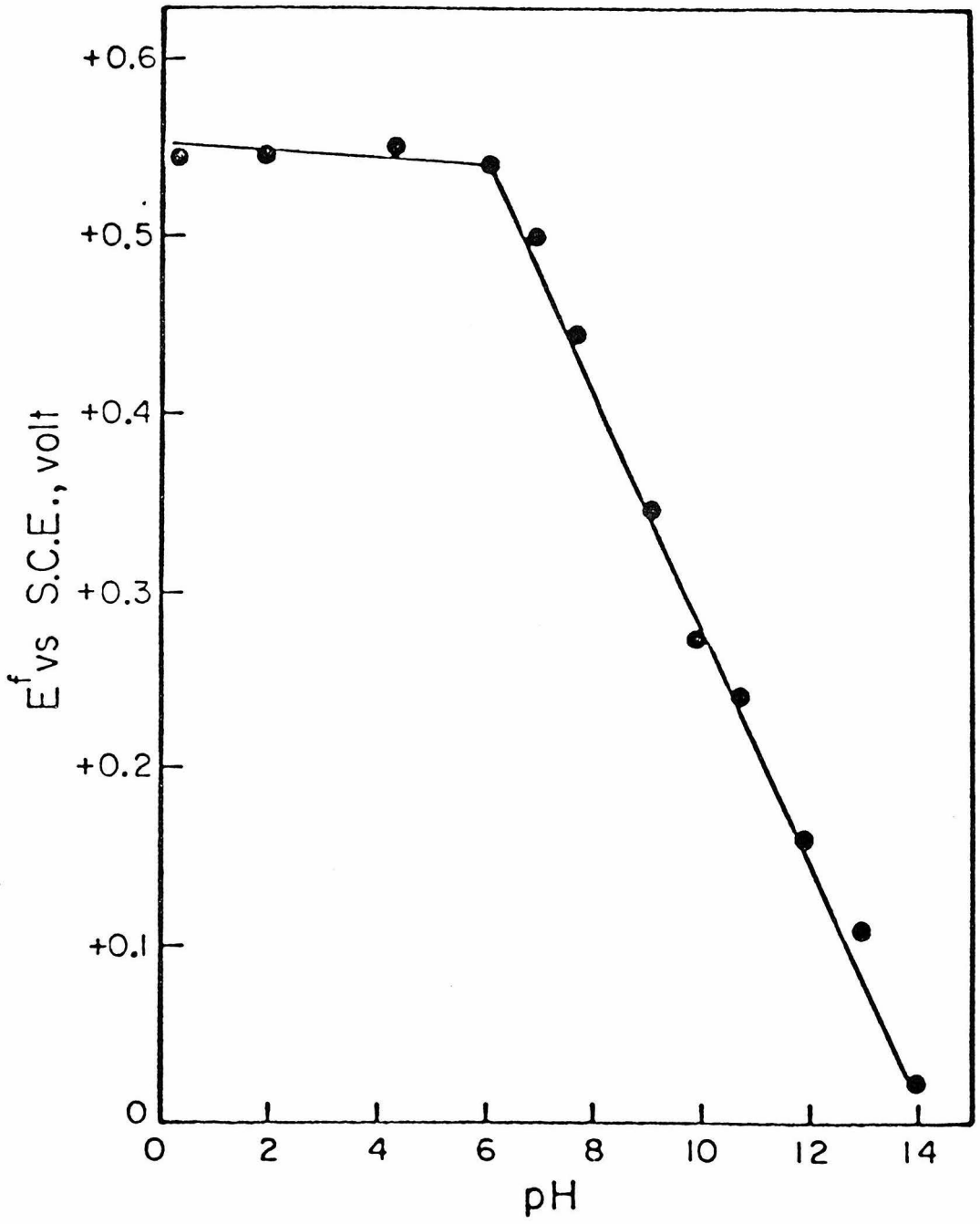
+0.6
+0.5
+0.4
+0.3
+0.2
+0.1
0
E^f vs S.C.E., volt
0
2
4
6
8
10
12
14
pH

Figure 4. Effect of imidazole on cyclic voltammograms of I adsorbed on graphite. Solid line: before addition of imidazole; dashed line: after solution was made 1 mM in imidazole. Supporting electrolyte: pH 9.2 buffer. Scan rate: 200 mV s^{-1}.

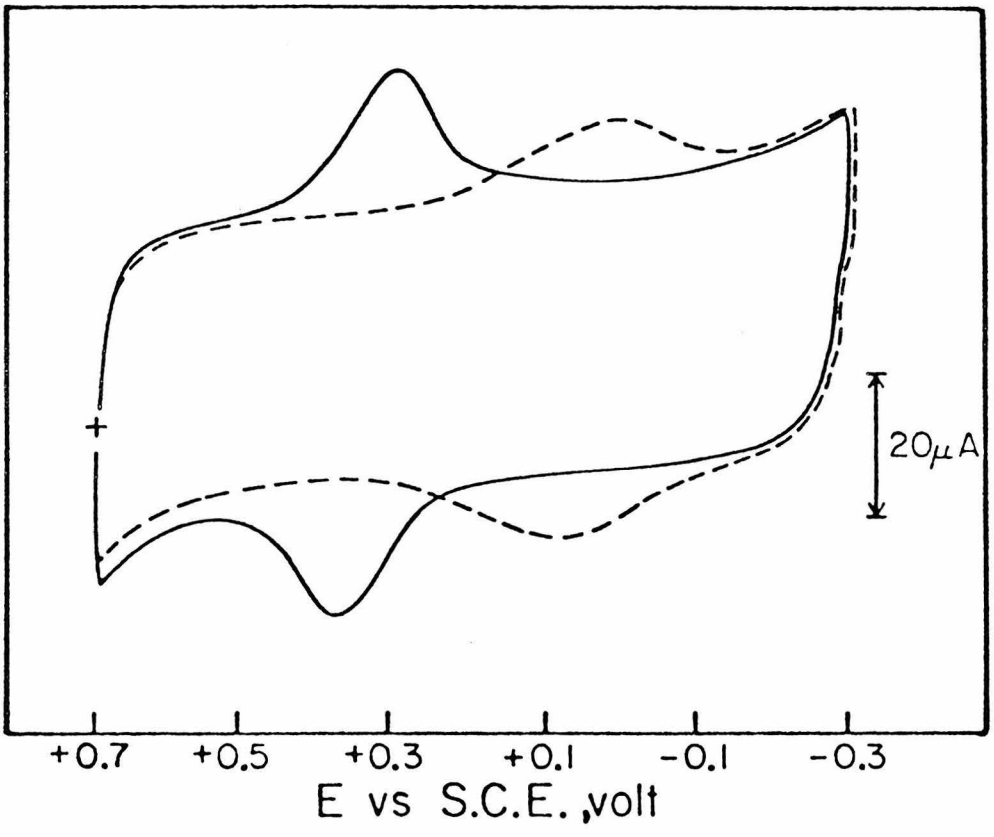
+
20μA
+0.7
+0.5
+0.3
+0.1
-0.1
-0.3
E vs S.C.E., volt

dependence in the absence of imidazole (Figure 3). This is to be expected if the addition of imidazole converts reaction (1) into reaction (3):

$$LCo^{III}Im + e \rightleftharpoons LCo^{III}Im \qquad (3)$$

(Im stands for imidazole.)

Voltammetry in the Presence of Dioxygen

In Figure 2B the catalyzed reduction of dioxygen at pyrolytic graphite electrodes coated with I is shown at a series of pH values. The corresponding responses at uncoated electrodes were negligible at the potentials where the prominent waves appear in Figure 2B. At all pH values the catalyzed reduction of O_2 proceeds at potentials well separated from the surface waves for the adsorbed catalyst so that these waves could be inspected (at higher current sensitivities) to determine if they are affected by exposure to dioxygen. In no case did the addition of dioxygen produce significant changes in the position or magnitude of the surface waves.

At pH 14 the cyclic voltammogram for the reduction of dioxygen at the coated electrode corresponds to a totally reversible, nearly nernstian couple (Figure 2A): essentially equal anodic and cathodic peak currents are obtained and the peak potentials are separated by 40 mV. The average of the anodic and cathodic peak potentials, 0.03 volt vs. SCE, is very close to the standard potential for the O_2/O_2H^- couple in 1 M NaOH, 0.08 volt.[10] A peak

splitting of 29 mV would be expected if the electrode reaction adhered to the Nernst equation. The slightly larger splitting observed may result from both uncompensated resistance in the cell and some small deviation from fully nernstian behavior. The most remarkable feature of the result is the ability of the adsorbed catalyst to transform the graphite surface into an electrode reversible to the O_2/O_2H^- couple. Mercury electrodes are known to respond reversible to the O_2/O_2H^- couple at high pH[11,12] and Figure 5 compares the responses of a mercury electrode with that of the graphite electrode coated with I. Their equivalence is apparent.

As the pH of the supporting electrolyte is decreased, the separation of the cathodic and anodic peak potentials for the O_2/O_2H^- couple increases (Figure 2B). The increasing separation results primarily from a shift of the anodic peak to more positive values while the cathodic peak remains relatively fixed down to pH 7. The magnitude of the anodic peak current also diminishes at pH values below ca. 12. This is also observed with solutions of H_2O_2 in the absence of dioxygen. It seems significant that the decrease in anodic current commences close to the pk_a of H_2O_2 (11.7) where the O_2H^- anions that presumably coordinate to the cobalt(II) centers of the catalyst in order to be oxidized are converted into much less nucleophilic H_2O_2 molecules.

Figure 5. Cyclic voltammograms of 1.0 mM H_2O_2 in 0.5M NaOH recorded at: (A) 0.032 cm^2 hanging mercury drop electrode; (B) 0.17 cm^2 graphite electrode coated with I. Scan rate: 100 mV s^{-1}. Initial potential: -0.5 volt.

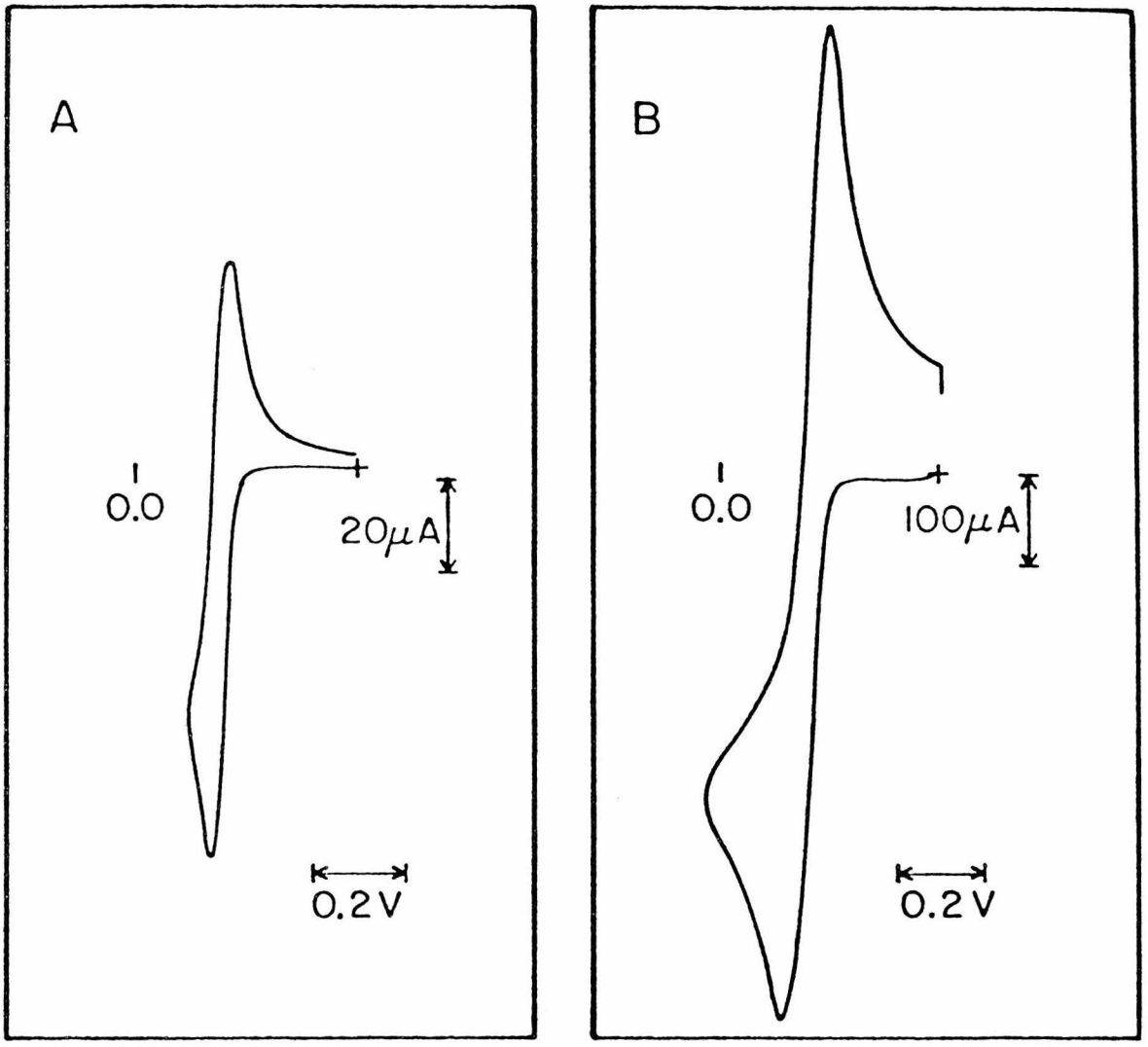
A
0.0
20μA
0.2V
B
0.0
100μA
0.2V

A similar dimunition of the H_2O_2 oxidation current results from the addition of imidazole at fixed pH (Figure 6). Note that the axial base also shifts the wave for the catalyzed reduction of dioxygen to more negative potentials. Both responses are in the direction expected if the imidazole were competing with H_2O_2 and O_2 for a coordination site on the cobalt center. It is also not surprising that the axial base is apparently more successful in competing with H_2O_2 than with O_2 for coordination to cobalt(II).

Effects of Increasing Scan Rates on the Current Responses

Figure 7 shows how the voltammograms for the adsorbed catalyst and the O_2/OH_2^- couple respond to large increases in the potential scan rate. The peak current of the cobalt catalyst increases more rapidly with scan rate than does that for the dioxygen reduction, as expected for an attached reactant. However, the dioxygen reduction wave becomes a flat plateau at scan rates above 10 Volt s^{-1}. This is the behavior expected if the electro-reduction step is preceded by a relatively rapid, potential-independent chemical reaction. Further evidence of the intervention of such a reaction will be presented in the section where the rotating disk studies are described.

The small separation in peak potentials and the undistorted shapes of the waves for the cobalt catalyst at the highest scan rates (Figure 7) show that it can be

Figure 6. Effect of imidazole on cyclic voltammograms for dioxygen reduction at graphite electrodes coated with I.

A) Dioxygen saturated solution before addition of imidazole;

B) After addition of 1 mM imidazole.

Supporting electrolyte: pH 10.8 buffer.

Scan rate: 200 mV s^{-1}.

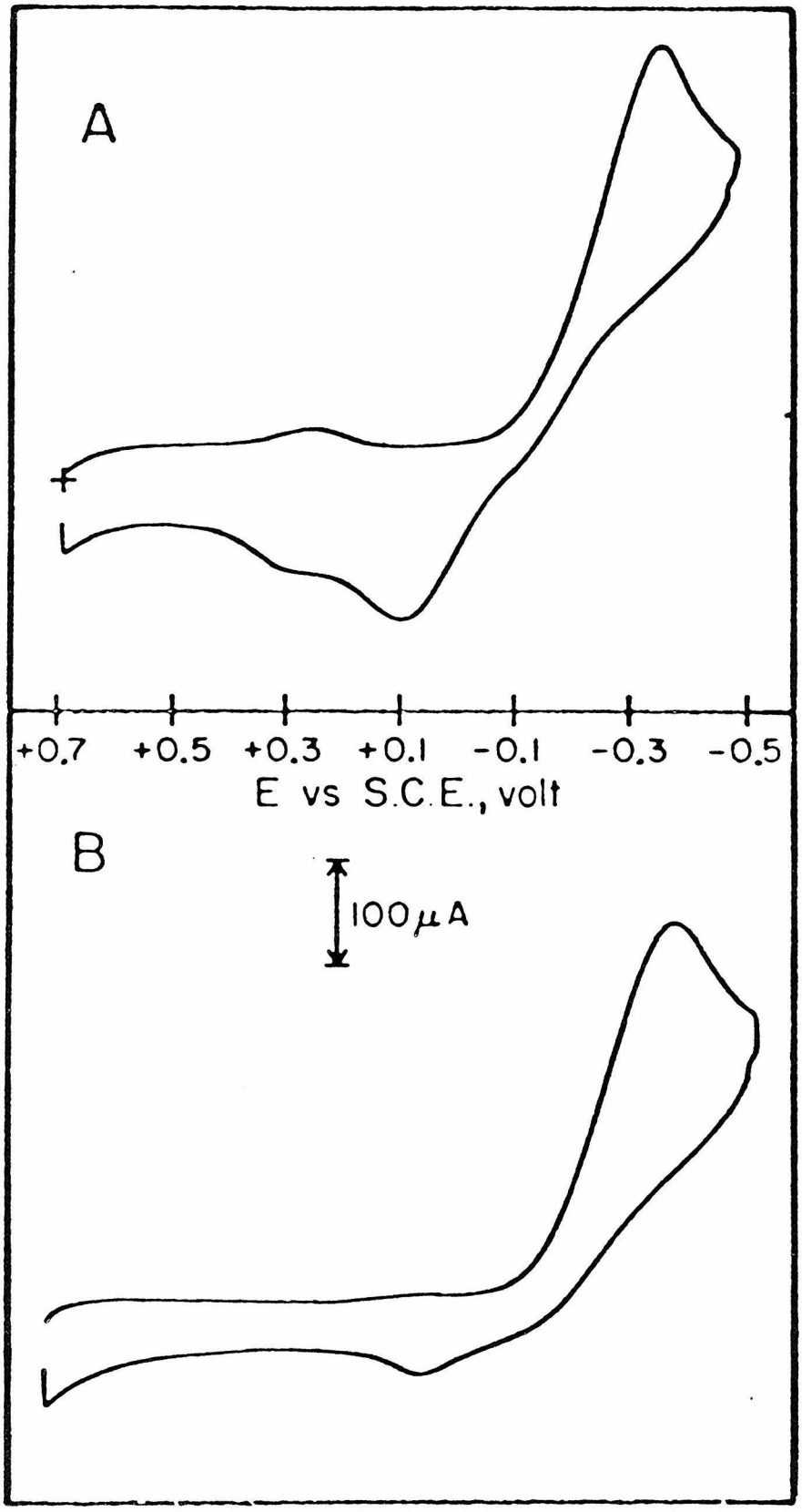
A
+0.7
+0.5
+0.3
+0.1
-0.1
-0.3
-0.5
E vs S.C.E., volt
B
100μA

Figure 7. Cyclic voltammograms for adsorbed I and the O_2/O_2H^- couple in 1 M NaOH at high scan rates. Dashed lines: argon saturated solutions. Solid line: dioxygen saturated solutions. Initial potential was 0.4 volt.

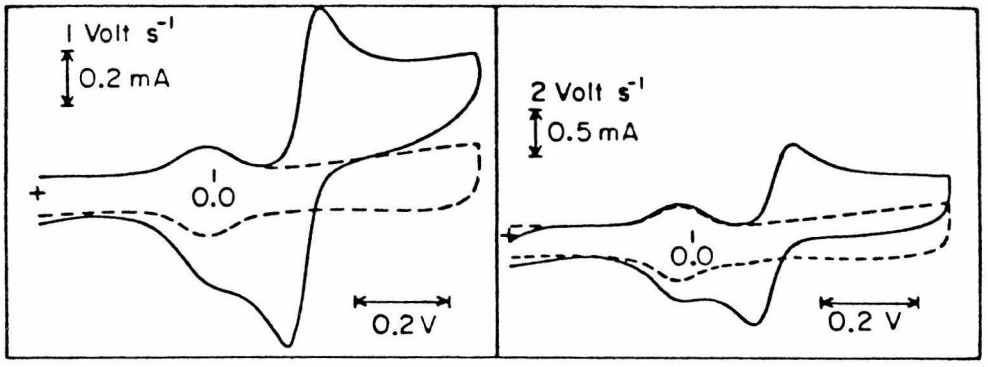
1 Volt s⁻¹
0.2 mA
0.0
0.2 V
2 Volt s⁻¹
0.5 mA
0.0
0.2 V

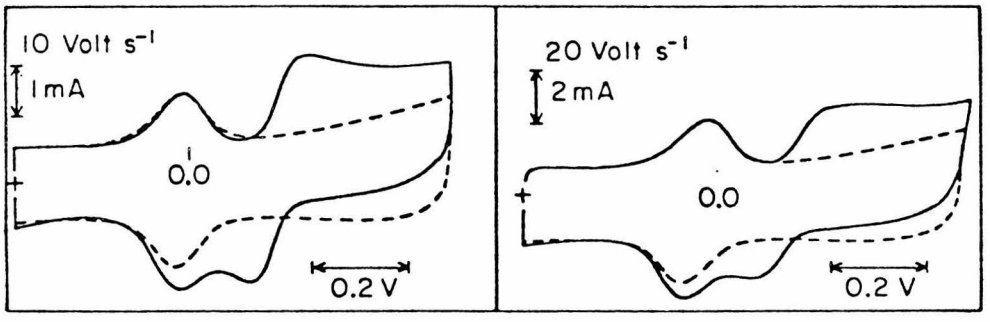
10 Volt s⁻¹
1 mA
0.0
0.2 V
20 Volt s⁻¹
2 mA
0.0
0.2 V

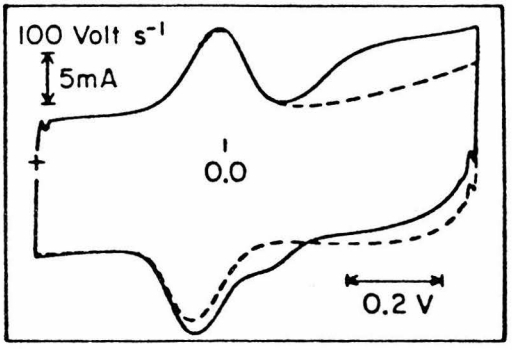
100 Volt s⁻¹
5 mA
0.0
0.2 V

cycled between its two oxidation states at very high rates at potentials close to its formal potential.

Anodic Peaks During Scans Towards More Negative Potentials

A revealing feature in the cyclic voltammograms for the O_2/O_2H^- couple at catalyst coated electrodes can be observed in the vicinity of the surface wave for the adsorbed catalyst. Curve A in Figure 8 shows the entire voltammogram recorded at a low current sensitivity so that the entire reversible O_2/O_2H^- response is observed. Curve B, recorded at a ten times higher sensitivity, shows the response from the attached catalyst when the electrode potential is cycled repeatedly but restricted to values ahead of the dioxygen reduction so that no H_2O_2 is formed. Curve C shows the response obtained when the potential is cycled repeatedly in an extended range where the reduction of dioxygen to H_2O_2 proceeds. On the second and all subsequent cathodic scans, a prominent oxidation peak appears near the potential where the cobalt catalyst is converted from cobalt(III) to cobalt(II). Curve D shows how the anodic peak, once formed, decays away if the potential range is again restricted to values ahead of the dioxygen reduction. This anodic peak that appears during scans to more negative potentials seems clearly to originate from the oxidation of H_2O_2 that is generated at the electrode while the electrode is at potentials on the dioxygen reduction wave. Much of the H_2O_2 is reoxidized at

Figure 8. Cyclic voltammograms of adsorbed I in dioxygen saturated 0.5 M NaOH. A) Low current sensitivity; potential scanned over the O_2/HO_2^- wave. B) High current sensitivity, potential scanned only to the foot of the O_2/HO_2^- wave. C) High current sensitivity, potential scanned repeatedly over the O_2/HO_2^- wave and then repeatedly to the foot of the wave. Scan rate: 100 mV s^{-1}. Current sensitivity: A) S = 100 μA; B,C,D) S = 10 μA. Initial potential: 0.4 volt.

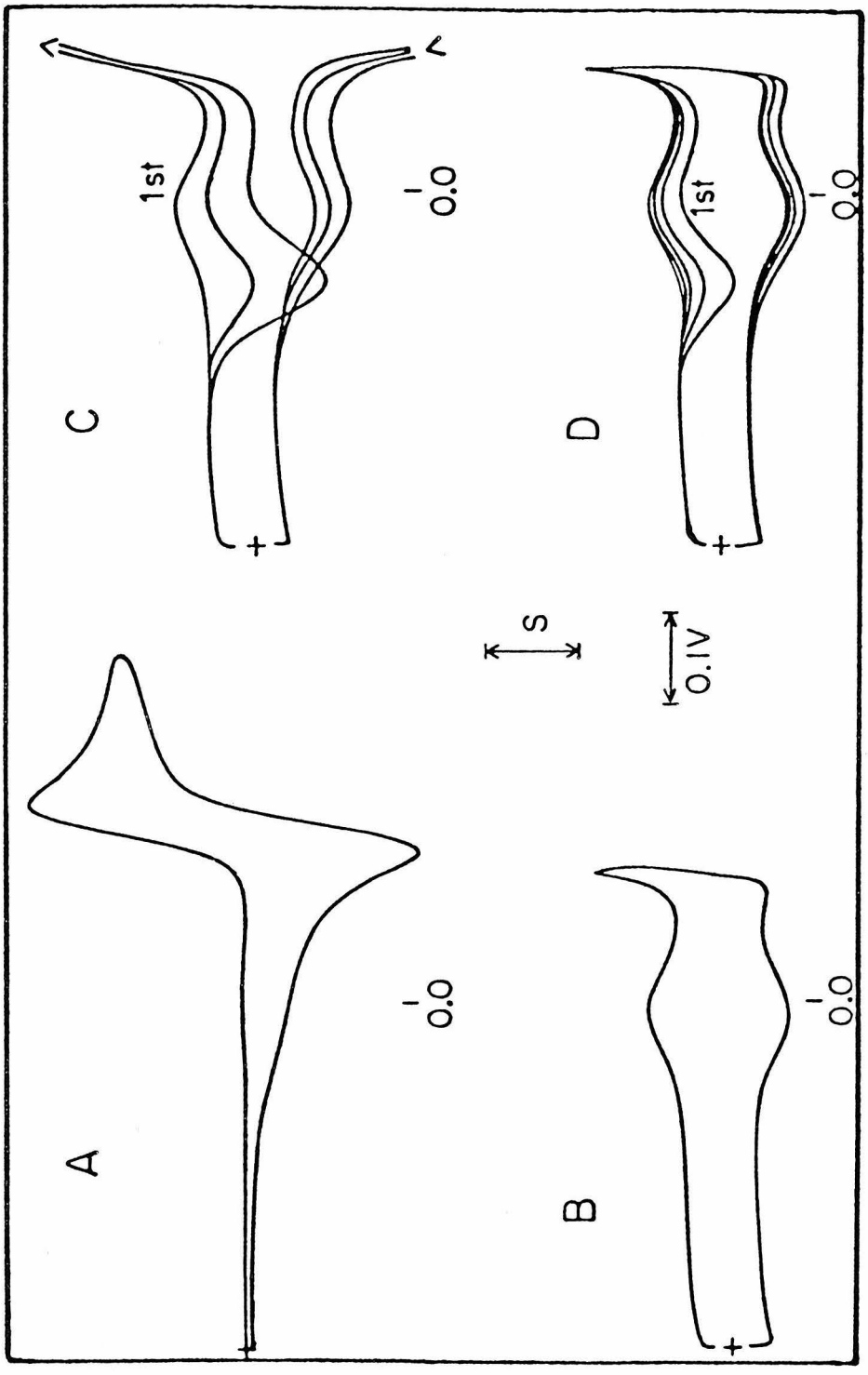
A
B
C
D
1st
1st
0.0
0.0
0.0
S
0.1V
+
+
+

potentials positive of the wave for the adsorbed catalyst. However, where the potential passes over the catalyst wave, converting the cobalt(II) to its catalytically unreactive cobalt(III) state, the oxidation of H_2O_2 can no longer proceed. Thus, the H_2O_2 that continues to diffuse to the electrode surface accumulates there until the electrode potential is returned to the value where the cobalt(III) is reduced again to cobalt(II). At that point the accumulated H_2O_2 can again be oxidized and the anodic peak results. The position of the anodic peak shifts with pH in the same way that peak potential of the wave for the cobalt catalyst shifts (Figure 3). Solutions of H_2O_2 in the absence of dioxygen also exhibit the unusual anodic wave. An initial scan to more positive potentials produces a normal anodic current peak but the current in the "tail" of the wave decays abnormally in the vicinity of the cobalt catalyst wave. The subsequent scan to more negative potentials exhibits a prominent anodic peak at the same potential as it appears in Figure 8.

The voltammetric behavior described here is somewhat unusual but the explanation proposed to account for it is not. Much higher activities of cobalt(II) than of cobalt(III) complexes have also been reported in the catalyzed disproportionation of hydrogen peroxide[13,14] and it is not surprising to see the same difference in reactivity reflected in the catalysis of the oxidation of H_2O_2 by the cobalt porphyrin catalyst.

Voltammetry at Catalyst-Coated Rotating Disk Electrodes

Figure 9A shows a set of current-potential curves for the reduction of dioxygen at a rotating disk electrode coated with the cobalt catalyst in 1M NaOH. The corresponding Levich plot[15] of limiting current vs. (rotation rate)$^{\frac{1}{2}}$ and the line calculated from the Levich equation[15] for the two-electron reduction of dioxygen are shown in Figure 9B. The evident deviations from the Levich line point to control of the limiting currents by a chemical step that precedes the reduction. Kinetic analysis of such systems is facilitated by means of Koutecky-Levich plots of (limiting current)$^{-1}$ vs. (rotation rate)$^{-\frac{1}{2}}$.[5,16] A typical plot is shown in Figure 10. These plots are interpreted on the basis of equation (4):

$$\frac{1}{i_{lim}} = \frac{1}{i_{lev}} + \frac{1}{i_k} \qquad (4)$$

where i_{lim} is the measured limiting current. The Levich current, i_{lev}, and i_k, the kinetic current, are defined by equations (5) and (6), respectively.

$$i_{lev} = 0.62\ nFAD^{2/3}\nu^{-1/6}C^b\omega^{1/2} \qquad (5)$$

where D and C^b are the diffusion coefficient and bulk concentration of dioxygen, respectively, ν is the kinematic viscosity of water, ω is the electrode rotation rate and the other symbols have their usual significance.

$$i_k = 10^3 nFAk\Gamma C^b \qquad (6)$$

where k is the rate constant ($M^{-1}s^{-1}$) governing the reaction of the catalyst with dioxygen and Γ (mole cm^{-2}) is

Figure 9. A) Current-potential curves for the reduction of O_2 in 1 M NaOH at a rotating graphite disk electrode coated with I. Electrode rotation rates in rpm are indicated on each curve. The electrode potential was scanned at 8.3 mV s^{-1}. B) Levich plot of the rotating disk limiting currents vs. (rotation rate)$^{\frac{1}{2}}$. The dashed line is the calculated response for the mass transfer-limited two-electron reduction of dioxygen.

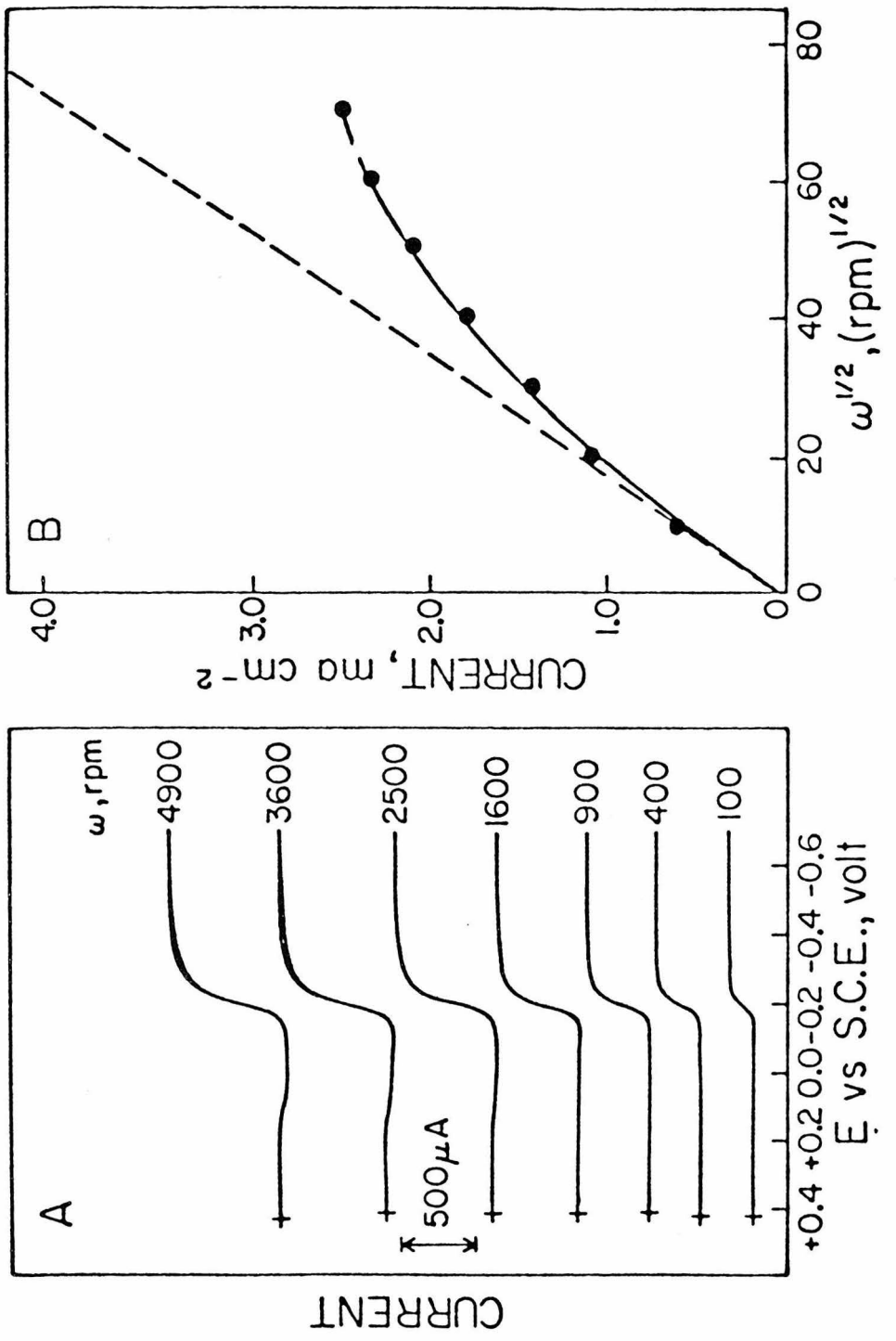
A
ω, rpm
4900
3600
2500
1600
900
400
100
500μA
CURRENT
+0.4 +0.2 0.0 -0.2 -0.4 -0.6
E vs S.C.E., volt
B
CURRENT, ma cm⁻²
4.0
3.0
2.0
1.0
0
0
20
40
60
80
ω^1/2, (rpm)^1/2

the quantity of catalyst on the electrode that participates in catalyzing the reaction.

The slope of the solid line shown in Figure 10 matches that of the dashed line that was calculated from equation (5) for the two electron reduction of dioxygen showing that hydrogen peroxide is the product of the electrode reaction. The intercept of the solid line in Figure 10 provides a measure of ($k\Gamma$).

Table I summarizes the values of ($k\Gamma$) and k evaluated from Koutecky-Levich plots for the catalyzed reduction of dioxygen at a series of pH values. All of the electrodes employed to obtain the data in Table I were coated by the procedure described above to produce the limiting porphyrin coverage of 4×10^{-10} mole cm^2. The measured values of k are not affected by changes in pH except at pH 14 where a somewhat smaller value of k results. It is noteworthy that the values of k listed in Table I are of the same magnitude as previously reported rate constants governing the kinetics of the coordination of dioxygen to a variety of cobalt(II) complexes in aqueous solution.[17]

Analogous experiments in which hydrogen peroxide is oxidized at the catalyst coated rotating disk electrode yielded the current potential curves shown in Figure 11. The decline in the limiting currents at potentials where the cobalt(II) catalyst is oxidized to cobalt(III) is evident. Intercepts of Koutecky-Levich plots for the

Table I

Rate constants obtained from the intercepts of Koutecky-Levich plots for the reduction of O_2 at graphite electrodes coated with I.

pH	$(k\Gamma)$, cm s^{-1}	k, $M^{-1}s^{-1}$
0.3	0.053	1.4×10^5
3.0	0.074	2.0×10^5
7.0	0.052	1.43×10^5
10.8	0.062	1.73×10^5
14	0.036	0.98×10^5

Figure 10. Koutecky-Levich plot of the current-rotation rate data from Figure 9. The dashed line corresponds to the dashed line in Figure 9.

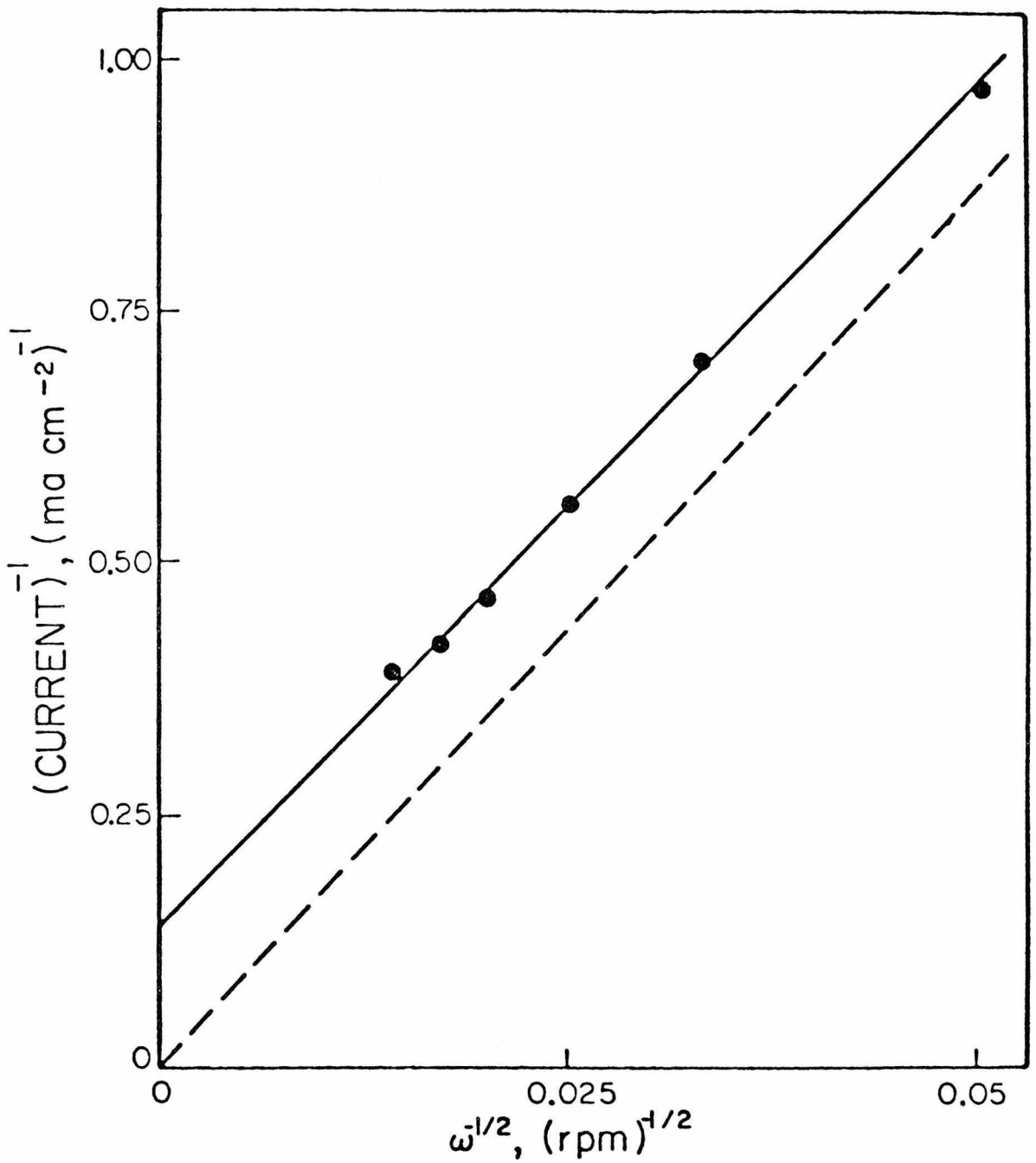
1.00
0.75
0.50
0.25
0
0
0.025
0.05
(CURRENT)$^{-1}$, (ma cm^{-2})$^{-1}$
$\omega^{1/2}$, (rpm)$^{1/2}$

Figure 11. Current-potential curves for the oxidation of 1 mM O_2H^- in 1 M NaOH at a graphite rotating disk electrode coated with I. Initial potential: -0.6 volt. Other conditions as in Figure 9.

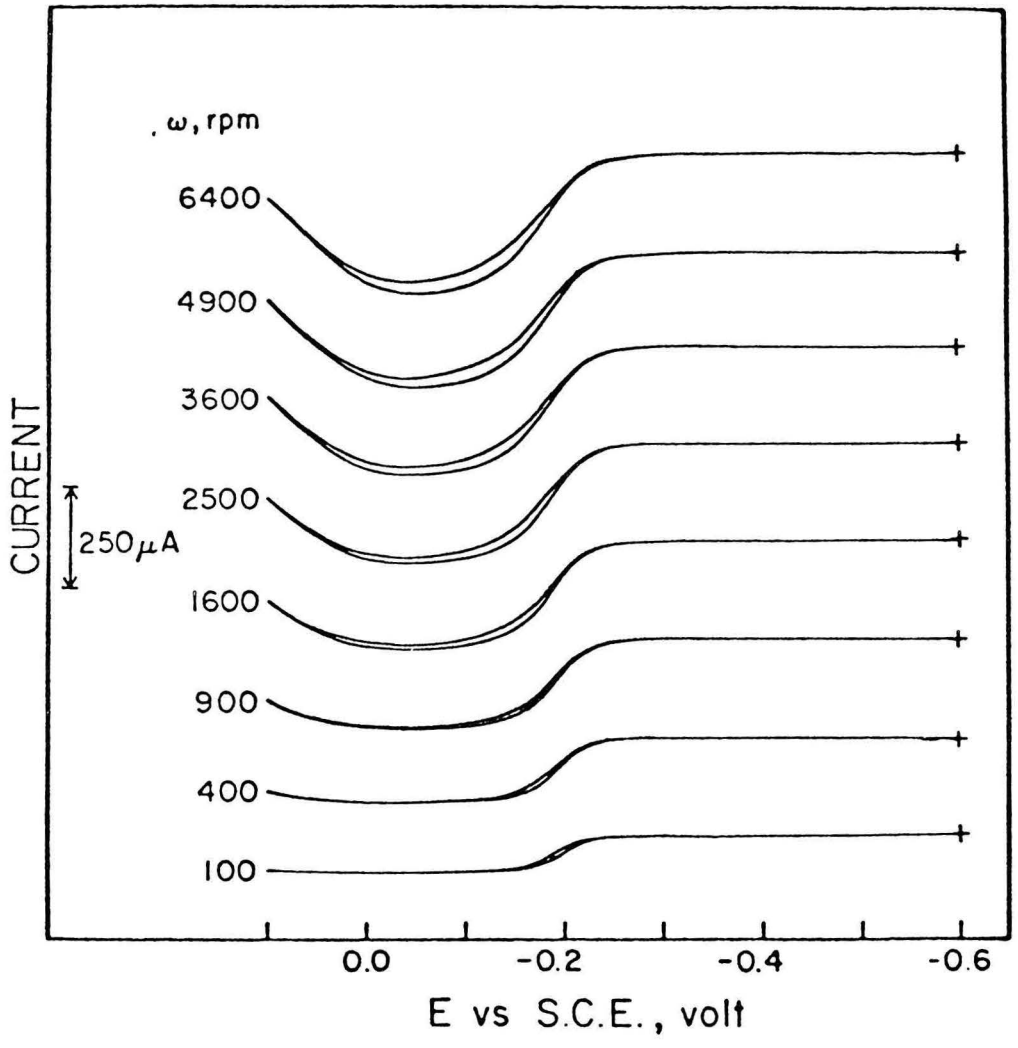
ω, rpm
6400
4900
3600
2500
1600
900
400
100
CURRENT
250μA
0.0
-0.2
-0.4
-0.6
E vs S.C.E., volt

oxidation of H_2O_2 were used to evaluate the rate constants listed in Table II. Measurements were limited to pH 12 or higher because the catalyst appeared to lose its potency to catalyze the oxidation at lower pH values. The values of rate constants in Table II are similar to those in Table I suggesting a common rate limiting step for both dioxygen reduction and hydrogen peroxide oxidation.

Voltammetry at a Rotating Ring-Disk Electrode

The rotating disk results already described were entirely consistent with the catalyzed reduction of dioxygen proceeding quantitatively to hydrogen peroxide. However, attempts to confirm this by means of a rotating graphite disk-platinum ring electrode were unsuccessful. Only 60-70% of the H_2O_2 believed to be generated at the catalyst-coated disk was detected at the platinum ring electrode held at potentials where H_2O_2 is oxidized. This discrepancy was traced to a fairly rapid "poisoning" of the platinum ring electrode toward H_2O_2 oxidation in most of the electrolytes employed. Similar observations in previous ring-disk experiments with the dioxygen-hydrogen peroxide system have been made in this laboratory[18] where repeated cleaning and "activation" of the platinum ring electrodes were required to assure quantitative oxidation of hydrogen peroxide reaching the ring. Such remedies were only partially successful with the electrolytes employed in the present experiments and we abandoned the use of the

Table II

Rate constants obtained from the intercepts of Koutecky-Levich plots for the oxidation of H_2O_2 at graphite electrodes coated with I.

pH	$(k\Gamma)$, cm s^{-1}	k, $M^{-1}s^{-1}$
12	0.022	6.0×10^4
14	0.034	9.4×10^4

ring-disk electrode to measure the quantities of H_2O_2 generated at the disk electrode. The best evidence that the catalyzed reduction of dioxygen produces only hydrogen peroxide is the slope of the Koutecky-Levich plot (Figure 10) which corresponds closely to the calculated value for n = 2 electrons.

DISCUSSION

One of the most striking features in the behavior of the cobalt porphyrin catalyst is the significant separation between the potentials where the catalyst is oxidized and reduced and the potentials where it exhibits its catalytic activity. The catalyst is reduced at potentials well ahead of those where dioxygen is reduced, suggesting that the formation of a cobalt(II)-O_2 adduct is a necessary but not a sufficient condition for the electroreduction of dioxygen to ensue. The potential of the electrode must also be made sufficiently negative to reduce the cobalt(II)-O_2 adduct. At pH 14, where the catalyst endows the electrode with full reversibility towards the O_2/O_2H^- couple, a possible reaction sequence for the catalyzed reduction is reaction 1 followed by the steps listed in Scheme I.

Scheme I

$$LCo^{II} + O_2 \rightleftharpoons LCo^{II}O_2 \qquad (A)$$

$$LCo^{II}O_2 + 2e \rightleftharpoons LCo^{II}O_2^{2-} \qquad (B)$$

$$LCo^{II}O_2^{2-} + H^+ \rightleftharpoons LCo^{II}O_2H^- \qquad (C)$$

$$LCo^{II}O_2H^- \rightleftharpoons LCo^{II} + O_2H^- \qquad (D)$$

All of the steps in this sequence are reversible but at high rates of reaction, the binding of the substrate to the catalyst, i.e., the forward direction of step A or the reverse direction of step D, become rate limiting. The insensitivity of the peak potentials of the reversible cobalt(III)/(II) couple of the adsorbed catalyst to the addition of O_2 or H_2O_2 (Fig. 2,6) is strong evidence that the equilibrium constants governing the formation of the Co(II) adducts of dioxygen and O_2H^- are not large, probably 1 M^{-1}. (The alternative possibility, that Co(II) and Co(III) bind O_2 (and O_2H^-) equally strongly, seems much less likely.) Thus, even if the proposed cobalt-dioxygen adduct were best regarded as a complex of cobalt(III) and superoxide, most of the cobalt centers in the adsorbed catalyst remain as Co(II) throughout the catalytic cycle.

The rate constants listed in Tables I and II for pH 14 give the specific rate of the forward direction of step A and the reverse direction of step D in Scheme I, respectively. It is unlikely that the rate could be limited by the decomposition of the products of the catalyzed reactions, i.e., by step D or the reverse of step A, because, as has already been argued, the equilibrium constants for steps A and D must be rather small and rather large, respectively.

The nearly equal values of the rate constants argues for a common rate determining step such as the loss of the ligand, probably H_2O, occupying the site of binding of the incoming O_2 or O_2H^- molecule to the cobalt porphyrin. The same argument has been used to account for the similarity in the rate of binding of dioxygen to a variety of different cobalt(II) complexes.[17,19]

At pH values between 7 and 11, the electrode process is less reversible because the oxidation of H_2O_2 moves to more positive potentials while the reduction of O_2 continues to proceed at virtually the same potential (Figure 2B). The dioxygen reduction probably continues to follow the same sequence (steps A to D) in the forward direction in this pH range while the oxidation of hydrogen peroxide must follow a somewhat different course such as that shown in Scheme II:

Scheme II

$$H_2O_2 \rightleftharpoons H^+ + O_2H^- \qquad (E)$$

$$HO_2^- + LCo^{II} \rightleftharpoons LCo^{II}O_2H^- \qquad (F)$$

$$LCo^{II}O_2H^- \rightleftharpoons LCo^{II}O_2 + H^+ + 2e^- \qquad (G)$$

$$LCo^{II}O_2 \rightleftharpoons LCo^{II} + O_2 \qquad (H)$$

This sequence accounts for the shift in the oxidation wave to more positive potentials as the pH decreases because the concentration of the proposed catalytically

active complex, $LCo^{II}O_2H^-$, is linked directly to the pH through steps E and F (the pK_a of H_2O_2 is 11.7).

At pH values below ca. 7, the dioxygen reduction peak begins to exhibit a pH dependence (Figures 2, 3). This can be explained if steps B and C in Scheme I are replaced by the following two steps:

$$LCo^{II}O_2 + H^+ \rightleftharpoons LCo^{II}O_2H^+ \qquad (J)$$

$$LCo^{II}O_2H^+ + 2e^- \rightleftharpoons LCo^{II}O_2H^- \qquad (K)$$

The oxidation of hydrogen peroxide at pH values below 7 could continue to proceed according to Scheme II.

On the rising portions of current-potential curves for dioxygen reduction at rotating disk electrodes, step C rather than step A in Scheme I would be rate limiting. Tafel plots of $\log(\frac{i}{i_{lim}-i})$ vs. E^{20} prepared from the rotating disk data recorded at the foot of the waves ($E>E_{\frac{1}{2}}$) were linear with slopes near 120 mV/decade at pH <11 (Table III) indicating that the addition of the first electron limits the rate of reduction of the cobalt(II)-dioxygen adduct. At pH 14, the slope decreased to 30 mV/decade as expected when the O_2/O_2H^- couple approached nernstian equilibrium.

Behavior of Related Catalysts

Several other cobalt porphyrins have been adsorbed onto graphite electrodes and compared to the species described above. The results for these catalysts are

Table III

Slopes of plots of $\log(\frac{i}{i_{lim}-i})$ vs. E for the reduction of O_2 at graphite disk electrodes coated with I.

pH	Slope, mV/decade
0.3	122
3.0	150
7.0	115
10.8	108
14	30

summarized in Table 4. It is apparent that as catalysts all these monomeric species behave similarly. The major distinction between complexes arises from the change in ligand itself. The electronic effects as the porphyrin structure changes are well documented.[21] The cobalt(III/II) reduction potentials are in the range of 0.3 to 0.8V vs. SCE. In all cases, the reduction of dioxygen appears at more negative and essentially constant potential to produce the same product, H_2O_2. This fact suggests all of these catalysts may function by a common mechanism. The only reported exception for monomeric cobalt porphyrin was described by Kuwana et al. in their study of cobalt tetrapyridylporphyrin.[22] A re-examination of this complex in this laboratory has been carried out.

The reduction of Co(III) to Co(II) was found by Kuwana to exist as a reversible wave at -0.05V in acidic medium under argon. In the presence of dioxygen the catalytic response appeared to be strongly coupled to this wave. Thus a mechanism in which the catalysis was governed by the Co(III/II) reduction potential was proposed.

Figure 12 shows a cyclic voltammogram of the cobalt tetrapyridylporphyrin adsorbed to an edge plane graphite electrode in presence and absence of oxygen in 0.5M HTFA. There is a very prominent reversible peak at +0.54V vs. SCE as well as a smaller response not attributable to the background response at +0.05V. The non-metalated ligand

Figure 12. Cyclic voltammograms of adsorbed CoTPyP in 0.5 M HTFA. A) Under argon, B) under O_2. Scan rate: 200 mV s^{-1}.

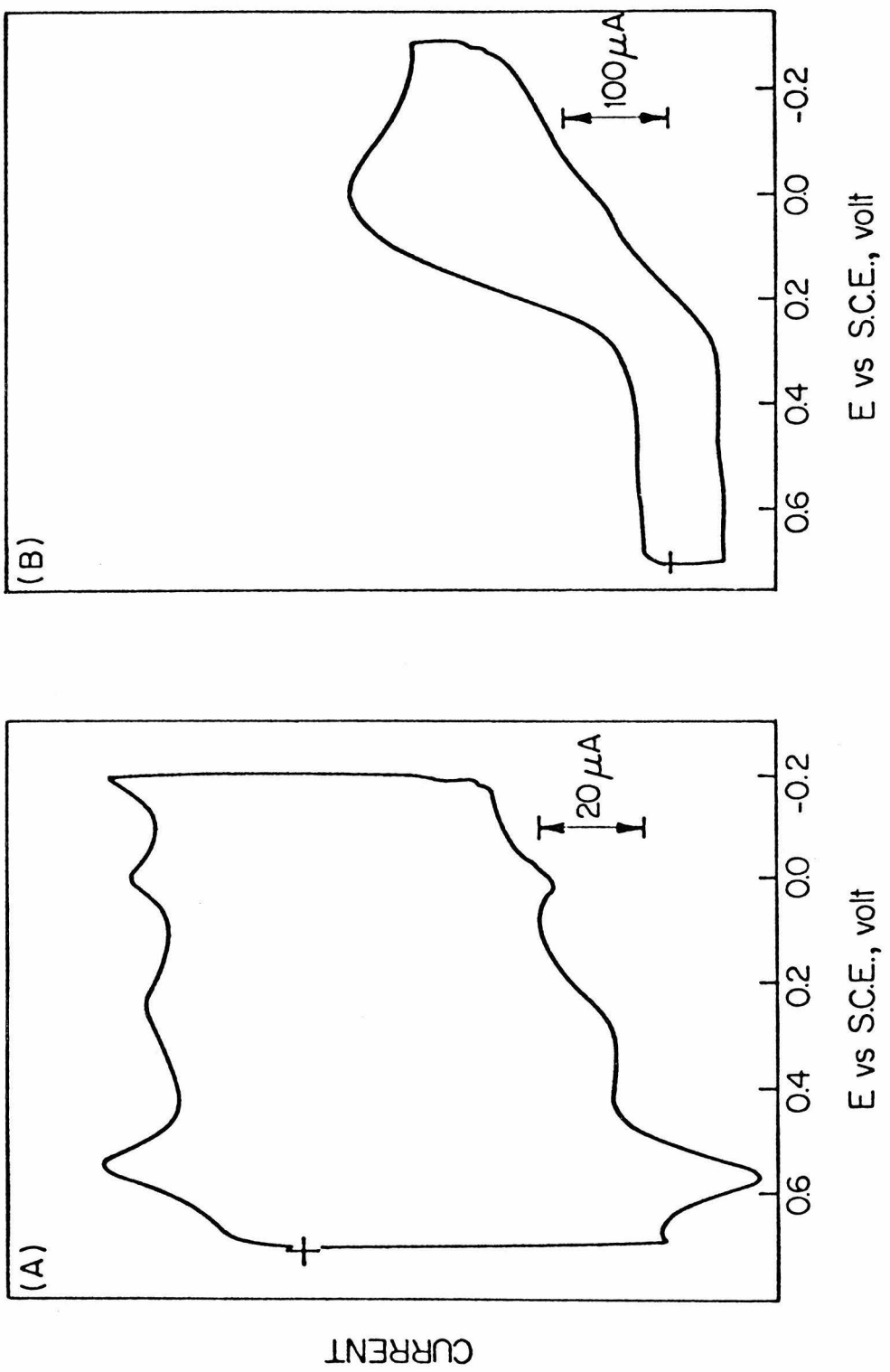
(A)
20 μA
0.6
0.4
0.2
0.0
-0.2
E vs S.C.E., volt
(B)
100 μA
0.6
0.4
0.2
0.0
-0.2
E vs S.C.E., volt
CURRENT

showed a wave near 0.0V vs. SCE as shown in Figure 13. The nature of this electroactivity is unclear, but it is similar in potential to the lesser response for the metalated complex and also to that obtained by Kuwana and co-workers in their study of the cobalt complex. The related cobalt tetra-N-methylpyridylporphyrin showed a Co(III/II) reduction at +0.55V under the same conditions utilized in this study.

Under O_2, the catalytic reduction occurs at more negative potentials than the Co(III/II) response as it does for the other porphyrins which have been examined. In the previous study of this complex,[22] the potentials scanned were limited such that the more positive response noted here would not be observed. The achievement of high purity for this complex may be difficult. It would be surprising that this particular porphyrin should show any unique features compared to the others noted in Table 4.

Further evidence for the large separation between the Co(III/II) reduction for CoTPyP and the potential at which oxygen is reduced was observed in strongly basic electrolyte. Successive scans over the O_2/HO_2^- wave produced the unusual anodic currents as observed for the more thoroughly examined Co monomer (Figure 1). This observation is consistent with the Co(III/II) reduction potential occurring positively with respect to the O_2/HO_2^- couple for the reasons already noted. As the pH decreases,

Table IV

Comparison of E^f(CoIII/II) and $E_{1/2}$ for O_2 reduction for electrodes (graphite disks) coated with various porphyrins.[a]

Porphyrin	E^f (V vs. SCE)	$E_{1/2}$ (V vs. SCE)	Comments
I	+0.52	+0.20	b
tetraphenylporphyrin	+0.75	+0.18	b
tetra(p-methoxy)phenylporphyrin	+0.64	+0.15	b
octaethylporphyrin	+0.60	+0.18	b
tetra(p-sulfonato)phenylporphyrin	+0.50	+0.20	b
tetra(N-methyl)pyridylporphyrin	+0.58	+0.18	b
tetrapyridylporphyrin	+0.55	+0.20	b
tetrapyridylporphyrin	+0.08*	+0.20*	c
tetra(p-amino)phenylporphyrin	+0.30*	+0.15*	d
tetrasulfonatophthalocyanine	+0.80*	-0.20*	e

a - 0.5M Trifluoroacetic acid; $E_{1/2}$ obtained from rotating disk voltammetry at 100 rpm

b - this work d - Reference 23 * - performed in H_2SO_4

c - Reference 22 e - Reference 24

Figure 13. Cyclic voltammogram of adsorbed TPyP ligand in argon saturated 0.5M HTFA. Scan rate: 100 mV s^{-1}.

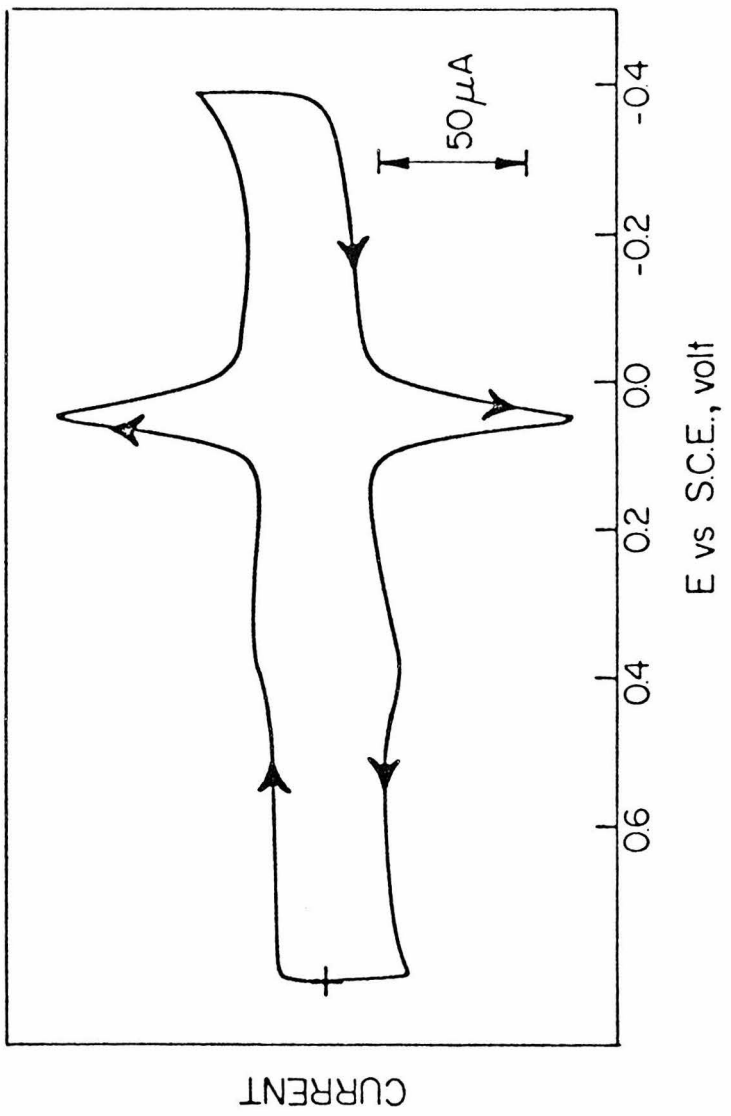
50μA
0.6
0.4
0.2
0.0
-0.2
-0.4
E vs S.C.E., volt
CURRENT

the Co(III/II) couple shows a potential shift to more positive values and always occurs prior to the oxygen reduction response. These observations suggest that the cobalt tetrapyridylporphyrin is not unique among the monomeric cobalt porphyrins.

Different porphyrin ligands show distinct Co(III/II) potentials. This may be related to the electronic effects of the substitution patterns. The effects of substitution on the catalytic activity of the monomeric cobalt porphyrin, I, have been considered. The mono-meso substituted nitro and cyano derivatives as well as a complex in which the B-pyrrole ester side chains have the carbonyl group directly attached to the porphyrin ring have been examined. Table 5 shows the comparison of the Co(III/II) reduction potentials for adsorbed catalysts in 1 M NaOH. The $E_{1/2}$ for oxygen reduction in 1 M NaOH occurs at the thermodynamic potential for all these complexes. In acidic solution, the oxygen reduction potential is unchanged by substitution. The Co(III/II) potentials are not as easily compared in acid as the voltammetric responses are distorted but trends similar to those observed in strong base were noted. The electron withdrawing nature of the substituents is manifested in the positive shift in the cobalt(III/II) potential. The change in Co(III/II) potential might be expected to alter the equilibrium binding affinity of dioxygen. The catalytic reduction of oxygen does not appear

Table V

Effects of substituents on Co(III/II) potentials for a Co monomer, I, adsorbed to graphite electrodes.*

Porphyrin	E^f (V vs. SCE)
Co monomer	+0.03
Co nitrated monomer	+0.19
Co cyanated monomer	+0.20
Co β-COOEt monomer	+0.12

*In 1 M NaOH electrolyte

to be influenced by this factor. The fact that the equilibrium constant is already very low for Co monomer porphyrin, I, may make the change less pronounced.

Relationship of the Co(III/II) Potential and the Oxygen Reduction Potential

The origin of the disparity between the Co(III/II) potential and the oxygen reduction potential is an important question to probe. Two arguments can be put forth to account for the behavior observed. It is conceivable that the Co(II) porphyrin can stabilize the reduction of oxygen to superoxide. The potential for the reduction of oxygen would be governed by the extent of superoxide stabilization. The feasibility of this argument will be further examined in Chapter 5 in the discussion of the non-aqueous chemistry of O_2 and $O_2^{\cdot-}$ reacting with a Co(II) complex. A second argument can be offered that the Co-O_2 adduct (i.e., the small quantity as dictated by the low equilibrium constant) is not reducible at the positive potentials at which Co(III) can be reduced. A possible qualitative rationalization for this second possibility is discussed below.

Molecular orbital and theoretical descriptions of dioxygen binding to low spin cobalt(II) complexes have been considered.[25-28] Regardless of the method utilized, the qualitative schemes embody predominantly the interaction of the d_{z2} orbital of Co(II) with the Π^* orbitals

of oxygen. A simplified interaction diagram is shown in Scheme III.

Scheme III

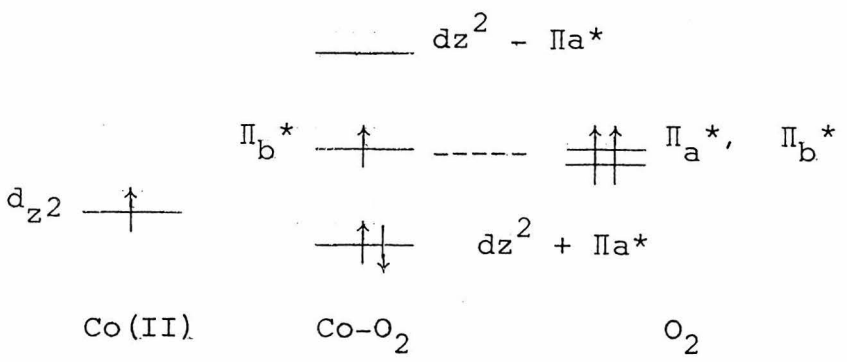

This MO scheme for the Co-O_2 adduct suggests that a single unpaired electron resides in an orbital which is predominantly based on oxygen and is of non-bonding character relative to cobalt and oxygen. The electronic structure of this adduct might be expected to be very similar for the various porphyrins under study. In the absence of a strong ligand field, the interaction of the d_{z2} orbital on cobalt and the Π^* orbitals on oxygen may be such that Co(III) is easier to reduce than the resultant adduct formed upon reduction. The magnitude of the Co(III/II) potential would not be expected to have a large effect on the reduction potential of the adduct if this explanation is correct. The conditions of these experiments provide weak ligand fields for the cobalt complex. The data for the variety of porphyrins examined in this study support the above rationalizations, but unambiguous

proof has not been obtained for such a scheme. It is obvious that other metal complexes will exhibit very different electronic structures and consequently different catalytic patterns than for cobalt porphyrins.

SUMMARY AND CONCLUSIONS

The mechanism of the catalysis of the electroreduction of dioxygen has been examined for a variety of cobalt porphyrins. All monomeric catalysts converted dioxygen to hydrogen peroxide. The mechanism appeared to be the same for all species. In this mechanism, the reduction of Co(III) occurred positive of the catalytic potential. The reversibility of the O_2/H_2O_2 response was found to be sensitive to the pH of the electrolyte. At pH 14, the response is nernstian and occurs at the reversible thermodynamic potential. The rate determining step has been attributed to the binding of dioxygen to cobalt (II).

REFERENCES AND NOTES

1. J. P. Collman, M. Marrocco, P. Denisevich, C. Koval, and F. C. Anson, J. Electroanal. Chem., 101, 117 (1979).

2. J. P. Collman, P. Denisevich, Y. Konai, M. Marrocco, C. Koval, and F. C. Anson, J. Am. Chem. Soc., 103, 6027 (1980).

3. J. P. Collman, F. C. Anson, S. Benscome, A. Chong, T. Collins, P. Denisevich, E. Evett, T. Geiger, J. Ibers, G. Jameson, Y. Konai, C. Koval, K. Meier, R. Oakley, R. Reitman, E. Schmitton, J. Sessler, in "Organic Synthesis Today and Tomorrow," B. M. Trost and C. R. Hutchinson, eds., Pergamon Press, New York, 1981.

4. N. Kobayashi, M. Fujihira, T. Osa, and T. Kuwana, Bull. Chem. Soc. Jpn., 53, 2195 (1980).

5. N. Oyama and F. C. Anson, Anal. Chem., 52, 1192 (1980).

6. E. Lauiron, Bull. Soc. Chem. Fr., 3717 (1967).

7. A. P. Brown and F. C. Anson, Anal. Chem., 49, 1589 (1977).

8. J. Manassen, Isr. J. Chem., 12, 1059 (1974).

9. L. A. Truxillo and D. G. Davis, Anal. Chem., 47, 2260 (1975).

10. W. M. Latimer, "Oxidation Potentials," Prentice-Hall, New York, N.Y. (1952).

REFERENCES AND NOTES

11. V. S. Bagotzky and I. E. Jablokowa, J. Phys. Chem. USSR, 27, 1665 (1953).

12. J. Koryta, Coll. Czech. Chem. Comm., 18, 206 (1953).

13. P. Waldmeier and H. Sigel, Chimia, 24, 195 (1970)

14. P. Waldmeier and H. Siegel, Inorg. Chim. Acta, 5, 659 (1971).

15. V. G. Levich, "Physicochemical Hydrodynamics," Prentice-Hall, Englewood Cliffs, N. J. (1962).

16. J. Koutecky and V. G. Levich, Zh. Fiz. Khim., 32, 1565 (1956).

17. R. D. Jones, D. A. Summerville, and F. Basolo, Chem. Rev., 79, 139 (1979).

18. T. Geiger and F. C. Anson, J. Am. Chem. Soc., 103, 7489 (1981).

19. R. G. Wilkins, Adv. Chem. Ser., 100, 111 (1971).

20. D. Jahn and W. Vielstick, J. Electrochem. Soc., 109, 849 (1962).

21. P. Worthington, P. Hambright, R. F. X. Williams, J. Reid, C. Burnham, A. Shamin, J. Turay, D. M. Bell, R. Kirkland, R. G. Little, N. Datta-Gupta, and V. Eisner, J. Inorg. Biochem., 12, 281 (1980).

22. A. Bettelheim, R. J. H. Chan, and T. Kuwana, J. Electroanal. Chem., 99, 291 (1979).

23. N. Kobayashi, T. Matsue, M. Fujihira, and T. Osa, J. Electroanal. Chem., 103, 427 (1979).

24. J. Zagal, R. K. Ser, and E. Yeager, J. Electroanal. Chem., 83, 207 (1977).

25. R. S. Drago and B. B. Corden, Acc. Chem. Res., 13, 353 (1980) and references cited therein.

26. W. A. Goddard III and B. D. Olafson, Proc. Natl. Acad. Sci. USA, 72, 2335 (1975).

27. A. Dedieu, M. M. Rohmer, and A. Veillard, J. Am. Chem. Soc., 98, 5789 (1976).

28. P. Fantucci and V. Valenti, J. Am. Chem. Soc., 98, 3832 (1976).

Chapter 3

Mechanistic Aspects of the Catalytic Reduction of Dioxygen by Cofacial Metalloporphyrins

INTRODUCTION

In previous accounts of the unusual catalytic potency of several dicobalt cofacial porphyrin molecules for the electro-reduction of dioxygen to water, [1-3] the catalytic mechanism was surmised on the basis of limited experimental data. In particular, the reduction and oxidation of the catalysts themselves in the absence of O_2 were difficult to observe above the background response from the surface of the pyrolytic graphite electrode on which they were adsorbed. The effects of changes in the proton concentration on the catalysis were also examined only cursorily although it was shown that the course of the reduction was substantially different at electrodes deprived of protons.[1-3]

Conditions have been found that permit the electrochemical responses of the adsorbed catalysts to be observed clearly and reproducibly both in the absence and in the presence of O_2 and over a wide pH range. The rate constant for the first step in the catalytic reaction has been measured and the effect of pH on the distribution of reduction products between H_2O_2 and H_2O has been determined. The catalytic activities of dicobalt cofacial porphyrins with six, five, four and three atoms in the amide bridges have been compared and the behavior of several new heterobinuclear cofacial porphyrins (Figure 1) has been examined. The results obtained have provided new insight into the mechanisms employed by these catalysts in reducing dioxygen.

EXPERIMENTAL

Materials. The detailed synthetic procedures employed to obtain the metalloporphyrin molecules utilized in this study are described elsewhere.[4] Figure 1 lists the porphyrins employed and the abbreviations used to identify them. Pyrolytic graphite electrodes were obtained and mounted as previously described (Chapter 2). Reagent grade chemicals and solvents were used as received. The electrodes were mounted to expose the edges rather than the basal planes of the pyrolytic graphite. Such edge plane electrodes cannot be cleaved to renew the electrode surface so their surfaces were prepared by polishing with 600 grade SiC paper (3M Co.).

Procedures. Pyrolytic graphite electrodes were coated with porphyrin catalysts by syringing small volumes of stock solutions in dichloroethane onto the electrode surface and allowing the solvent to evaporate. Coulometric assays of the resulting coatings performed by measuring the areas under cyclic voltammograms recorded in the absence of dioxygen showed that they typically contained 2 to 4 x 10^{-10} mole which corresponds to a few close-packed monolayers on a smooth surface or to a single monolayer on a graphite surface with a roughness factor of two to three. This quantity of adsorbed electractive catalyst was reproducibly obtained whether or not larger excesses of catalysts were applied to the electrode surface in the adsorption step.

Conventional cyclic and rotating disk voltammetry were carried out with the previously described apparatus and procedures. For cyclic voltammetry at scan rates above 1 volt s^{-1}, a digital oscilloscope (Tektronix Model 5223) was employed to acquire the voltammetric data which were subsequently read out with an x-y recorder for precise measurements of peak potentials and currents. Potentials were measured and are quoted with respect to a saturated calomel reference electrode (SCE).

RESULTS

Behavior of Co_2 FTF4 in Acidic Electrolytes. The most impressive catalysis of the reduction of dioxygen is achieved by the dicobalt cofacial porphyrin in which four atoms comprise the two bridging groups that link the porphyrin rings, Co_2FTF4, (Figure 1). Therefore, most of the attention has been concentrated on the behavior of this molecule. The pair of prominent cyclic voltammetric waves exhibited by this catalyst when it is adsorbed on a pyrolytic graphite electrode and examined in the absence of O_2 are shown in Figure 2. The wave appearing near 0.6 volt is easily distinguished from the background current but the wave near 0.3 volt falls close to that of a component of the background response (dashed curve in Figure 2) believed to arise from the presence of reducible quinone-like functional groups on the graphite surface. The position of

Figure 1. Molecular structures and abbreviations for the metalloporphyrins examined in this study.

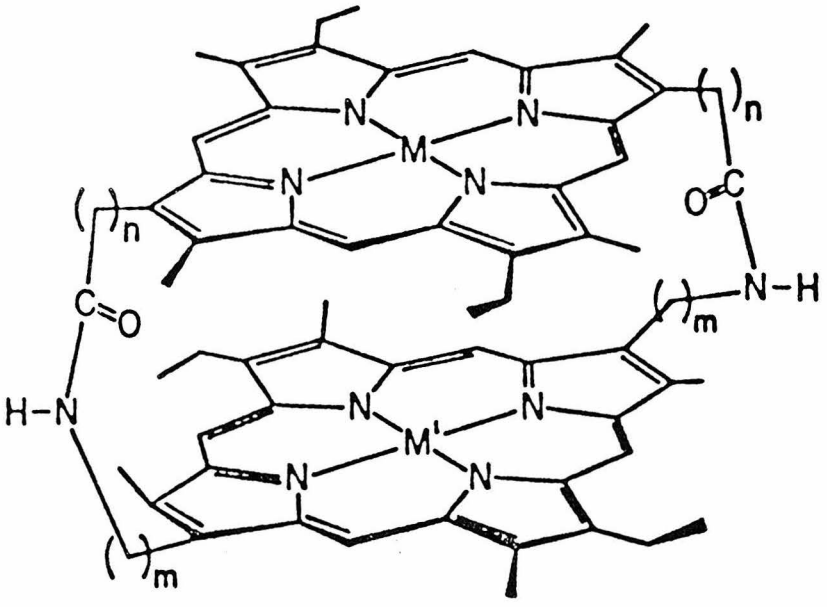

M	M′	n	m	Abbreviation
Co	Co	2	2	Co_2FTF6
Co	Co	1	2	Co_2FTF5
Co	Co	1	1	Co_2FTF4
Co	Co	0	2	Co_2FTF4^*
Co	Co	0	1	Co_2FTF3
Co	2H	1	1	CoH_2FTF4
Co	Fe	1	1	CoFeFTF4
Co	Mn	1	1	CoMnFTF4
Co	Ag	1	1	CoAgFTF4
Co	Al	1	1	CoAlFTF4
Ag	Ag	1	1	Ag_2FTF4

Figure 2. Cyclic voltammogram of Co_2FTF4 adsorbed on an edge-plane pyrolytic graphite electrode in the absence of O_2. Supporting electrolyte: 1 M CF_3COOH saturated with argon. Scan rate: 0.1 volt s^{-1}. The dashed line is the background response of the pyrolytic graphite before the porphyrin was adsorbed.

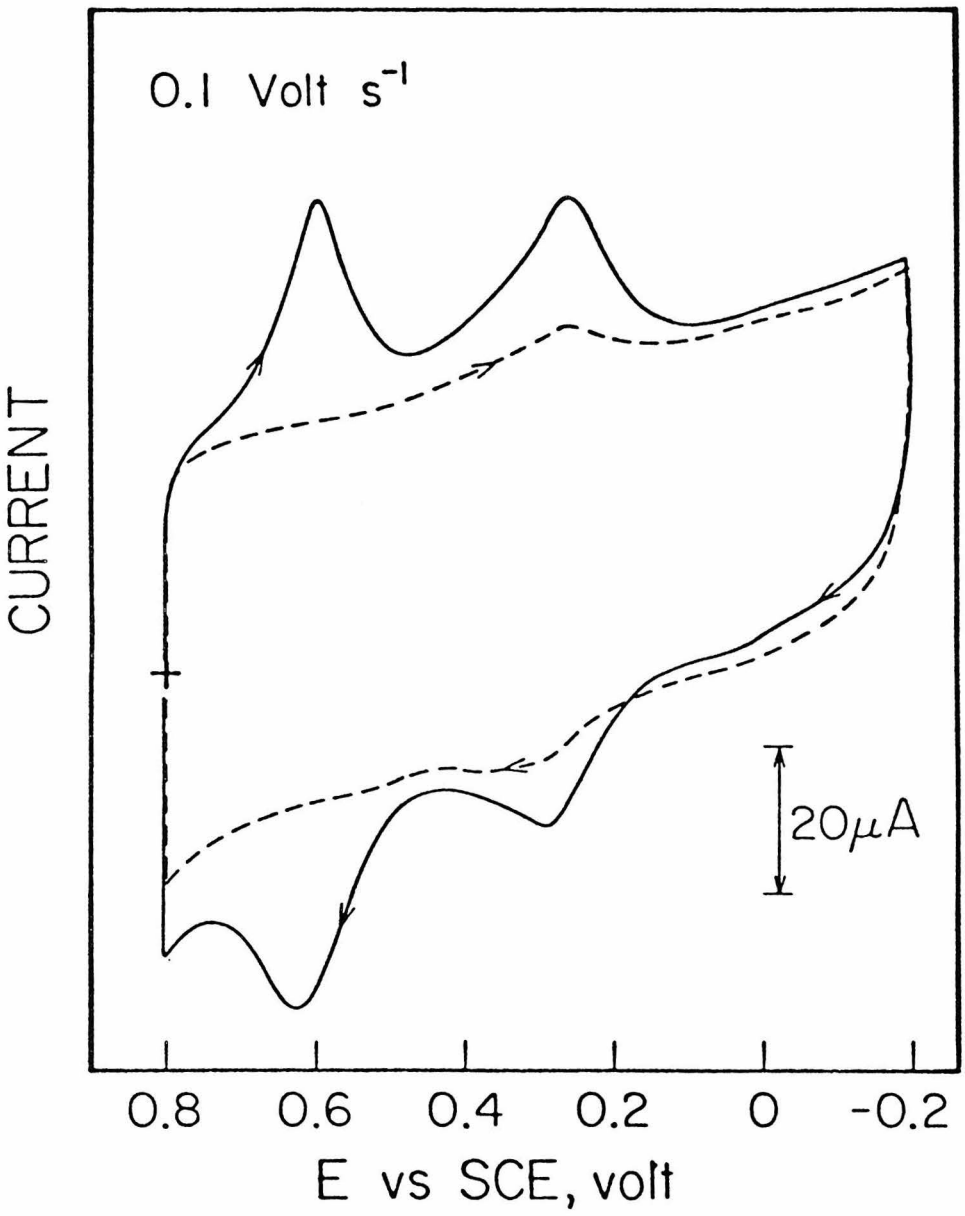
0.1 Volt s⁻¹
CURRENT
20μA
0.8
0.6
0.4
0.2
0
-0.2
E vs SCE, volt

the latter wave depends upon pH while the catalyst waves show no pH dependence below pH 6. This feature permits the background wave to be shifted away from the catalyst waves so that the formal potentials corresponding to both waves of the adsorbed catalyst can be measured under conditions where the background reactions do not interfere. The resulting values are E^f = 0.62 and 0.27 volt.

The shapes of the waves for the reduction of the adsorbed complex resemble those expected for a one-electron, surface-confined couple that exhibits small deviations from the Nernst equation. For example, Figure 3 shows how the experimental wave differs from that calculated from the Nernst equation for the same peak potential and quantity of adsorbed reactant. A reasonable fit of the experimental curves results if a non-ideality parameter is introduced into the Nernst equation[5] as shown by the solid points in Figure 3. This non-ideal behavior arises from the fact that the surfaces activities of adsorbed reactants may differ from the surface concentrations. There may be repulsive or attractive interactions between molecules which are manifested in the shape of the voltammetric response. The non-ideality parameter can be extracted from an analysis of the voltammetric wave shape. For the Co_2FTF4 complex adsorbed to graphite, a parameter was obtained which suggests deviation from nernstian behavior due to repulsive interactions.

Figure 3. Comparison of the background corrected voltammetric wave of Co_2FTF4 at +0.27 V (solid line) with the calculated nernstian response (dashed line). The solid points represent the calculated response when a non-ideality parameter is introduced into the Nernst equation as described in reference (5). The best fit resulted with $r\Gamma_T = -0.7$.[5]

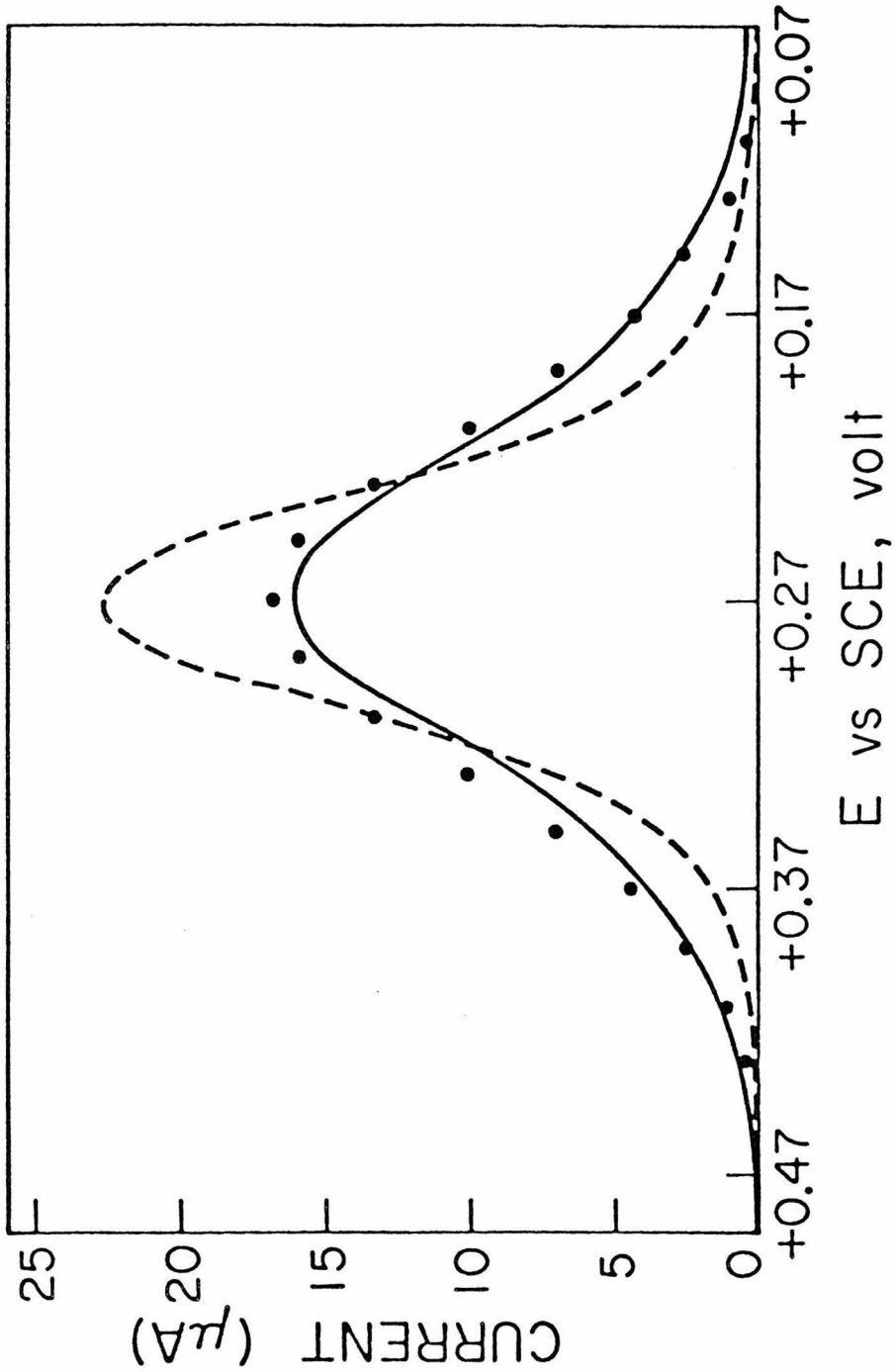
CURRENT (μA)
25
20
15
10
5
0
+0.47
+0.37
+0.27
+0.17
+0.07
E vs SCE, volt

The presence of two waves for the adsorbed Co_2FTF4 molecule is expected on the basis of its cyclic voltammetry in non-aqueous solution where two waves are also obtained.[6] Both waves result from the reduction of the virtually identical cobalt(III) centers to cobalt(II). The reductions appear at different potentials because of the repulsive interactions between the cobalt centers that are held in close proximity (~4Å) by the structure of the ligand. The splitting of cyclic voltammetric waves by such intramolecular interactions in reactant molecules has been discussed in several previous studies.[7-9]

The peak potentials of the waves in Figure 2 are shifted only slightly when the scan rate is increased to 100 volt s^{-1} showing that the catalyst can be reduced and re-oxidized rapidly at potentials close to its formal potential.

Catalyzed Reduction of O_2 in Acidic Electrolytes. The reduction of dioxygen at an electrode surface on which Co_2FTF4 is adsorbed is shown in the cyclic voltammogram in Figure 4. The first reduction peak for the adsorbed catalyst can be seen followed by the large current resulting from the catalyzed reduction of O_2. The peak potential for the reduction of O_2 (0.42 volt) is near the foot of the second reduction wave for the catalyst with a peak potential of 0.27 volt (Figure 2). This indicates, as proposed previously on the basis of less well-resolved

Figure 4. Cyclic voltammogram for the reduction of O_2 at a graphite electrode on which Co_2FTF4 is adsorbed. Supporting electrolyte: 1 M CF_3COOH saturated with O_2. Scan rate: 0.1 V s^{-1}.

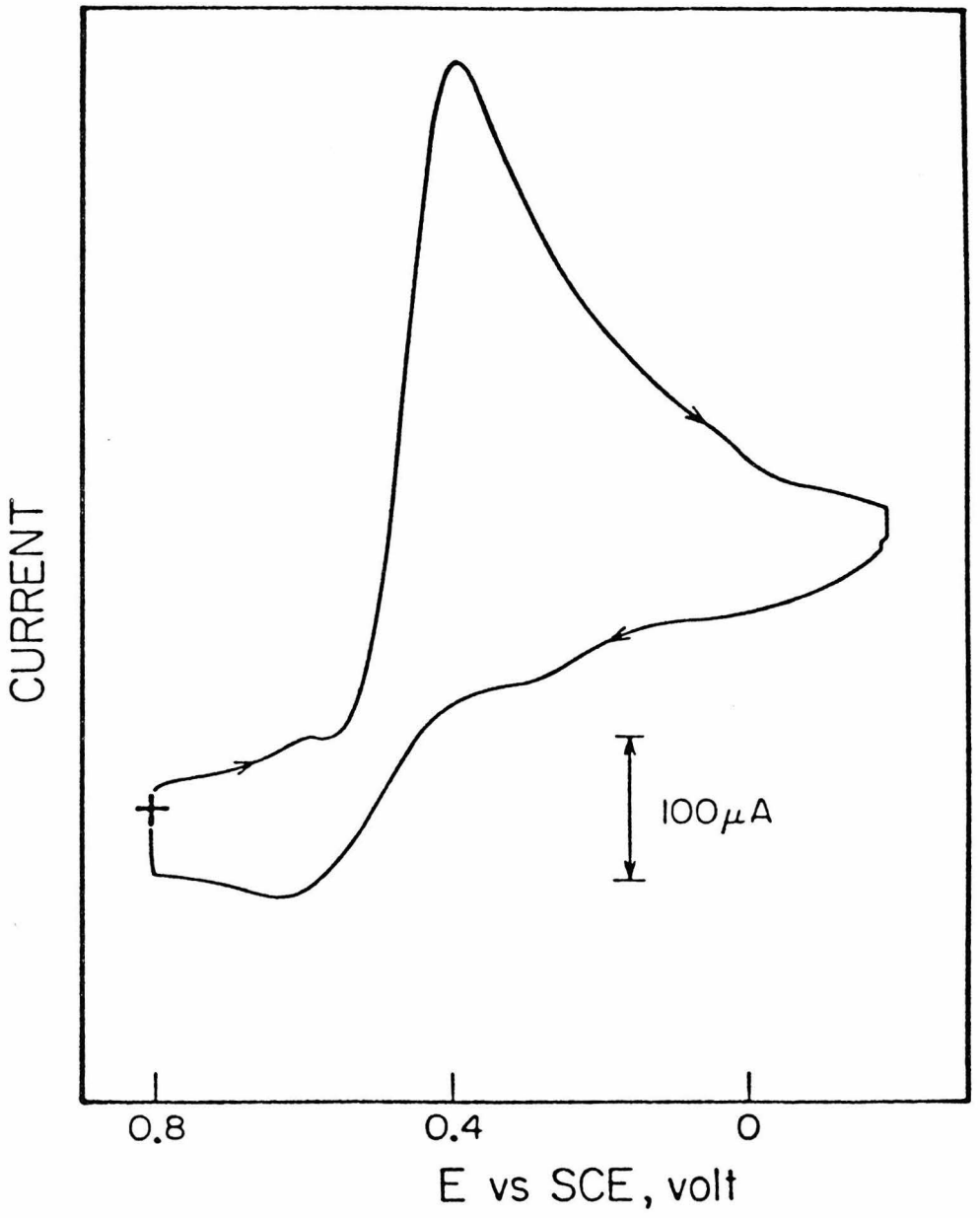
CURRENT
100μA
0.8
0.4
0
E vs SCE, volt

voltammograms,[1-3] that reduction of the second cobalt center in the adsorbed catalyst to cobalt(II) produces the dicobalt(II) species that is active towards the reduction of dioxygen. It should be noted that the first reduction peak was not affected by the presence of O_2. This suggests that the binding constant of O_2 to the first reduced cobalt site is very low. For all complexes examined here, except the Co_2FTF4*, there was no effect of O_2 on the first voltammetric peak. For Co_2FTF4*, there was a large shift, suggesting distinctly different equilibrium binding characteristics. The origin of this change for Co_2FTF4* has not yet been established.

The effect of changes in the proton concentration on the reduction of dioxygen was investigated at a rotating disk electrode coated with Co_2FTF4. At low rotation rates (~100 rpm) the limiting disk currents obey the Levich equation,[10] and the half-wave potentials depend on the pH of the supporting electrolyte in the way shown in Table 1. Between pH 0 and 3 the half-wave potential shifts by about 60 mV per pH unit even though the peak potential for the reduction of the adsorbed catalyst shows no pH dependence in this range. The sensitivity of the catalyzed reduction to the proton concentration must arise from a step in the catalytic cycle subsequent to the reduction of the catalyst.

The magnitudes of the Levich currents[9] for dioxygen reduction show a small decrease between pH 0 and 3 but remain close to the value expected for a four-electron reduction (Table 1). At higher pH values the Levich current decreases towards the value corresponding to a two-electron reduction from which it may be concluded that the dioxygen is being reduced to a mixture of hydrogen peroxide and water. Tests showed that Co_2FTF4 is not a catalyst for the reduction or the disproportionation of hydrogen peroxide so that these Levich currents indicate that direct reaction pathways for both two- and four-electron reductions of O_2 must be accessible.

Behavior of Co_2FTF4 at High pH. When a catalyst-coated electrode that yields voltammograms such as those in Figure 2 is transferred to a dioxygen-free solution at pH 14, the voltammogram shown in Figure 5A is obtained. The pair of waves observed at low pH is replaced by a single wave at a much more negative potential. The area under the single wave is no greater than that under either of the waves in Figure 2 and the single wave does not have the narrower width expected for a two-electron nernstian process.[5] Thus, it does not appear that the waves present in acidic media have merged to form the single wave at pH 14. The diminished response is not the result of loss of catalyst from the surface because both of the original

Figure 5. Cyclic voltammograms of Co_2FTF4 adsorbed on graphite. Supporting electrolyte: 1 M NaOH saturated with argon. Scan rates: (A) 1, (B) 10, (C) 20, (D) 100 volt s^{-1}. The dashed curves show the result of reversing the direction of potential scan before the second reduction peak is traversed.

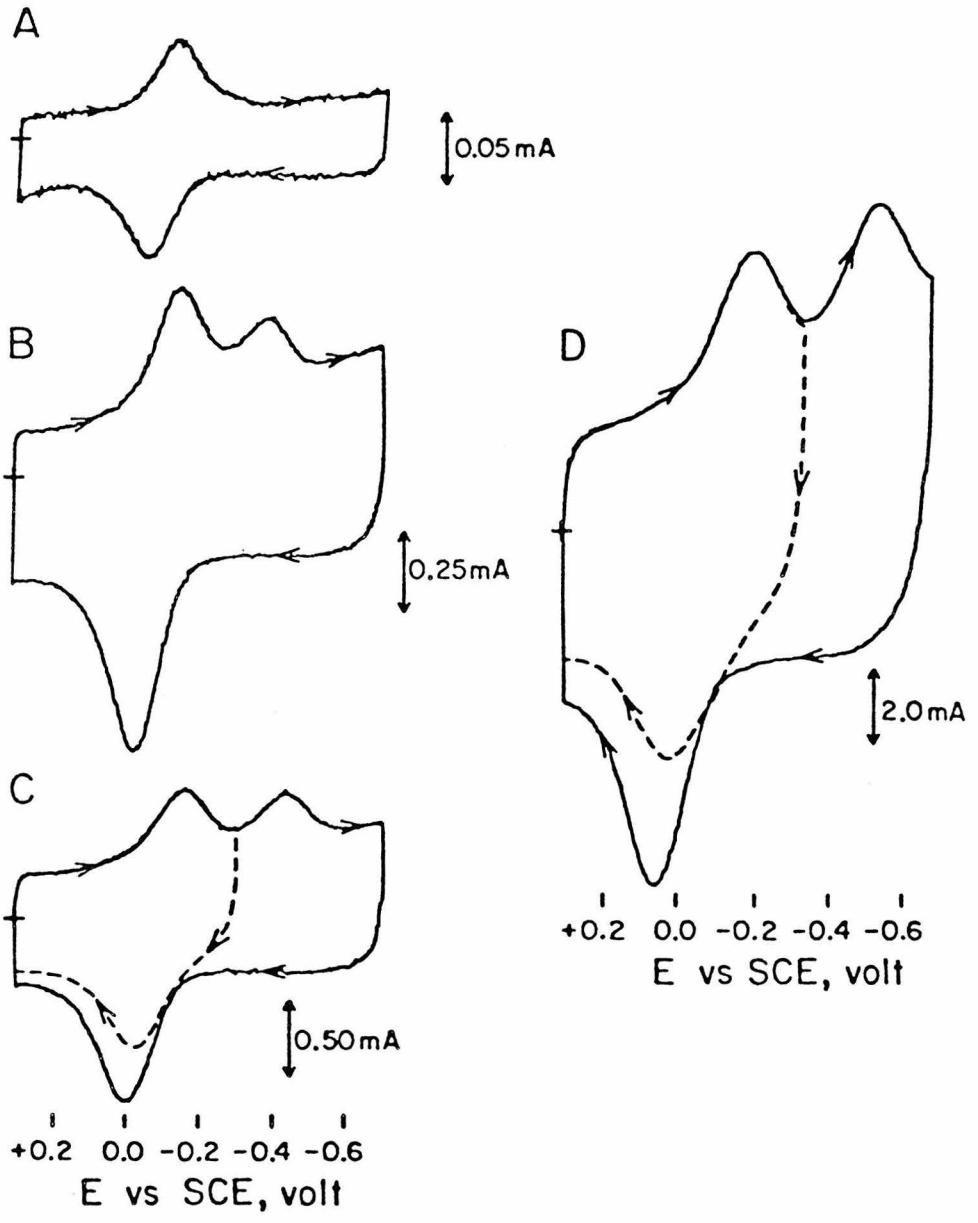
A
0.05 mA
B
0.25 mA
C
0.50 mA
D
2.0 mA
+0.2 0.0 -0.2 -0.4 -0.6
E vs SCE, volt
+0.2 0.0 -0.2 -0.4 -0.6
E vs SCE, volt

waves reappear with the same magnitudes if the electrode is returned to acidic supporting electrolytes.

The single reduction wave shown in Figure 5A develops a satellite wave at scan rates above ca. 1 volt s^{-1} that grows at the expense of the original wave as the scan rate increases (Figure 5B, C, D). However, only a single oxidation wave is present under the same conditions and its magnitude is influenced by both of the reduction waves when two are present (Figure 5, curves C and D). Increasing the solution temperature to 80°C eliminates the satellite wave while decreasing the temperature to 5°C causes the satellite wave to appear at lower scan rates. Decreasing the pH from 14 to 12 (at 25°C) diminishes the magnitude of the satellite wave. Once the peak currents of the satellite wave and the original wave become about equal their relative magnitudes are insensitive to further increases in scan rate.

A less prominent satellite wave develops at high scan rates when the Co_2FTF5 catalyst, with five atoms in the struts separating the porphyrin rings, is substituted for Co_2FTF4. With Co_2FTF6, with six atoms in the bridges, no satellite wave is observed at scan rates up to 100 volt s^{-1}. The same is true for both Co_2FTF3, with three atoms in the bridges, and the monomeric cobalt porphyrin I (Figure 1). Co_2FTF4*, in which the four atoms in the bridges have been rearranged so that the carbonyl group of amide linkage is

directly attached to one porphyrin ring, gives voltammograms in which the satellite wave appears at scan rates as low as $0.1\ V\ s^{-1}$.

To account for the behavior of the adsorbed Co_2FTF4 catalyst at high pH, we suggest equilibria such as those depicted in Scheme I in which μ-oxo and μ-hydroxo bridges are assumed to form within the cavity of the catalyst. In writing Scheme I we have assumed that the cofacial porphyrin molecules adsorb on the electrode because of strong interactions between one of the porphyrin rings and the graphite surface. We have no direct evidence for the orientation of the adsorbed molecules but the maximum obtainable coverages are consistent with a monolayer of porphyrin rings adsorbed in a flat orientation and it is known that flat molecules with aromatic centers show high affinities for graphite surfaces.[11,12] This implies that the axial ligand site on the cobalt ion in the adsorbing ring may be inaccessible to ligands other than those that are present on the graphite itself.[13] The lower ring in the molecules shown in Scheme I is assumed to be bound to the electrode surface.

If the oxo- and hydroxo-bridged dicobalt(III) complexes in Scheme I were reduced at different potentials the double waves in Figure 5 could be understood. As the distance separating the two cobalt centers increased, such bridging would become less likely and this could account for the

Scheme I

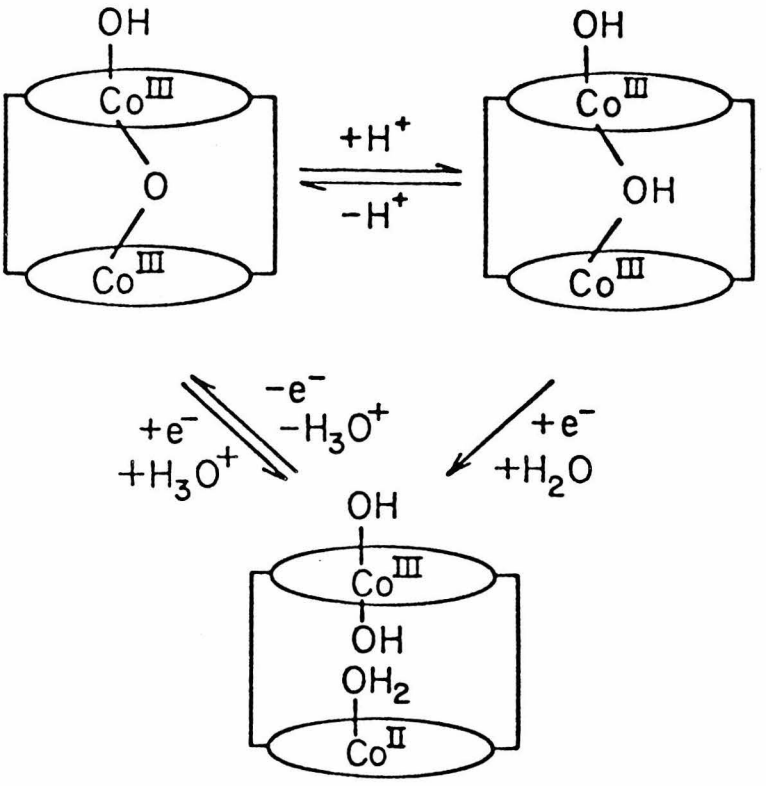
OH
Co^III
O
Co^III
+H+
-H+
OH
Co^III
OH
Co^III
-e-
-H3O+
+e-
+H3O+
+e-
+H2O
OH
Co^III
OH
OH2
Co^II

decrease in the magnitude of the satellite wave with Co_2FTF5 and its disappearance with Co_2FTF6. The relative magnitudes of the waves for the reduction of the μ-oxo and μ-hydroxo species would depend on the rate with which these two forms could be interconverted.

The lack of the satellite peak in the voltammograms of Co_2FTF3 could reflect the absence of intercavity bridging when the separation of the cobalt centers becomes too small. The appearance of the satellite peak at lower scan rates with Co_2FTF4* than with Co_2FTF4 might be the result of a somewhat smaller separation between the cobalt centers in Co_2FTF4* arising from conjugation of the carbonyl groups in the amide bonds with the porphyrin rings. One result might be a somewhat smaller ring-to-ring separation in Co_2FTF4* than in Co_2FTF4. The rate of interconversion between the two bridged complexes proposed in Scheme I might also be altered and this could account for the appearance of the satellite peak at lower scan rates with Co_2FTF4* than Co_2FTF4.

At sufficiently high potential scan rates the magnitudes of the peak currents for the two waves in Figure 5 should become independent of scan rate and provide a measure of the equilibrium concentration of each form of the complexes. These predictions are in qualitative accord with the behavior shown in Figure 5, although quantitative features, such as the relative magnitudes of the two peak

currents at pH 12 and 14, are not. The origin of this discrepancy remains uncertain.

The cobalt(III) center in the half-reduced form of the catalyst shown in Scheme I is proposed to be converted to a dihydroxo complex. If the reduction of this species were kinetically much slower or had a formal potential that lay at inaccessibly negative values, the lack of a second catalyst reduction wave would be explained. Previously we have observed that the reduction wave of the adsorbed monomeric cobalt porphyrin, I, remains clear and undiminished at pH 14 (Chapter 2). This is the anticipated result if the formation of the trans-dihydroxo form of the monomer were blocked by its adsorption on the electrode surface similar to the lower rings in the dimeric porphyrins of Scheme I.

There is only one form of the half-reduced catalyst in Scheme I so that only one oxidation wave is expected even at scan rates where the reduction wave is split into two parts. This accords with the behavior shown in Figure 5. Scheme I would also predict that the reduction of O_2 would proceed to H_2O_2 instead of H_2O in alkaline media if each end of the O_2 molecule must be coordinated to a cobalt center as the O_2 is reduced in order to avoid the release of H_2O_2. This also corresponds to the observed result (vide infra).

Attempts were made to do non-aqueous electrochemistry of Co_2FTF4 in the presence of OH^-. It was extremely difficult to produce a solvent/electrolyte system free of decomposition problems. Although Scheme I manages to accommodate most of the experimental observations, the mechanistic implications to which it leads are reasonable possibilities, not demonstrated facts.

Catalyzed Reduction of O_2 at High pH. The reduction of dioxygen from pH 14 solutions at electrodes coated with Co_2FTF4 is a reversible process that yields hydrogen peroxide quantitatively. Figure 6 shows a typical cyclic voltammogram. The magnitude of the cathodic peak current matches that calculated from the Randles-Sevcik equation[14] for a two-electron nernstian reduction and the equal magnitude of the anodic wave confirms that hydrogen peroxide is the only reduction product. The response obtained is indistinguishable from that exhibited by the monomeric cobalt porphyrin, I, under the same conditions (Chapter 2). This suggests that at high pH Co_2FTF4 catalyzes the reduction of O_2 by a pathway that does not involve the participation of more than one of the cobalt centers in the catalyst molecule.

The adsorbed catalyst is not permanently altered by exposure to 1 M NaOH because transferring the electrode used to record Figure 6 to an acidic solution saturated with dioxygen produces the same, four-electron reduction

Figure 6. Reduction of O_2 at a graphite electrode on which Co_2FTF4 is adsorbed. Supporting electrolyte: 1 M NaOH saturated with O_2. Scan rate: 0.1 V s^{-1}.

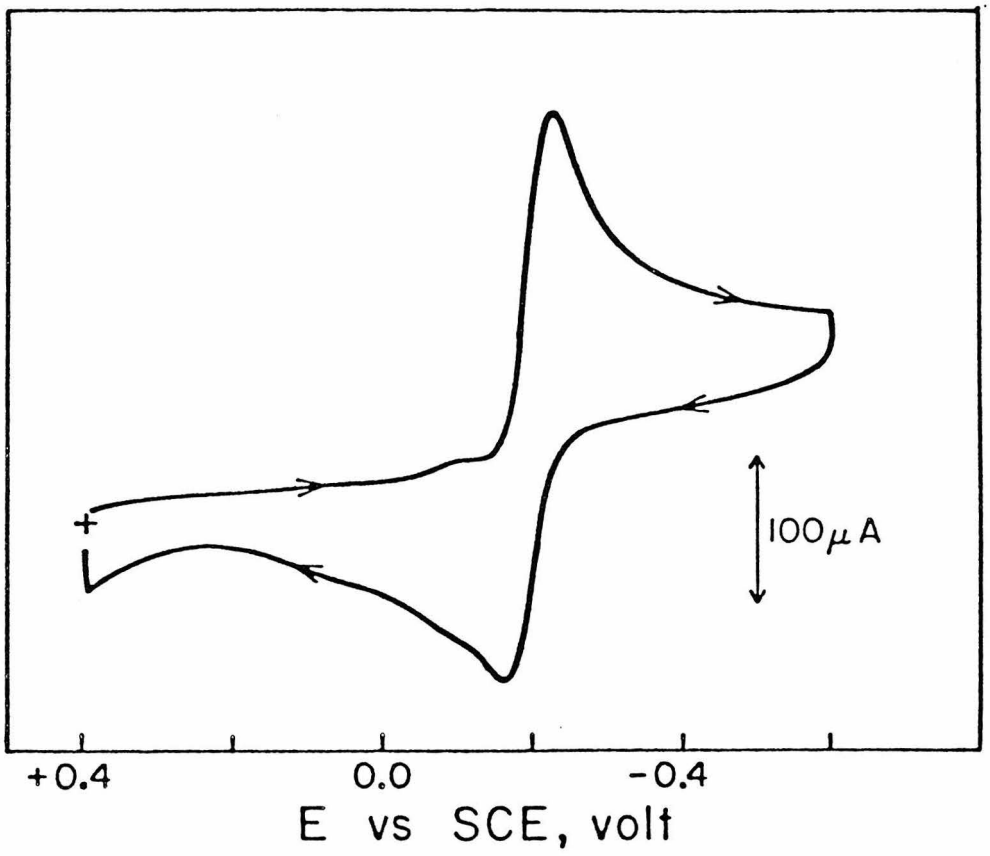
+
100μA
+0.4
0.0
-0.4
E vs SCE, volt

of dioxygen that is obtained in the acidic solution with a freshly coated electrode.

Rotating Disk Voltammetry. In previous reports[1-3] current-potential curves for the reduction of dioxygen at rotating disk electrodes coated with Co_2FTF4 were recorded only in acidic electrolytes. Data for a wider pH range are now available and they reveal a pronounced pH dependence in the responses (Table 1). As noted earlier, at pH 0 and 1 the Levich currents are essentially equal to the current calculated for the four-electron reduction of dioxygen. Above pH 3 the Levich current falls below this value signaling an increase in the formation of hydrogen peroxide. The Levich current at pH 14 is less than half of that at pH 0 because of the decreased solubility of dioxygen in 1 M naOH. When this factor is accounted for, the current at pH 14 matches that expected for the quantitative two-electron reduction of dioxygen to hydrogen peroxide.

In unbuffered solutions between pH 4 and 6 the current potential curve exhibits two waves with relative magnitudes that are affected by the concentration of protons at the electrode surface (Figure 7). At potentials on the first wave the reduction of O_2 proceeds to H_2O as indicated by the absence of ring current in Figure 7. When this process consumes all of the available protons, the pH at the electrode surface increases substantially and the reduction shifts to more negative potentials. The corresponding

Table I

Half-Wave Potentials and Limiting Levich Current Densities for the Reduction of O_2 at Rotating Graphite Disk Electrodes Coated with Co_2FTF4 [a]

pH [b]	$E_{1/2}$, volt vs. SCE	I_{lim} ma cm^{-2}
0	0.47	1.3 [c]
1	0.40	1.3
2	0.33	1.2
3	0.27	1.2
4	0.23, -0.15 [d]	0.9 [d]
7	-0.07	0.9
10.8	-0.17	0.8
14	-0.21	0.55

a. The electrode was rotated at 100 rpm in dioxygen-saturated solutions.

b. Phosphate buffers were used for pH 7 and 10.8. Other solutions were not buffered.

c. The calculated Levich current density for the four-electron reduction of O_2 is 1.3 ma cm^{-2}.

d. Two waves present, see text. The value of I_{lim} is the total plateau current on the second wave.

Figure 7. Disk and ring current vs. disk potential for the reduction of O_2 at a rotating disk electrode coated with Co_2FTF4. Rotation rate: 100 rpm. Supporting electrolyte: 0.1 M CF_3COONa saturated with air and adjusted with CF_3COOH to pH (A) 4.0, (B) 4.5, (C) 5.0. The platinum ring was maintained at +0.85 volt. The values of S for disk and ring currents are 100 and 10 μA, respectively.

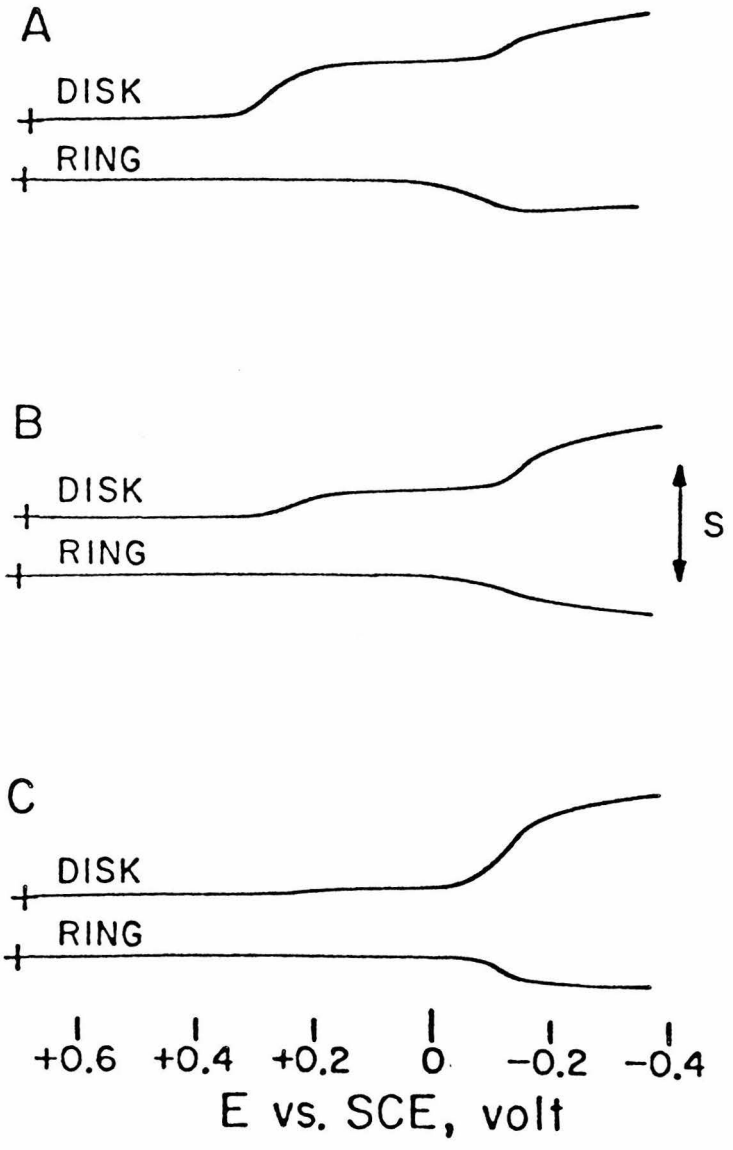
A
DISK
RING
B
DISK
RING
S
C
DISK
RING
+0.6
+0.4
+0.2
0
−0.2
−0.4
E vs. SCE, volt

anodic ring current shows that H_2O_2 is now a significant reduction product.[15] The data in Table 1 indicate clearly that the stoichiometry of the reduction of dioxygen as catalyzed by Co_2FTF4 is influenced strongly by the hydrogen ion concentration.

Between pH 0 and 2 the limiting disk currents at low rotation rates (e.g., $\omega<400$ rpm) increase linearily with $\omega^{1/2}$ which shows that the currents are controlled by the convective transport of O_2 to the electrode surface. The shape of the rising part of the rotating disk current-potential curves recorded under these conditions was analyzed by plotting log $(\frac{I}{I_{lim} - I})$ vs. E. A typical plot, shown in Figure 8, is linear with a slope of 90 mV per decade. To analyze the slopes of such plots it was desirable to compare them with the potential dependence of the quantity of the reduced form of the Co_2FTF4 catalyst on the electrode surface. This was calculated from the solid curve in Figure 3 and is shown in the form of a plot of log $(\frac{\Gamma_{red}}{\Gamma_{tot}})$ vs. E in Figure 8 (Curve B). The slope of the linear portion of the curve that lies in the potential range where the catalyzed reduction of O_2 is observed is ca. 85 mV per decade. The agreement between the two slopes is the expected result if the current is controlled by the quantity of reduced catalyst on the electrode surface. This observation was important in deriving the catalytic mechanism described in the Discussion Section.

Figure 8. Potential dependences of (A) the catalyzed dioxygen reduction current, (B) the concentration of doubly reduced Co_2FTF4 on the electrode surface. Data for line A (left-hand ordinate) were recorded in 1 M CF_3COOH saturated with air at ω = 400 rpm. Curve B (right-hand ordinate) was obtained by measuring the area under the solid curve in Figure 3 up to each potential of interest.

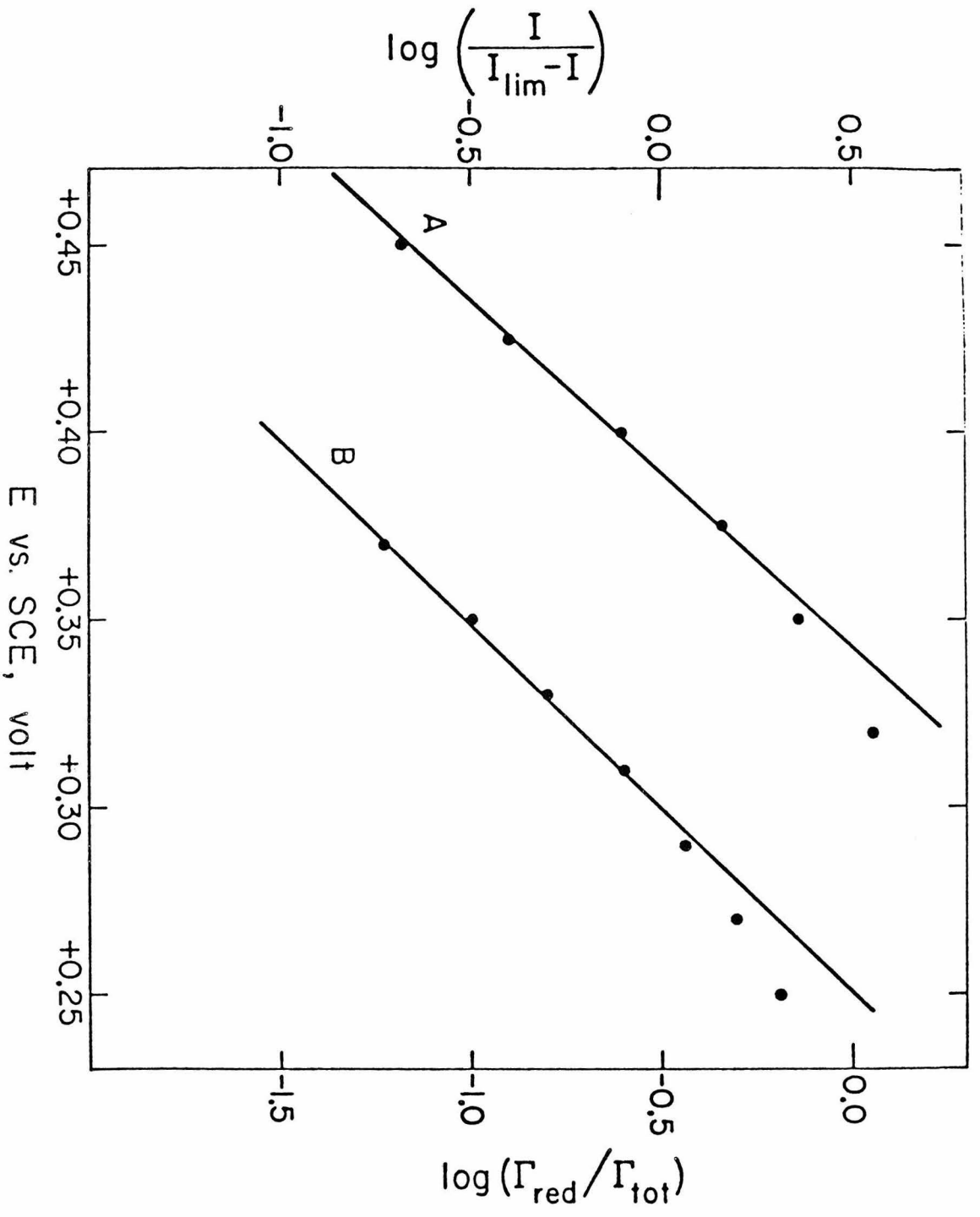
log (I / (I_lim - I))
-1.0
-0.5
0.0
0.5
A
B
+0.45
+0.40
+0.35
+0.30
+0.25
E vs. SCE, volt
-1.5
-1.0
-0.5
0.0
log (Γ_red / Γ_tot)

Levich plots (I_{lim} vs. $\omega^{1/2}$)[10] of the limiting dioxygen reduction current are shown in Figure 9A for a 1 M CF_3COOH solution. The increasing deviations from linearity at higher rotation rates reflect the intervention of a potential-independent chemical step as the current limiting factor. The reaction between the reduced catalyst and dioxygen is the most likely such step[1-3] and its rate may be estimated from the intercepts of Koutecky-Levich plots (I_{lim}^{-1} vs. $\omega^{-1/2}$)[16] such as the two shown in Figure 9B for air- and dioxygen-saturated solutions. The reciprocal of two intercepts of the lines, I_{int}, can be related to the rate constant of the current-limiting reaction, k, via equation 1:[16]

$$I_{int} = nF\ k\ C_{O_2}\ \Gamma_{cat} \qquad (1)$$

where n is the number of electrons consumed in the reduction of dioxygen, i.e., 4, F is the Faraday, C_{O_2} is the concentration of oxygen in the bulk of the solution and Γ_{cat} is the surface concentration of catalyst (assumed to be uniformly accessible to the dioxygen). The chemical reaction that limits the current is assumed to be first order in dioxygen and in catalyst. This was confirmed for dioxygen by noting that the values of I_{int} differ by a factor of 5 in dioxygen- and air-saturated solutions. The rate constants evaluated from the two lines in Figures 9B are 2 X 10^5 and 3 X 10^5 M^{-1} s^{-1}. Using the average of these constants and an estimate of the uncertainty in the

Figure 9. Levich (A) and Koutecky-Levich (B) plots of rotating disk limiting currents in air-(0) and dioxygen-saturated (Δ) 1 M CF_3COOH. The dashed lines represent the calculated responses for the mass transfer-limited, four-electron reductions of dioxygen in air- and dioxygen-saturated solutions.

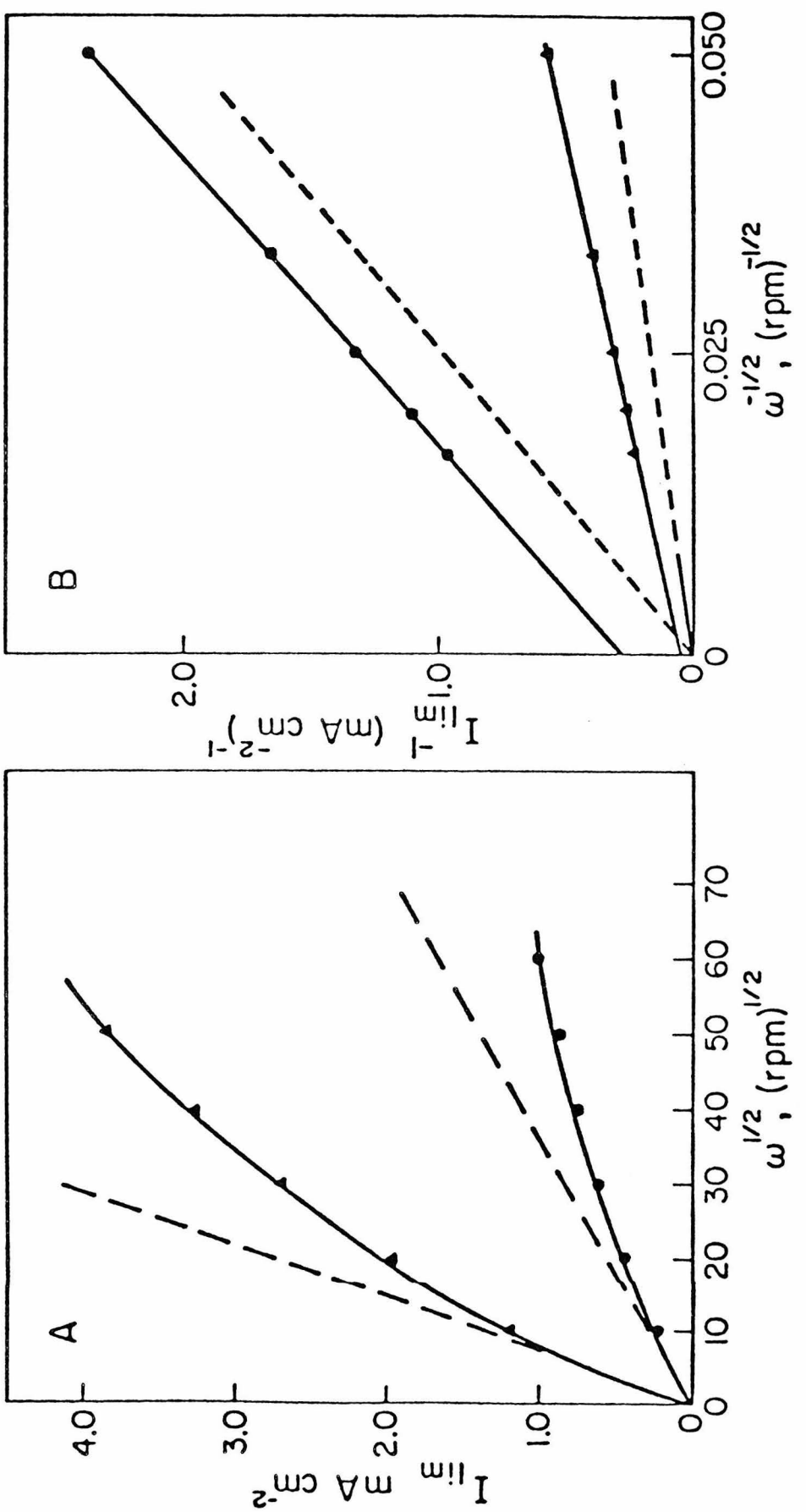
A
B
I_{lim} mA cm^{-2}
I_{lim}^{-1} (mA cm^{-2})$^{-1}$
$\omega^{1/2}$, (rpm)$^{1/2}$
$\omega^{-1/2}$, (rpm)$^{-1/2}$
0
10
20
30
40
50
60
70
1.0
2.0
3.0
4.0
0.025
0.050

measurement of the quantity of catalyst present on the electrode surface, we calculate a catalyst turn-over number of $(4 \pm 2) \times 10^2$ per second in a dioxygen-saturated solution. This number compares very favorably with turn-over numbers that have been estimated for platinum based catalysts[17,18] and is within an order of magnitude of the rates of turn-over achieved by some biological dioxygen reduction catalysts such as cytochrome c oxidase.[19,20]

Related Heterobinuclear Cofacial Porphyrins. In order to compare the catalytic effectiveness of Co_2FTF4 with that obtained if a different metal cation (or two protons) were substituted for one of the two cobalt ions, the behavior of several new binuclear cofacial porphyrins was examined. These included the Co-Fe(II), Co-Mn(III), Co-Al(III), Co-Ag(II) and Co-H_2 complexes. The behavior of the Co-Pd(II) complex was reported in our previous studies.[1-3] Table 2 lists the formal potentials of the cobalt centers in the adsorbed catalysts measured in the absence of dioxygen, the half-wave potential of the catalyzed dioxygen reduction wave for each catalyst at a graphite disk electrode rotated at a low rate and the corresponding limiting reduction (Levich) currents. The responses obtained are clearly quite sensitive to the nature of the second cation in the cofacial complexes which supports the previous contention[1-3] that interactions of both metal centers of the catalyst with the O_2 molecule are

Table II

Electrochemical Responses of Cofacial Metalloporphyrins Towards the Catalysis of the Reduction of Dixoygen [a]

Porphyrin	E_f, [b] V vs. SCE	E'_f, [c] V vs. SCE	$E_{1/2}$, [d] V vs. SCE	I_{lim}, [e] ma cm^{-2}
Co_2FTF4	0.62	0.27	0.47	1.3
CoFeFTF4	0.60	f	0.25, -0.07	0.7, 1.2
CoAlFTF4	f	f	0.22	0.8
CoAgFTF4	0.59	(0.25)	0.38	1.1
CoMnFTF4	f	f	0.23 [g]	0.8 [g]
CoH_2FTF4	0.60	-	0.20	0.8
Co monomer, I	0.54	-	0.20	0.8

a. All data refer to 1 M CF_3COOH supporting electrolyte.

b. Formal potential of the cobalt center in the adsorbed porphyrin. Evaluated from cyclic voltammetric peak potentials recorded under argon at 100 mV s^{-1}.

c. Formal potential of the second metal center (if any).

d. Half-wave potential of the dioxygen reduction wave recorded in dioxygen-saturated solution with a coated disk electrode rotated at 100 rpm.

e. Limiting current density for the reduction of dioxygen at 100 rpm.

f. No clear peak evident above the background current.

g. A more positive $E_{1/2}$ (0.32 V) and a higher current (0.9 mA cm^{-2}) can be obtained by soaking the electrode in basic solution (see text).

involved in determining the course of the catalyzed reduction reaction.

CoFeFTF4. A single redox wave for the $Co^{III/II}$ couple appeared near 0.6 volt with electrodes coated with this catalyst in the absence of dioxygen in 1 M CF_3COOH. This potential corresponds closely to that observed with the monomeric cobalt porphyrin, I, (Chapter 2). By comparison with monomeric iron porphyrins[21] the $Fe^{III/II}$ response would be expected to appear at potentials about 0.5 volt negative of the cobalt response but we were unable to observe a clear wave above the background current. In dioxygen-saturated solutions, electrodes coated with CoFeFTF4 exhibited the two-step reduction shown in Figure 10, curve A. The first step appears at potentials considerably more negative than the potential where the catalyst is reduced. This behavior resembles the response obtained at electrodes coated with monomeric cobalt porphyrins (Chapter 2) where the catalyzed reduction proceeds only to hydrogen perioxide. The second reduction step in Figure 10 appears at about the same potential that adsorbed, monomeric iron porphyrins are active catalysts for the reduction of hydrogen peroxide[21] and the total limiting current on the second plateau is closer to that expected for the four-electron reduction of dioxygen.

When the experiment was repeated with a dioxygen-free solution of hydrogen perioxide, only the second reduction

wave remained with a limiting current corresponding to a two-electron reduction (Figure 10, curve B). Thus, the two metal centers in the CoFeFTF4 catalyst appear to function independently to yield behavior characteristic of monomeric porphyrin catalysts containing the same metal cations. Indeed, an electrode coated with a one-to-one mixture of monomeric cobalt and iron porphyrins produced a current potential curve very similar to that in Figure 10A.

CoMn-, CoAl-, CoPd- and CoH_2FTF4. The behavior of all four of these catalysts is similar and resembles that obtained with the monomeric cobalt porphyrin: Limiting reduction currents at catalyst-coated rotating disk electrodes correspond to the two-electron reduction of dioxygen with half-wave potentials between 0.20 and 0.23 volt vs. SCE (Table 2). Although the identity of the second metal has some influence on the potential where the cobalt center is reduced, these heterobinuclear cofacial porphyrins are catalytically no more effective than the monomeric cobalt porphyrin, I. The corresponding monomeric porphyrin complexes of the second metals show no activity towards the reduction of dioxygen.

As noted in Table 2, if the adsorbed CoMnFTF4 was soaked in an alkaline solution and transferred back to an acidic supporting electrolyte, some changes resulted in the limiting current and half-wave potential. The monomeric

Figure 10. Rotating disk voltammograms at electrodes coated with CoFeFTF4. Supporting electrolyte: 1 M CF_3COOH. (A) Dioxygen-saturated solution; (B) Argon-saturated solution + ~1 mM H_2O_2. Scan rate 0.5 V min^{-1}. Electrode rotation rate: 100 rpm. Potential scanned at 0.5 volt min^{-1}.

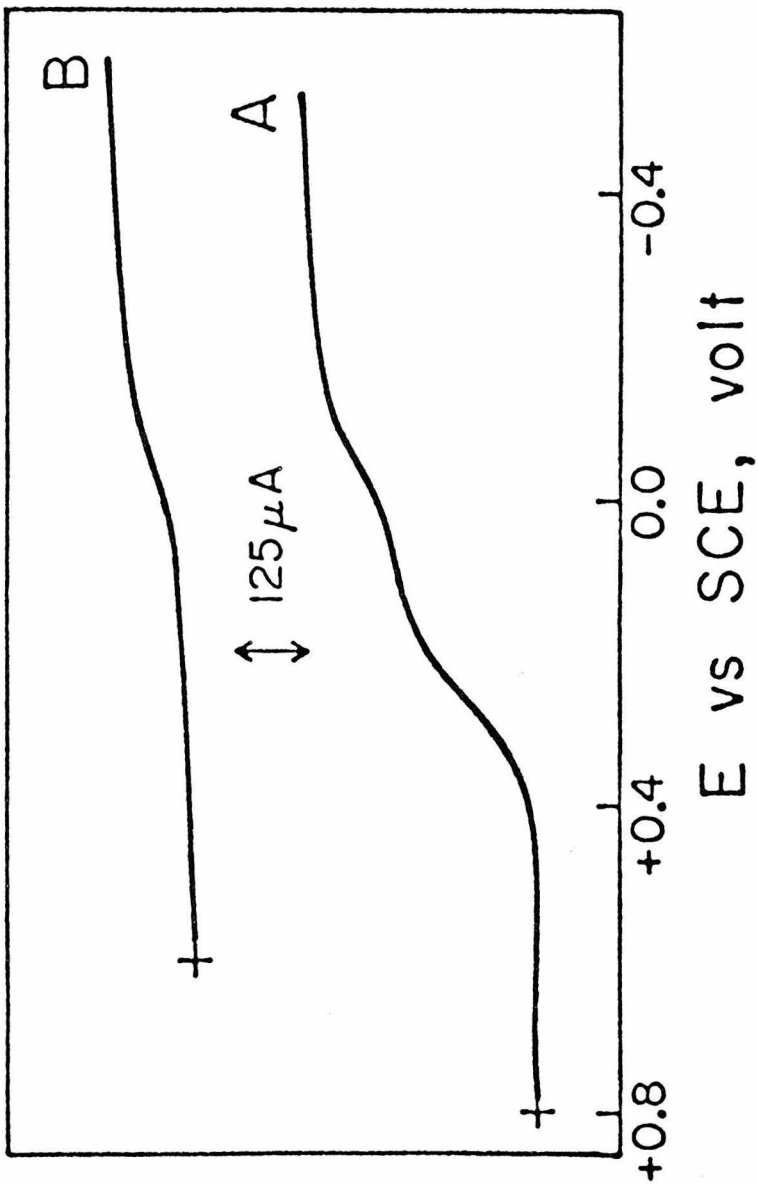
B
A
125μA
+0.8
+0.4
0.0
-0.4
E vs SCE, volt

manganese porphyrin exhibited no changes when subjected to the same treatment. It is possible that axial ligands initially coordinated to the Mn center are removed by exposure to alkaline solutions but the phenomenon was not studied sufficiently to establish its origin.

CoAgFTF4. In contrast to the other heterobinuclear catalysts, the cofacial porphyrin containing cobalt and silver ions shows two reduction waves when inspected under argon (Figure 11A). The more positive wave remains at about the same potential observed with the other porphyrins and seems clearly to arise from the cobalt center. The less positive wave probably originates in the silver center as it appears at a potential typical for the $Ag^{III/II}$ couple in porphyrins.[22] The reduction of dioxygen at a graphite rotating disk electrode coated with CoAgFTF4 is shown in Figure 11B. The reduction proceeds at positive potentials and the limiting currents are well above the value corresponding to a two-electron reduction of dioxygen. The slope of the Koutecky-Levich plot prepared from curves such as those in Figure 11B corresponds to 2.9 electrons suggesting that the reduction proceeds by two parallel pathways, one leading to hydrogen perioxide and the other to water.

Electrodes coated with a monomeric silver porphyrin or the disilver analog, Ag_2FTF4, showed no catalytic activity towards the reduction of dioxygen or hydrogen peroxide.

Figure 11. (A) Cyclic voltammogram of CoAgFTF4 adsorbed on graphite. Supporting electrolyte: 1M CF_3COOH saturated with argon. Scan rate: 0.1 volt s^{-1}. (B) Rotating disk voltammograms for reduction of O_2 at graphite electrodes coated with CoAgFTF4. Supporting electrolyte: 1 M CF_3COOH saturated with air. A new coating of complex was applied before each curve was recorded. Scan rate 0.5 V min^{-1}.

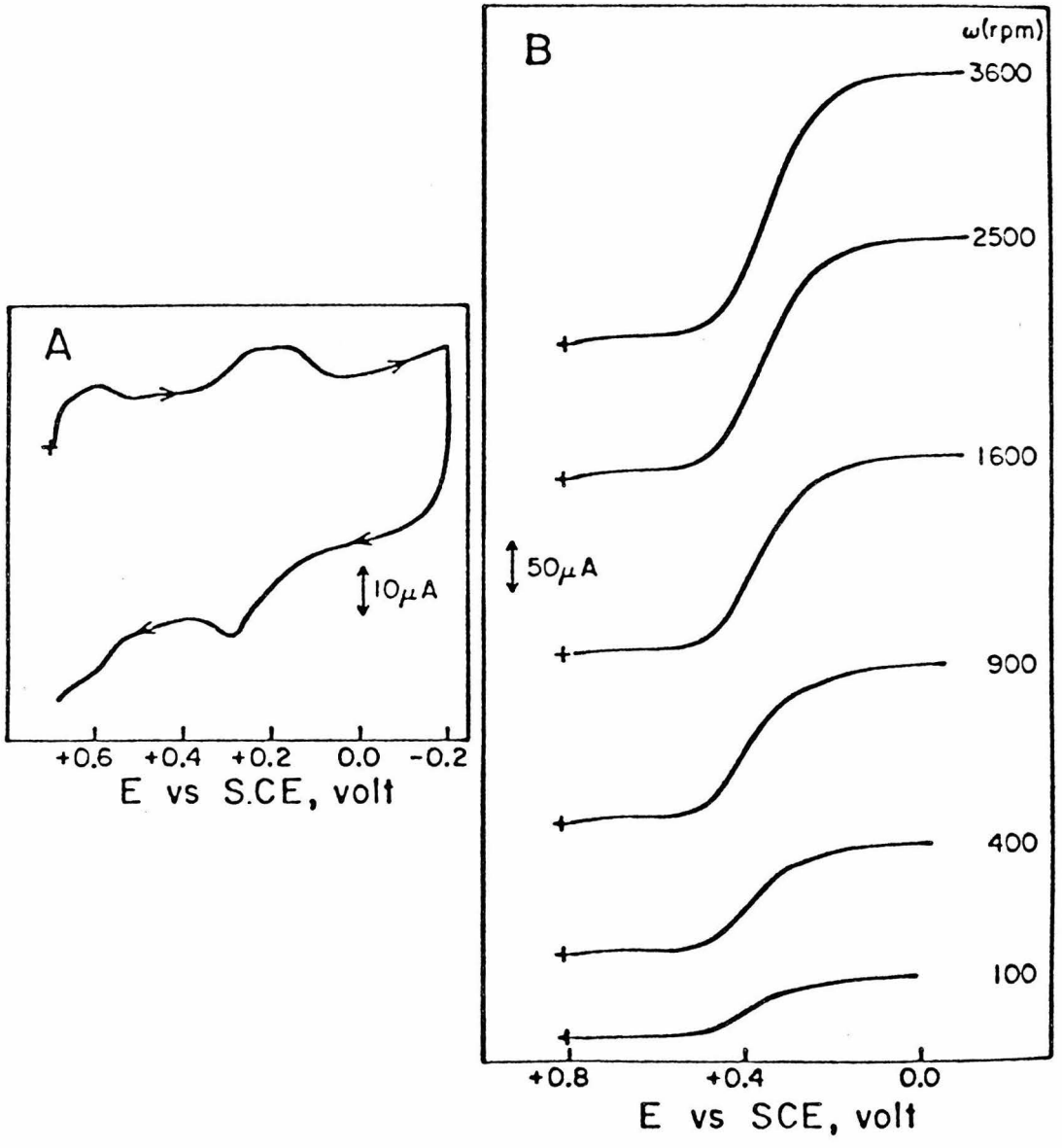
A
10μA
+0.6
+0.4
+0.2
0.0
-0.2
E vs S.CE, volt
B
ω(rpm)
3600
2500
1600
900
400
100
50μA
+0.8
+0.4
0.0
E vs SCE, volt

Adsorption of a mixture of monomeric cobalt and silver porphyrins produced an electrode with a response similar to that obtained from the cobalt monomer alone. The CoAgFTF4 complex resembles Co_2FTF5 in its ability to catalyze the reduction of O_2. It is the most active cofacial porphyrin catalyst we have encountered that does not contain two cobalt centers and the circumstantial evidence points strongly to the participation of both metal centers in generating the enhanced catalytic activity.

Variation in the Length of the Bridging Groups in Dicobalt Cofacial Porphyrins. Dicobalt cofacial porphyrins with three, four, five and six atoms in the bridging groups have now been synthesized and tested as dioxygen reduction catalysts. Table 3 summarizes the results that have been obtained. The optimum separation between the porphyrin rings appears to have been reached with the four-atom bridge as indicated by the less positive value of $E_{1/2}$ and smaller limiting currents obtained for both Co_2FTF3 and Co_2FTF5.

The effect of changing the order of the bridging atoms is clear from the difference in the behavior of Co_2FTF4 and Co_2FTF4*. The magnitude of the limiting O_2 reduction current obtained with Co_2FTF4* points to H_2O_2 as the primary reduction product. The half-wave potential of the catalyzed wave obtained with Co_2FTF4* is more positive than any peroxide-producing catalyst previously encountered.

Table III

Effects of Increasing the Distance Between Porphyrin Rings on Electrochemical Responses of Dicobalt Cofacial Porphyrins [a]

Porphyrin	E_f, V vs. SCE	E_f', V vs. SCE	$E_{1/2}$, V vs. SCE	I_{lim}, ma cm^{-2}
Co_2FTF3	0.64	0.34	0.40	0.8
Co_2FTF4	0.62	0.27	0.47	1.3
Co_2FTF4*	0.64	0.35	0.44	0.8
Co_2FTF5	0.60	b	0.38	1.1
Co_2FTF6	0.59	b	0.32	0.8

a. See Table II for explanation of column headings.

b. Wave not discerned.

Kinetics of the Reaction Between Catalysts and Dioxygen. The rotating disk procedure described earlier for measuring the rate constant governing the reaction of Co_2FTF4 with O_2 was also applied to several additional porphyrins. The results, summarized in Table 4, show that the reaction rate constant does not vary extensively from porphyrin to porphyrin suggesting a common rate limiting step such as the substitution of dioxygen in the inner coordination sphere of cobalt(II).

DISCUSSION

Dicobalt Porphyrins. The catalyst waves shown in Figure 2 are much more clearly defined than was true in our previous reports,[1-3] probably because the samples of Co_2FTF4 used to coat the electrode in the present study were more abundant and more highly purified.[4] The two reversible waves observed in the absence of dioxygen represent the reduction of the dicobalt(III, III) complex successively to the (III, II) and (II, II) states. The absence of a pH dependence of the peak potentials below pH 6 indicates that hydroxy complexes of the oxidized and half-reduced catalyst are not important in this pH range. In proposing a possible mechanism for the catalytic action of Co_2FTF4 in dioxygen reduction several facets of its behavior must be accommodated. These include the relative positions and pH dependences of the waves corresponding to the reduction of the catalyst itself and of dioxygen, the conversion of the

Table IV

Rate Constants for the Reaction of Adsorbed Porphyrins with Dioxygen

Porphyrin	10^{-5} k M^{-1} s^{-1}
Cobalt monomer, I	1.4
Co_2FTF3	1.2
Co_2FTF4	3
CoAgFTF4	2.2
CoAlFTF4 [a]	1.0
CoMnFTF4 [a]	2.0

a. The quantities of these catalysts on coated electrodes were taken to be the same as that measured for Co_2FTF4 becuase the voltammetric responses were not sufficiently well defined for reliable measurements to be made.

dioxygen reduction product from water to hydrogen peroxide as acidic supporting electrolytes are made neutral or alkaline, the shape of the current-potential curve for the catalyzed reduction of dioxygen and the intervention of a potential-independent step in the reaction mechanism when high rates of reaction are demanded by increasing the flux of dioxygen reaching the electrode surface. Scheme II presents a mechanism for acidic electrolytes that accommodates most of these points. As in Scheme I, it is assumed for each molecule shown in Scheme II that the lower porphyrin ring is adsorbed on the graphite surface so that the axial ligand site on the corresponding cobalt center is blocked. For purposes of exposition we have depicted the first step in the catalytic sequence as the formation of an adduct between O_2 and a Co(II) center in which the formal oxidation states of the two reactants do not change. The actual electronic distribution within the adduct could, of course, differ from that depicted.

The reduction of dioxygen is catalyzed by Co_2TFT4 at potentials near the foot of the second reduction wave of the catalyst (Figure 4) whose formal potential is labeled E_2 in Scheme II. The first catalyst wave, at potential E_1, is not altered in position or magnitude by the presence of O_2. This insensitivity of the first wave to O_2 shows that the equilibrium constants for the formation of adducts such as F and G in Scheme II are not large. If

Scheme II

POSSIBLE CATALYTIC CYCLE IN ACIDIC MEDIA

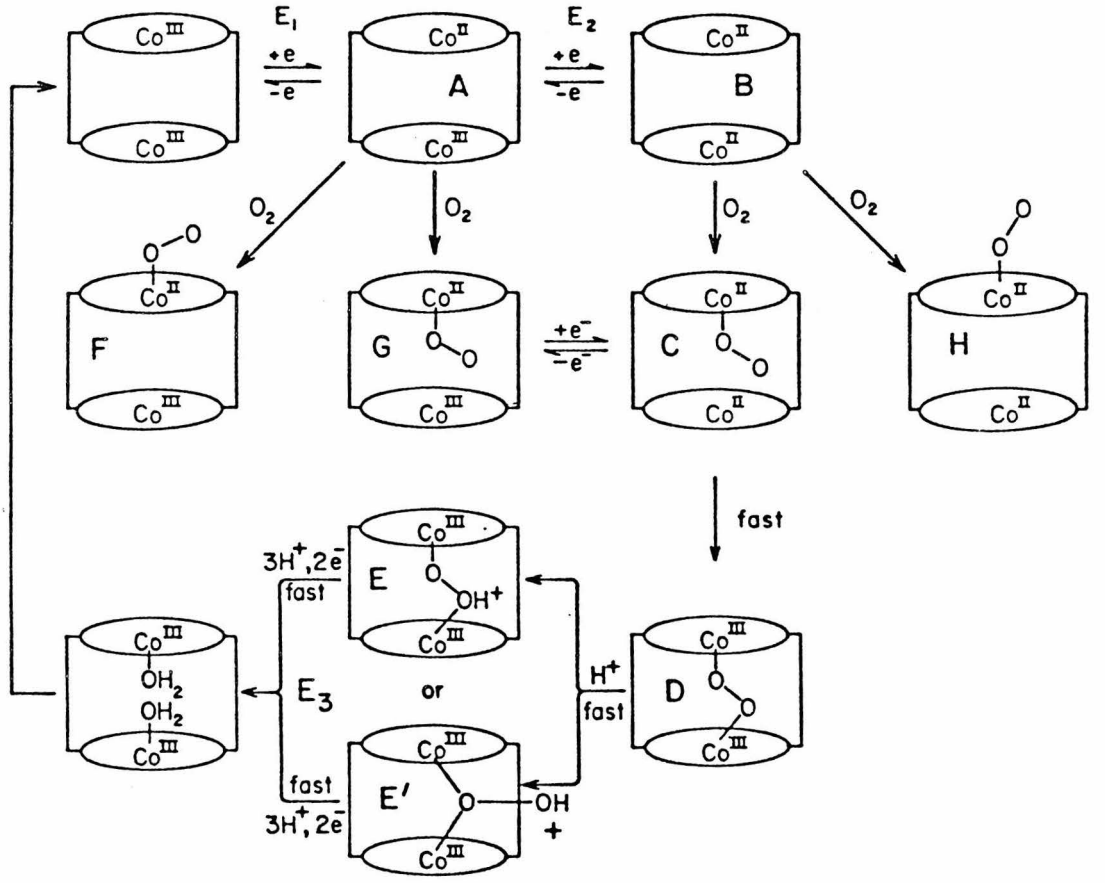

significant quantities of these species were formed, the peak potential of the first catalyst wave would be shifted towards more positive values in the presence of O_2. The same observation was made recently for the monomeric cobalt porphyrin, I, whose single reduction wave precedes that for O_2 and is not affected by the presence of O_2 (Chapter 2).

The dioxygen group present in F and G is not reducible before the second cobalt(III) center in species A or G is reduced to yield species B and C, respectively. At this point the catalyzed reduction of O_2 to H_2O ensues via species D and E. The potential, E_3, required for the reduction of the μ-hydroperoxo group in species E is assumed to lie positive of E_2 so that the final step of the reduction proceeds rapidly at the potential where species B is generated at the electrode. The dioxygen complex that is catalytically active in the four-electron pathway is proposed to be C, with the dioxygen molecule inside the cavity separating the two porphyrin rings, rather than F or H, because of the dramatic difference in behavior between Co_2FTF4 and the monomeric porphyrin, I, or Co_2FTF5, with only one additional atom in the bridging groups.[1-3] Although species such as F and H do not participate in the electrochemistry at potentials near E_2 because they are not reduced there, such O_2-adducts are reducible to H_2O_2 at more negative potentials (Chapter 2). This accounts for

the appearance of H_2O_2 and the decrease in limiting disk currents when catalyst-coated electrodes are scanned to sufficiently negative potentials.[1-3] Further support for this proposal is provided by the behavior of Co_2FTF3 with only three atoms in the amide bridging groups. Coatings of Co_2FTF3 catalyze the reduction of O_2 to H_2O_2 but not to H_2O, a result to be expected according to Scheme II if the dioxygen molecule were unable to fit between the two porphyrin rings.

The formation of species E, the μ-hydroperoxodicobalt (III) complex, is proposed in order to account for the unique ability of Co_2FTF4 to avoid the formation of H_2O_2. The release of H_2O_2 from species D and E should be slowed down by the need to break two cobalt-oxygen bonds. Rapid protonation of D produces a hydroperoxo group with both ends coordinated to a cobalt center. We propose that this μ-hydroperoxo group is more easily reduced than any of its predecessors in the reaction sequence. Once formed, it rapidly accepts two electrons from the electrode to complete the reduction to H_2O and regenerate the catalyst. The μ-hydroperoxo- rather than the μ-peroxodicobalt(III) complex is proposed as the rapidly reducible intermediate in order to account for the positive shift in the half-wave potential of the O_2 reduction wave produced by increases in the concentration of protons (Table 1). Scheme II is compatible with this observation if the rate at which the

dicobalt(II) form of the catalyst is consumed irreversibly by reaction with O_2 depends on the proton concentration. Indeed, if the formation of species E from species B and O_2 were fast, irreversible and first order in H^+, the observed 60 mV change in $E_{1/2}$ for each ten-fold change in proton concentration could be rationalized.[23]

Scheme II includes the possibility that the hydroperoxide intermediate formed in the catalytic cycle leading to H_2O might be isomer E' because analagous μ-hydroperoxocobalt ammine complexes are known[24-27] and in one case[28] such a complex was shown to be a more reactive oxidant than the corresponding μ-peroxo isomer. The molecular geometric requirements for the formation of E and E' certainly differ and all of the evidence indicates that the catalytic effectiveness of the cofacial porphyrins is exceedingly sensitive to the relative configurations of the two cobalt centers. For example, although both Co_2FTF4 and Co_2FTF4* have been shown by ESR to form μ-superoxodicobalt(III) complexes in non-aqueous media,[4] they are not equally effective as dioxygen reduction catalysts: Co_2FTF4* catalyzes the two-electron reduction instead of the four-electron reduction achieved by Co_2FTF4. The ESR spectra of the two μ-superoxo complexes show dissimilarities that suggest less structural symmetry in the Co_2FTF4* complex. This apparent structural difference has major consequences in the catalytic behavior of the two complexes. Recent ESR

studies on similar cofacial cobalt porphyrins by Chang et al.[29] suggest that cis and trans isomers of oxygen bound to the two cobalts may be possible. It is conceivable that tampering with the geometry of the cavity may alter the reactivity patterns of these isomers.

Mixed Metal Porphyrins. The results obtained with the heterobinuclear cofacial porphyrins adds support to the mechanism depicted in Scheme II in that the metal center present in addition to cobalt is catalytically inert unless it is electroactive at potentials prior to that where species such as F, G or H are reduced to H_2O_2. For example, the CoAgFTF4 catalyst, with two electroactive metal centers, yielded currents well in excess of those corresponding to the two-electron reduction of O_2 and at potentials more positive than any catalyst except Co_2FTF4. A reaction pathway leading to H_2O as the reduction product is apparently accessible with this catalyst and it can be traversed in parallel with the pathway leading to H_2O_2 that is shared by all the catalysts. Since neither Ag_2FTF4 nor the monomeric silver porphyrin analogous to I shows catalytic activity toward the reduction of O_2 or H_2O_2, the apparent activity of the reduced silver center in CoAgFTF4 may reflect its ability to react with the unbound end of the O_2 molecule in the species corresponding to G of Scheme II to produce a hydroperoxo intermediate that is

reduced to H_2O at the electrode in the same potential range where the O_2 in the species corresponding to F and H are reduced to H_2O_2.

By contrast, the CoFeFTF4 complex, which also contains two electroactive metal centers, is no more active than the monomeric cobalt porphyrin because the electroactivity of the iron(III) center lies at potentials well beyond those where the O_2 in the species corresponding to F is reduced to H_2O_2.

Catalytic Mechanism in the Absence of Protons. In neutral and alkaline solutions the catalyzed reduction of O_2 occurs at significantly more negative potentials and leads to H_2O_2 instead of H_2O. In highly alkaline solutions this change could be interpreted in the light of Scheme II as resulting from μ-hydroxo- or μ-oxo-groups competing successfully against O_2 molecules for the cavity in the catalyst, access to which is required for the four-electron reduction according to Scheme II. The catalyzed reaction may then be forced to proceed via species such as F and H in Scheme II which require more negative potentials for reduction of the coordinated O_2 and lead only to H_2O_2.

In neutral solutions, where the O_2 molecules may continue to be able to enter the cavity of the catalyst, the four-electron pathway may be blocked by the lack of protons necessary to convert the μ-peroxo intermediate, D, into species E (or E'), the only form of the intermediate

that is reducible at the potential where it is generated. The coordinated peroxide is therefore released from the cavity as depicted in Scheme III instead of being further reduced. The resulting H_2O_2 accumulates in the solution because Co_2FTF4 is inert towards the reduction of H_2O_2 at any pH.

SUMMARY

The observations described here have helped to identify several important facts about the catalytic cycle by which cofacial porphyrins reduce O_2 to H_2O;

i) the distribution of reduction products (H_2O_2 or H_2O) is strongly influenced by proton concentration;

ii) there are specific geometric requirements within the porphyrin dimer cavity for four electron activity;

iii) the two metal redox sites must have similar reduction potentials in order to produce the four electron reduction;

iv) the potential at which the catalytic reduction of O_2 occurs is governed by second metal centered reduction;

v) a key intermediate in the formation of H_2O appears to be a protonated bridging peroxide;

vi) the rate limiting step is the initial formation of an oxygen adduct.

Scheme III

POSSIBLE CATALYTIC CYCLE IN ABSENCE OF ACID

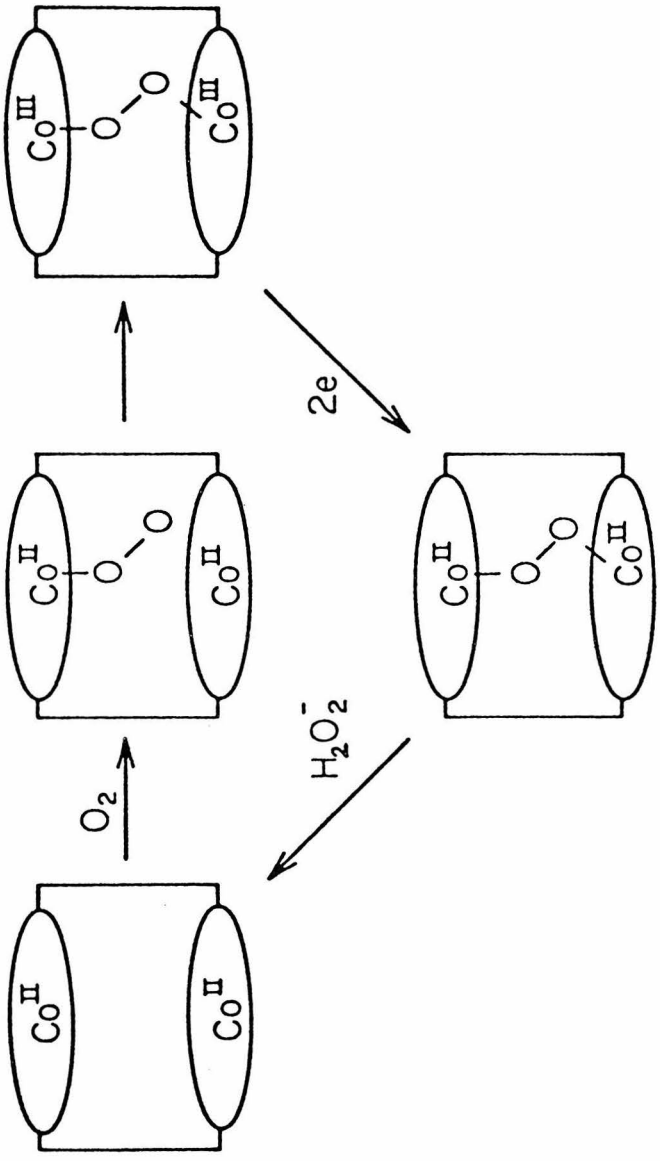

The features outlined above emphasize the complexity of the catalytic cycle. For example, ii and v are interrelated since the electroreduction in acidic media of μ-peroxodicobalt complexes of some macrocyclic complexes produce cobalt(II) and H_2O_2, not H_2O.[30] Thus, the μ-peroxo group in the complex formed by Co_2FTF4 is apparently unusually reactive towards protonation and further reduction. The combination of steric and electronic constraints imposed simultaneously by the cofacial porphyrin ligand with four atoms in its amide bridge seems of crucial importance to its unique catalytic action. A more thorough understanding of the coordination chemistry of the cofacial porphyrins is required to determine the specific steric and electronic factors which account for their unique activity.

REFERENCES AND NOTES:

1. J. P. Collman, M. Marrocco, P. Denisevich, C. Koval, and F. C. Anson, J. Electroanal. Chem., 101, 117 (1979).

2. J. P. Collman. P. Denisevich, Y. Konai, M. Marrocco, C. Koval, and F. C. Anson, J. Am. Chem. Soc., 102, 6027 (1980).

3. J. P. Collman, F. C. Anson, S. Bencosme, A. Chong, T. Collins, P. Denisevich, E. Evitt, T. Geiger, J. Ibers, G. Jameson, Y. Konai, C. Koval, K. Meier, R. Oakley, R. Pettman, E. Schmittou, and J. Sessler, in "Organic Synthesis, Today and Tomorrow," B. M. Trost and C. R. Hutchinson, eds., Pergamon Press, New York, p. 29, 1981.

4. J. P. Collman, F. C. Anson, C. E. Barnes, S. Bencosme, T. Geiger, E. R. Evitt, R. P. Kreh, K. Meier, R. B. Pettman, J. Am. Chem. Soc., 105, 2694 (1983). J. P. Collman, F. C. Anson, S. Bencosme and R. R. Durand, Jr., and R. P. Kreh, ibid., 105, 2699 (1983). J. P. Collman, S. Bencosme, C. E. Barnes, and B. D. Miller, ibid., 105 2704 (1983).

5. A. P. Brown and F. C. Anson, Anal. Chem., 49, 1589 (1977).

6. P. Denisevich, Ph.D. Thesis, Stanford University, (1979).

7. D. S. Polcyn and I. Shain, Anal. Chem., 39, 370 (1966).

REFERENCES AND NOTES

8. R. L. Myers and I. Shain, Anal. Chem., 41, 980 (1969).

9. F. Ammar and J. M. Saveant, J. Electroanal. Chem., 47, 215 (1973).

10. V. G. Levich, "Physicochemical Hydrodynamics," Prentice-Hall, Englewood Cliffs, N.J., 1962.

11. A. P. Brown, C. Koval, and F. C. Anson, J. Electroanal. Chem., 72, 379 (1976).

12. A. P. Brown and F. C. Anson, J. Electroanal. Chem., 83, 203 (1977).

13. C. Koval and F. C. Anson, Anal. Chem., 50, 223 (1978).

14. A. J. Bard and L. Faulkner, "Electrochemical Methods," J. Wiley and Sons, New York, 1980.

15. In previous studies difficulties were often experienced in maintaining a constant sensitivity of the platinum ring electrode towards the oxidation of H_2O_2 in buffered supporting electrolytes at pH values above ca. 2. For this reason it is preferred to use the magnitude of disk currents as a more reliable indicator of the stoichiometry of the reduction of O_2. However, the presence or absence of ring current remains a highly reliable qualitative means for detecting H_2O_2 among the reduction products.

16. J. Koutecky and V. G. Levich, Zh. Fiz. Khim., 32, 1565 (1958).

REFERENCES AND NOTES

17. P. N. Ross, Jr. and F. T. Wagner, Report to Los Alamos National Laboratory (Contract No. CRI-7090 W-1) March, 1982.

18. J. Bett, J. Lundquist, E. Washington, and P. Stonehart, Electrochimica Acta, 18, 343 (1973).

19. C. R. Hartzell, H. Beinert, B. F. van Gelder, and T. E. King, Methods Enzymol., 53, 54 (1978).

20. S. B. Vik and R. A. Capaldi, Biochem. Biophys. Res. Commun., 94, 348 (1980).

21. K. Shigehara and F. C. Anson, J. Phys. Chem., 86, 2776 (1982).

22. K. Kadish, D. G. Davis, and J. M. Fuhrhop, Angew. Chem. Intl. Ed., 11, 1014 (1972).

23. L. Nadjo and J. M. Saveant, J. Electroanal. Chem., 44, 327 (1973).

24. M. Mori and M. A. Weil, J. Am. Chem. Soc., 89, 3732 (1967).

25. V. Thewalt and R. A. Marsh, J. Am. Chem. Soc., 89, 6364 (1967).

26. R. Davies and A. G. Sykes, J. Chem. Soc. (A), 2840 (1968).

27. M. R. Hyde and A. G. Sykes, J. Chem. Soc. Dalton, 1550 (1974).

28. R. Davies, M. G. Stevenson and A. G. Sykes, J. Chem. Soc. (A), 1261 (1970).

REFERENCES AND NOTES

29. H. Y. Liu, M. J. Weaver, C. B. Wang, and C. K. Chang, J. Electroanal. Chem., 145, 439 (1983).

30. T. Geiger and F. C. Anson, J. Am. Chem. Soc., 103, 7489 (1981).

Chapter 4

Dissolution of Insoluble Cobalt Porphyrins in Concentrated Acids to Produce Increased Stability in their Catalysis of Dioxygen Reduction

INTRODUCTION

In the previous studies of the electrocatalytic activity of metalloporphyrins adsorbed on graphite toward oxygen reduction, the films were cast from organic solution (Chapters 2 and 3). The electrolyte media were aqueous with the pH ranging from 0-14. The catalysts are insoluble under these conditions. These complexes have now been found to dissolve in more strongly acidic electrolytes (>5M) and in neat phosphoric acid. Both monomeric and dimeric cobalt porphyrins have been found to solubilize without demetalation in 5.6M trifluoromethanesulfonic acid (HTFMS) and neat H_3PO_4. The lack of demetalation was noted by UV-visible spectroscopy and in catalytic studies of the dissolved complexes. Cyclic voltammetry and rotating ring-disk voltammetry have been utilized to examine oxygen reduction by these catalysts. There was an advantageous effect on the catalytic properties for both the monomeric and dimeric species when they are dissolved in the electrolyte solution. Of particular interest was the observation that the cofacial cobalt porphyrin, Co_2FTF4, appears to have a much improved stability under conditions in which some catalyst resides in solution.

EXPERIMENTAL

The two complexes utilized in this study were prepared as described previously (see references in Chapter 2 and Chapter 3). Trifluoromethane sulfonic acid was obtained from 3M Company and was distilled prior to use. Reagent grade phosphoric acid (Baker analyzed) was used as received.

Electrochemical instrumentation has been described in preceding chapters. Spectra were obtained on HP 8450A UV-visible spectrometer.

RESULTS AND DISCUSSION

Solubility of Cobalt Porphyrins in Strong Acids

The monomeric cobalt(II) porphyrin examined in Chapter 2 was observed to dissolve in a variety of very concentrated acid solutions. The extent of demetalation and solubility was variable. In the cases of 5.6M HTFMS and neat H_3PO_4, the solubility was high while the extent of demetalation was low. Figure 1 shows the visible spectra for the free base porphyrin and the corresponding cobalt derivative in 5.6M HTFMS. The spectrum obtained for the free base porphyrin was characterized as arising from the dication resulting from protonation of two nitrogens of the porphyrin core.[1] The spectrum of the cobalt complex was very distinct from the free base species. It was more similar to a spectrum of the cobalt porphyrin obtained in non-aqueous solvents. Clear spectral distinction was also

Figure 1. The UV-visible spectra of the monomeric free ligand (solid line) and the corresponding cobalt complex (broken line).

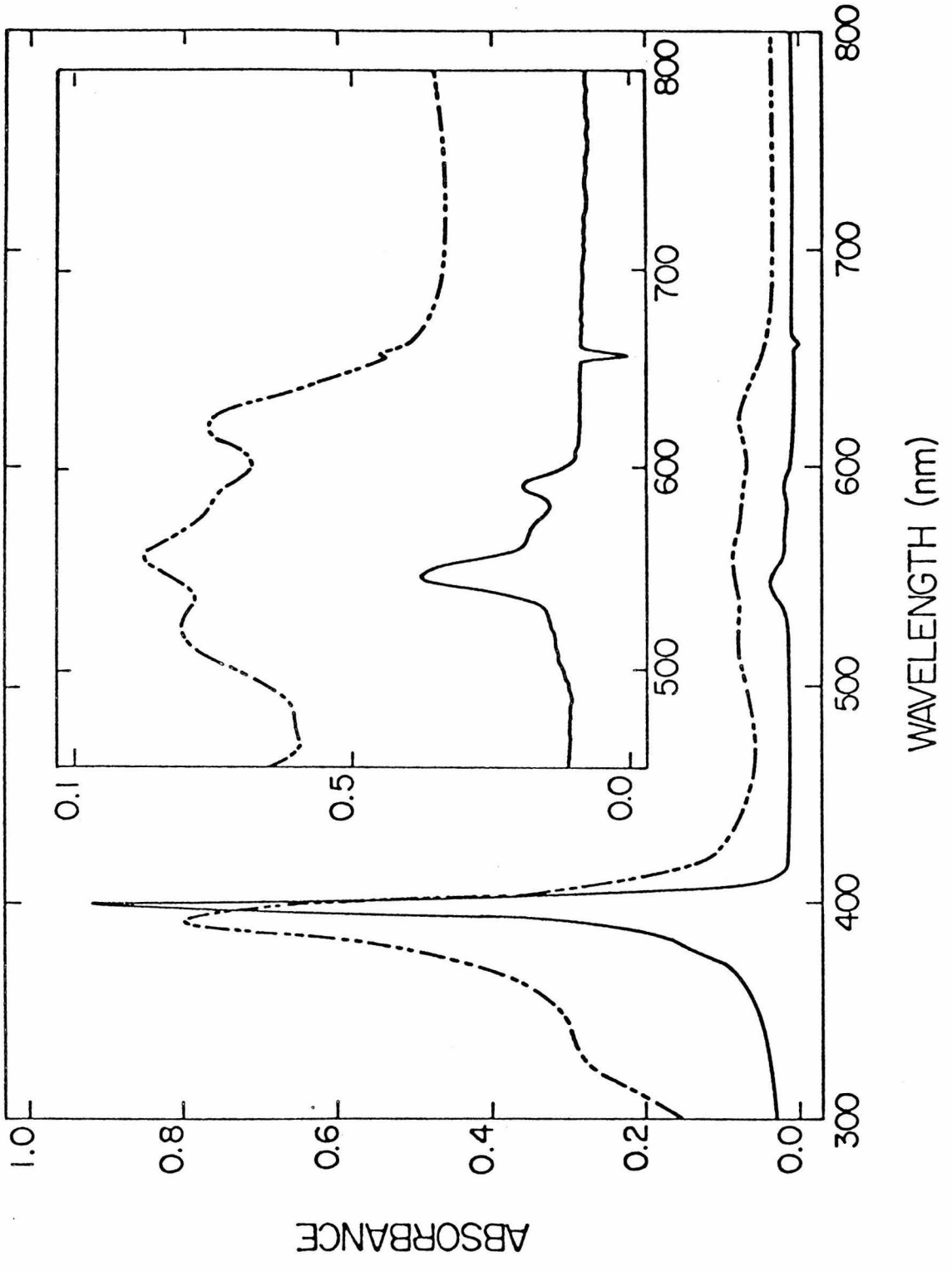
ABSORBANCE
1.0
0.8
0.6
0.4
0.2
0.0
300
400
500
600
700
800
WAVELENGTH (nm)
0.1
0.5
0.0
500
600
700
800

made between free base and metalloporphyrin in neat phosphoric acid.

The cofacial dimer, Co_2FTF4, also showed distinct spectral features from a non-metallated precursor; however, it does not appear to be related to spectra obtained in non-aqueous solution. The rate of solubilization appeared to be faster for the dimer compared to the monomer. The solutions of dissolved monomeric or dimeric complexes could be diluted without spontaneous precipitation of the complexes. Even when dilution factors were high enough to produce acidities near pH 0-2, the complexes were very slow to precipitate.

Normally, free base porphyrins are insoluble in aqueous media, unless they contain ionizable substitutents (e.g., pyridyl, amino, carboxyl, or sulfonate groups) or they are exposed to strong acid. The resulting porphyrin dication imparts an overall +2 charge on the molecule to render it more soluble. If a metalloporphyrin is exposed to strong acid, then it is very common for demetalation to occur. The acidic demetalation of metalloporphyrins is a common synthetic procedure.[2] The extent or ease of demetalation is influenced by the nature and oxidation state of the metal center, as well as the strength and type of acid employed. Empirical measures of the relative thermodynamic stability of metalloporphyrins toward acid have been proposed.[3] Other qualitative classifications

have been established to order the various metalloporphyrins toward the ease of demetalation.[4,5] For divalent metals, the relative order of the 1st row transition metals is:

$$Ni > Cu > Co >> Fe \simeq Zn$$

where the ease of demetalation increases to the right. Higher oxidation states which are less labile tend to be even more stable toward acid. Under proper conditions the cobalt porphyrins can withstand acidic electrolytes reasonably well.

The origins for the solubility of the cobalt complexes of the porphyrins might be expected to be distinct from the free ligands. The protonation of the nitrogens in the porphyrin core is not likely. The molecules examined here do contain ester or amide groups which can be protonated. The acid dissociation constants for representative esters and amides are 10^6 and 10^1, respectively.[6] The ester group is not expected to undergo significant protonation under the conditions described here. A cobalt porphyrin derivative of the octaethylporphyrin free ligand was found to have similar solubility properties as the ligand containing an ester group. For the amide bridge of the cofacial porphyrin, a significant amount of protonation is possible. This may account for the observation that the dimeric complex dissolves more readily than the monomeric precursor. Another contributing factor to solubilizing the metalloporphyrins may arise from the oxidation of the metal

centers to produce cationic species. There is also a possibility that the much lower activity of water in these solutions could favor dissolution of hydrophobic ions. The solubilization properties of these complexes are complex and warrant further investigation.

Catalytic Activity of Dissolved Cobalt Porphyrins

5.6M HTFMS

Cyclic voltammograms of Co monomer and Co_2FTF4 were examined for 5.6M HTFMS and concentrated phosphoric acid in the absence and presence of dioxygen. Solutions containing 0.1mM complex could easily be obtained. Figure 2 shows the cyclic voltammetric behavior for Co_2FTF4 in 5.6M HTFMS in the absence and presence of oxygen. It was evident that adsorption of the complex was complicating the response. In oxygen saturated electrolyte, the catalytic reduction of oxygen was noted (Figure 2B). Transfer of the same electrode examined in a solution of the complex to pure 5.6M HTFMS or 1M trifluoroacetic acid showed that the catalyst had adsorbed to the electrode spontaneously. The cyclic voltammetric response was identical to that noted upon initial exposure of a coating cast from organic solution to these electrolytes. These observations suggested that the complex was not undergoing irreversible chemical changes which affect its catalytic activity when exposed to strongly acidic media.

Figure 2. Cyclic voltammograms at an edge plane pyrolytic graphite electrode in 5.6M HTFMS. (A) under argon; (B) under oxygen. Scan rate: 100mV/sec.

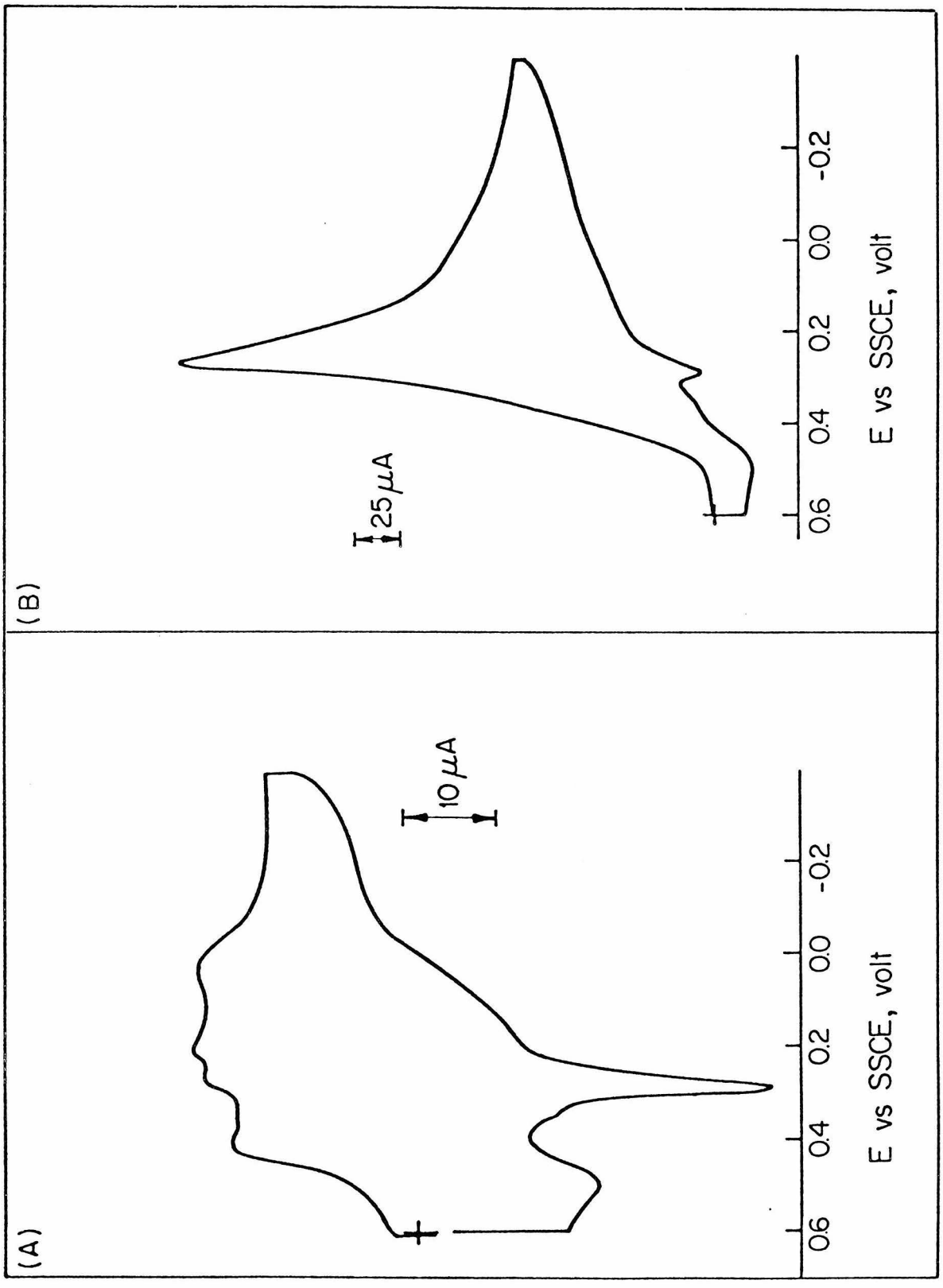
(A)
(B)
10 μA
25 μA
0.6
0.4
0.2
0.0
-0.2
E vs SSCE, volt
CURRENT

Rotating ring-disk voltammetry was performed to examine the catalytic activity of solutions of the porphyrin complexes in 5.6M HTFMS. Figures 3 and 4 are the responses for the Co monomer and Co_2FTF4 in oxygen saturated 5.6M HTFMS. The Co monomer exhibited a response occurring at more positive potentials than previously observed (see Chapter 2). The multiple wave response at the disk and ring electrodes reflects a more complex reaction sequence than results when only the catalyst on the electrode surface was employed. Although it is difficult to quantitate the number of electrons involved in the reduction, the response at the Pt ring held at 1.1V vs. SCE (sufficiently positive to oxidize H_2O_2) indicated that significant amounts of H_2O_2 were produced. As the disk potential was scanned more negative, less H_2O_2 was observed at the ring. The further consumption at the disk electrode of generated H_2O_2 appeared to be possible. A rotating ring-disk voltammogram obtained in a deaerated H_2O_2 solution in the presence of the cobalt complex exhibited a catalytic reduction response. Similar behavior could be obtained from solutions in which the concentration of the catalyst complex was much lower (μM).

The Co_2FTF4 complex exhibited ring-disk behavior similar to the monomeric species when dissolved in 5.6M HTFMS. Only 10% more disk current was observed, but much lower ring currents were noted. The smaller ring current

Figure 3. The rotating ring-disk voltammograms obtained for Co_2FTF4 (ca. 0.1mM) in 5.6M HTFMS. The dashed line represents the background response under O_2 at bare graphite. (A) Oxygen saturated; (B) Argon saturated. S_1 = 125 μA for the ring. S_2 = 25 μA for disk and 10 μA for ring. Scan rate: 0.5 V/min.

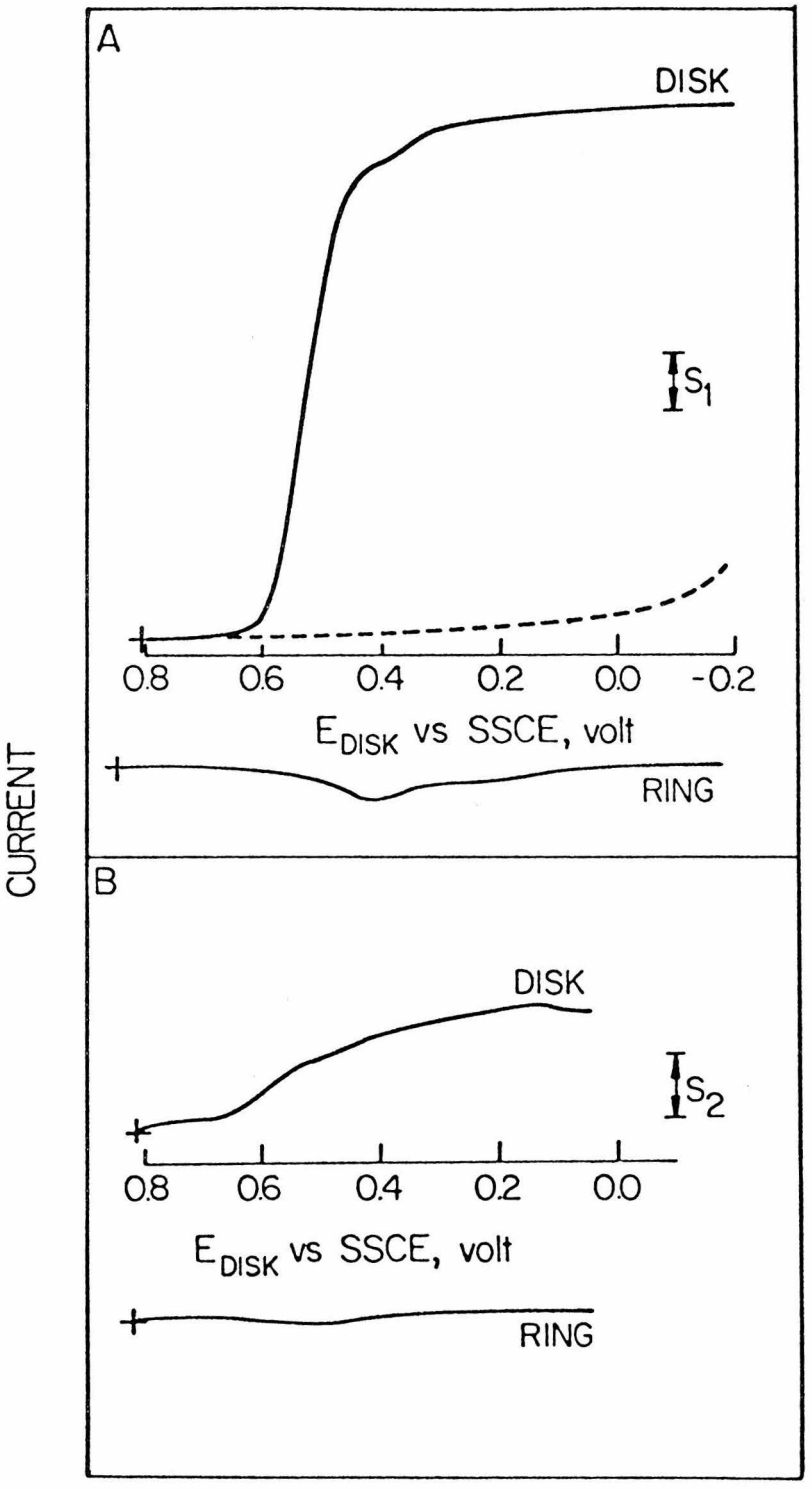
A
DISK
S_1
0.8
0.6
0.4
0.2
0.0
-0.2
E_{DISK} vs SSCE, volt
RING
CURRENT
B
DISK
S_2
0.8
0.6
0.4
0.2
0.0
E_{DISK} vs SSCE, volt
RING

Figure 4. The rotating ring-disk voltammogram obtained for Co monomer porphyrin (0.2 mM) in oxygen saturated 5.6M HTFMS. S = 125 μA for disk and 25 μA for the ring. Scan rate: 0.5 V/min.

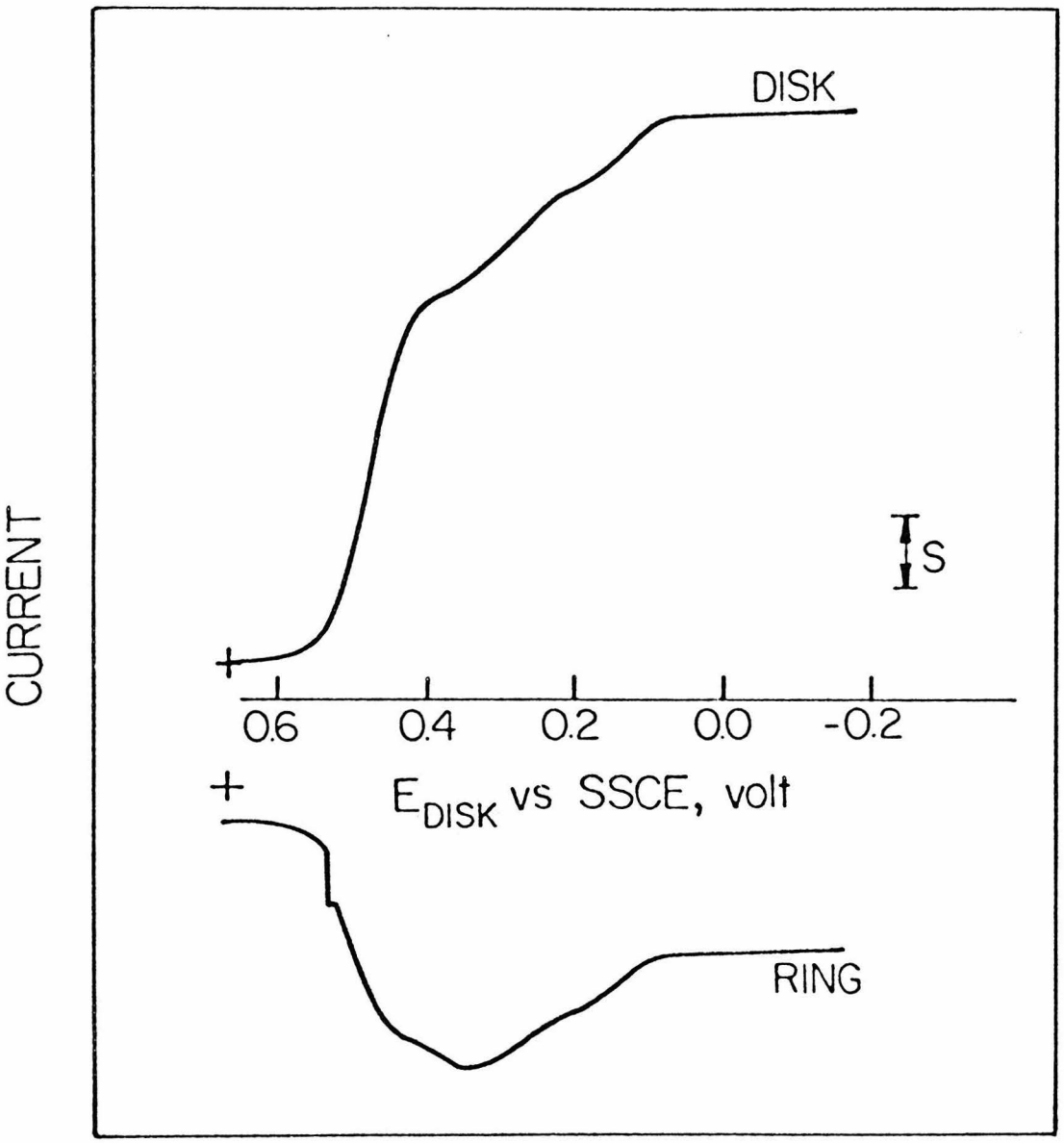
CURRENT
DISK
Is
+
0.6
0.4
0.2
0.0
-0.2
+
E_{DISK} vs SSCE, volt
RING

observed for the dimer suggests that a cleaner reduction to water was occurring than for the monomer. The shapes of the disk and ring responses were unusual in that inflections were noted in a narrow potential region where H_2O_2 was produced. The ring response showed further consumption of H_2O_2 was possible as it was for the monomer. The Co_2FTF4 did show a catalytic response toward H_2O_2 reduction in a deaerated electrolyte solution of hydrogen peroxide.

The stability of the Co_2FTF4 as an O_2 reduction catalyst was vastly improved when some of the catalyst resides in solution. Figure 5 shows a comparison of the rotating disk responses for an electrode coated from an organic solution of Co_2FTF4 and a micromolar solution of Co_2FTF4 in 5.6M HTFMS. In Figure 5A, the scans of the catalyst coated disk electrode taken five minutes apart are denoted by curves 1 and 2. The limiting current had dropped 30% in this time and the $E_{1/2}$ for the reduction had shifted negative by ca. 100mV. The responses in Figure 5B correspond to that obtained for a μM solution of Co_2FTF4 in 5.6M HTFMS. Curve 1 was the initial disk voltammogram and curve 2 is the response at the disk after about one hour in which the electrode was held at a potential on the limiting plateau (-0.17V). Although the shape of the curve changes slightly, the limiting current is unchanged and the $E_{1/2}$ value is shifted negative by only 20mV. There

Figure 5. The rotating disk voltammograms obtained for Co_2FTF4 in oxygen saturated 5.6M HTFMS. (A) Response for catalyst coated disk (1). The response on the next cycle five minutes later after holding E = +0.80V is denoted by (2); (B) Co_2FTF4 in solution (ca. μM) curve (1) is the initial scan and (2) is one hour later after holding potential at -0.17 V. S_1 = 125 μA; S_2 = 250 μA. Scan rate = 0.5 V/min.

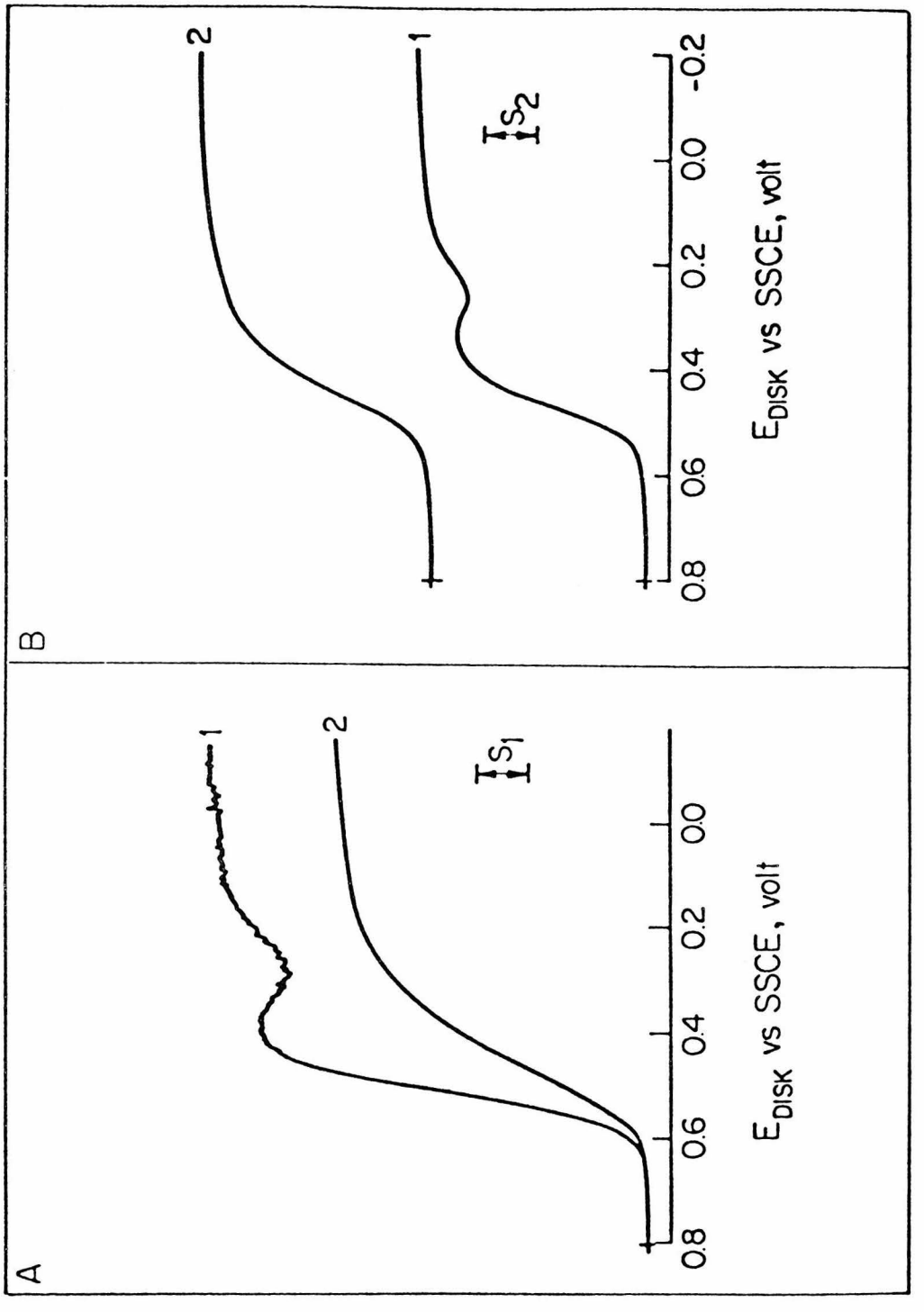
A
B
1
2
I_{S_1}
I_{S_2}
0.8
0.6
0.4
0.2
0.0
-0.2
E_{DISK} vs SSCE, volt
CURRENT

is a remarkable improvement in stability when the catalyst resides in the electrolyte solution. The fact that only low concentrations of catalyst were needed to improve stability over time suggests that fresh catalyst coatings are maintained by the equilibrium adsorption/desorption characteristics of the catalyst.

The behavior of Co monomer and Co_2FTF4 at a graphite disk in 5.6M HTFMS at various rotation rates has been examined. There was a distinct deviation from the predicted Levich current.[7] The Koutecky-Levich plots also showed non-zero intercepts.[8] Both these observations imply, as previously noted for a catalyst strictly confined to the electrode, that kinetic limitations are important. Analysis of these data is very difficult due to the fact that there is active catalyst in solution and on the surface.

Concentrated H_3PO_4

The responses of the catalysts dissolved in neat H_3PO_4 were similar to those in 5.6M HTFMS. The magnitude of the catalytic currents were much smaller, since the solubility of oxygen is lower and viscosity of the solvent is much higher. Figure 6 shows the rotating ring-disk behavior of Co_2FTF4 in H_3PO_4. The magnitude of the current and the $E_{1/2}$ for the reduction of oxygen is very similar to the response obtained for a P+ electrode under the same

Figure 6. The rotating ring-disk response obtained for Co_2FTF4 (0.1 mM) in oxygen saturated concentrated H_3PO_4. Scan rate: 0.5 V/min.

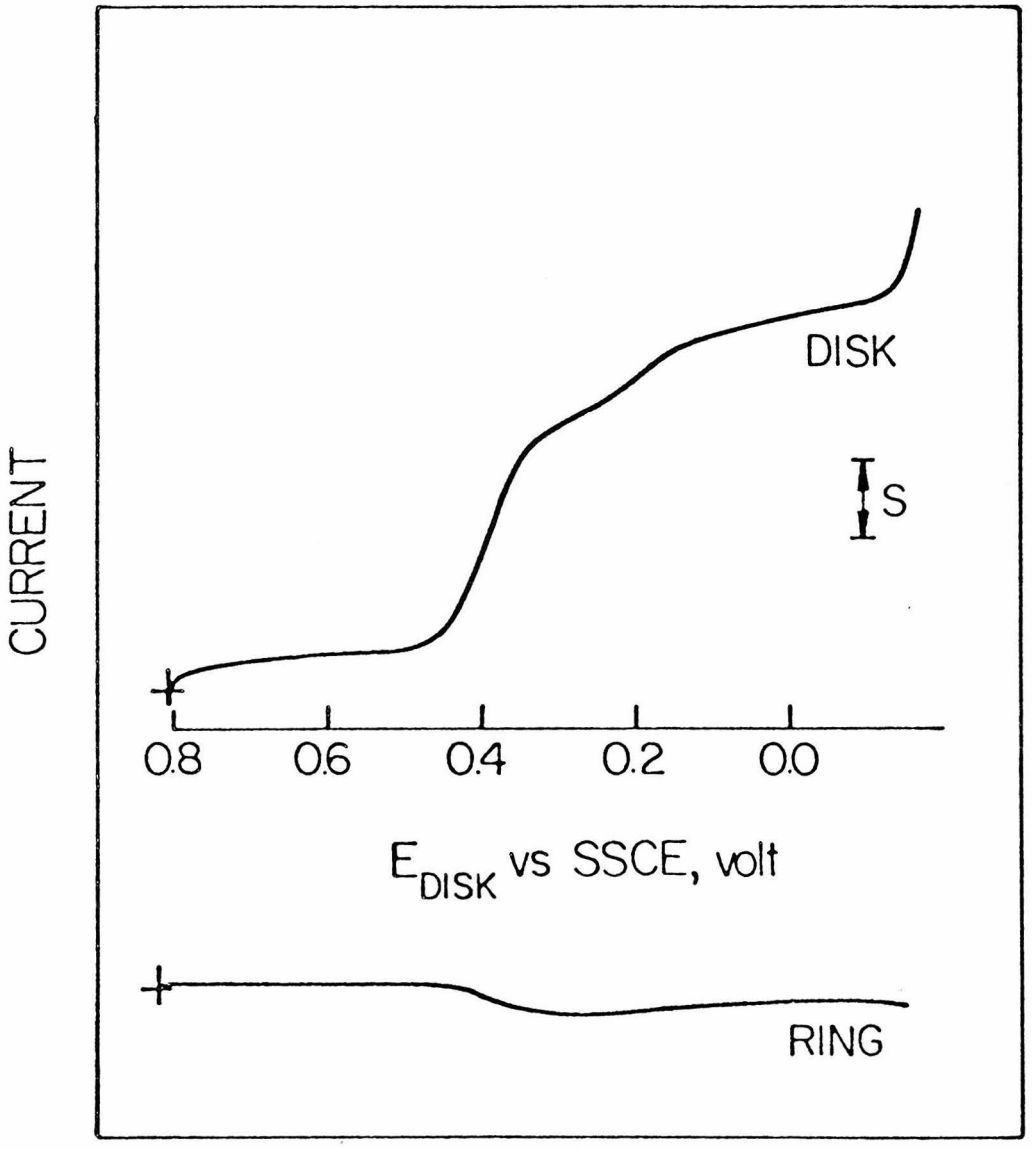
CURRENT
DISK
S
0.8
0.6
0.4
0.2
0.0
E DISK vs SSCE, volt
RING

conditions. Some H_2O_2 is detected at the ring electrode for the Co_2FTF4. The Co monomer shows more H_2O_2 at the ring with less current at the disk.

A comparison of the observed currents for the monomeric or dimeric complexes to those predicted by the Levich equation has been made. Values for the concentration of oxygen and diffusion coefficient in H_3PO_4 are known.[9,10] If one assumes that only mass transport limitations exist, then the Levich equation can be used to calculate the expected currents for two or four electron reduction. At 25°C, the values of $C_{O_2} = 3 \times 10^{-7}$ moles/cm^3 and $D_{O_2} = 2 \times 10^{-6}$ cm^2/sec were used to calculate the predicted current at 400 rpm from the Levich equation. For n = 4, a calculated disk current of 51 μA was obtained. The observed currents for Co_2FTF4 and Co monomer are 45 μA and 38 μA, respectively. Both of these values exceed that expected for an overall two electron reduction. Improvements in the stability of the catalysts were also noted in H_3PO_4. Exposure of catalyst solution to high temperatures (~150°C) did not completely destroy its activity, although it did diminish it. The results in H_3PO_4 are of particular significance with respect to practical utility of these catalysts for fuel cells.

SUMMARY AND CONCLUSIONS

The solubilization of cobalt porphyrins in strong acid media without demetalation has been demonstrated. The catalytic reduction of dioxygen can be carried out by dissolved catalysts. The results described here suggest that both the monomeric and dimeric cobalt catalysts have additional mechanistic pathways available in strongly acidic electrolytes. The ability to solubilize the metalloporphyrin complexes has been shown to provide improve stability over longer times. Finally, the solubilization of catalyst complexes may allow other techniques such as spectroscopy to be more effectively utilized in future investigations.

REFERENCES AND NOTES

1. P. Hambright in, "Porphyrins and Metalloporhyrins," K. M. Smith (ed.), Elsevier, Amsterdam, p. 233 (1975).
2. J. E. Falk, "Porphyrins and Metalloporphyrins," Elsevier, Amsterdam (1964).
3. F. J. C. Rosotti in "Modern Coordination Chemistry," J. Lewis and R. G. Wilkins, eds., Interscience, New York (1960).
4. J. N. Phillips, Rev. Pure Appl. Chem., 10, 35 (1960).
5. J. W. Buchler, L. Pappe, K. Rhohbock, and H. H. Schneehagg, Ann. N.Y. Acad. Sci., 206, 116 (1973).
6. R. B. Homer and C. D. Johnson in "The Chemistry of Amides," Jacob Zabicky, ed., (1970).
7. V. G. Levich, "Physicochemical Hydrodynamics," Prentice-Hall, Englewood Cliff, New Jersey (1962).
8. J. Koutecky and V. G. Levich, Zh, Fiz. Khim., 32, 1565 (1956).
9. K. Klinedinst, J. A. S. Bett, J. MacDonald, and P. Stonehart, J. Electroanal. Chem., 57, 281 (1974).
10. K. E. Gubbins and R. D. Walker, J. Electrochem. Soc., 112, 469 (1965).

Chapter 5

An Electrochemical Study of the Reaction of Superoxide Anion with a Macrocyclic Cobalt(II) Complex in Dimethylsulfoxide

INTRODUCTION

Dioxygen can be reduced by one electron to produce the superoxide anion radical. In aqueous media, the superoxide ion does not have a long lifetime.[1] It can be generated at steady state levels via pulse radiolysis.[2] As a consequence of its instability in aqueous solution, its reactivity as a nucleophile or redox reagent is hard to examine. In aprotic media, stable superoxide solutions can be prepared by the electrochemical reduction of dioxygen or by the dissolution of a superoxide salt (e.g., KO_2) with the aid of solubilizing agent such as a crown ether.[3] The potency of the superoxide ion as a reactant is better evaluated in non-aqueous solvents. Under such conditions, it has been shown to act as a moderately strong nucleophile (e.g., superoxide reacts with esters to form carboxylic acids and alcohols).[4] It can also act as a mild one electron reducing or oxidizing agent.[5,6] Singlet oxygen can be produced by the reaction of superoxide ion with ferricenium ion.[7]

The observations of $O_2^{\cdot-}$ by ESR from dioxygen-utilizing enzymes have generated interest in the reactions of superoxide with metal complexes.[8] Suggestions have been made that some metalloproteins function to catalyze the disproportionation of superoxide (i.e., superoxide dismutases).[9] Copper and zinc metal ions are known to be at the active sites of these enzymes. The reactions of model metal complexes with superoxide have been examined.[10,11] Superoxide

ion was found to act as a nucleophile in coordinating to zinc or copper complexes to form relatively stable adducts. The coordination chemistry of superoxide may also have relevance to the role of superoxo complexes in other oxygen-involving enzymes (e.g., oxidases).

In an attempt to understand the details of the mechanism by which macrocyclic cobalt complexes catalyze dioxygen reduction, the interactions of superoxide with cobalt(II) complexes were examined. By investigating the reaction of Co(II) with $O_2^{\cdot-}$ in a non-aqueous electrolyte, it was possible to study reactions that may be obscured by the catalytic sequence occurring in aqueous media. There have been few studies of the reactions of Co(II) macroyclic complexes with superoxide ion. Hoffman and Simic studied the reactions of two cobalt(II) macrocycles with superoxide generated by pulse radiolysis in aqueous solution.[12] The reaction was extremely rapid ($k \sim 10^9 M^{-1}s^{-1}$). An adduct with a lifetime of several minutes appeared to be formed. This adduct was not characterized. The reaction of a cobalt(II) tetraphenylporphyrin with superoxide in non-aqueous solution has been reported by Russian investigators.[13] They claimed that a stable oxygenated complex of the form shown in equation (1) was obtained.

$$2\ \text{Co(II)TPP} + O_2^{\cdot-} \rightleftharpoons \text{TPPCo(II)} - O_2^{\cdot-} - \text{Co(II)TPP} \qquad (1)$$

The evidence for this binuclear adduct was predominantly from UV-visible spectroscopy. A very important complica-

ion was noted by these investigators in that the superoxide ion was thermodynamically capable of reducing Co(II) to Co(I) for this porphyrin complex. This redox complication may cast doubt on the interpretation of these investigators.

The possible role of superoxide as an intermediate during the catalytic reduction of dioxygen has been suggested in Chapter 2. The large difference between the Co(III/II) reduction potential and the catalytic O_2 reduction potential may be the result of the reaction of superoxide with the catalyst. The Co(II) porphyrin can act to stablize the reduction of O_2 to superoxide by the concerted scheme noted in equation (2).

$$Co(II) + O_2 + e^- \rightleftharpoons Co(II) - O_2^{\cdot-} \text{ (or } Co(III - O_2^{2-}) \quad (2)$$

Reaction (2) is meant to imply that Co(II) stabilizes the oxygen to accept an electron to produce an adduct which can be described as a cobalt(II) superoxide complex or a cobalt(III) peroxide. It is conceivable that the potential at which oxygen is reduced is governed by the extent of stabilization of the superoxide ion. If this is true, the similarities among various cobalt porphyrins catalysts arise from their interaction with superoxide. Further investigation of the reactions of $O_2^{\cdot-}$ with Co(II) were necessary to test the above hypothesis.

A model macrocyclic cobalt(II) complex was examined in this study. The complex was one used by Hoffman and Simic in their aqueous studies, Co(II) (4,11-diene)N_4 (Figure 1). This complex had distinct advantages over the

Figure 1. Molecular structure of the complex Cobalt(II)Me_6(4,11 diene)N_4.

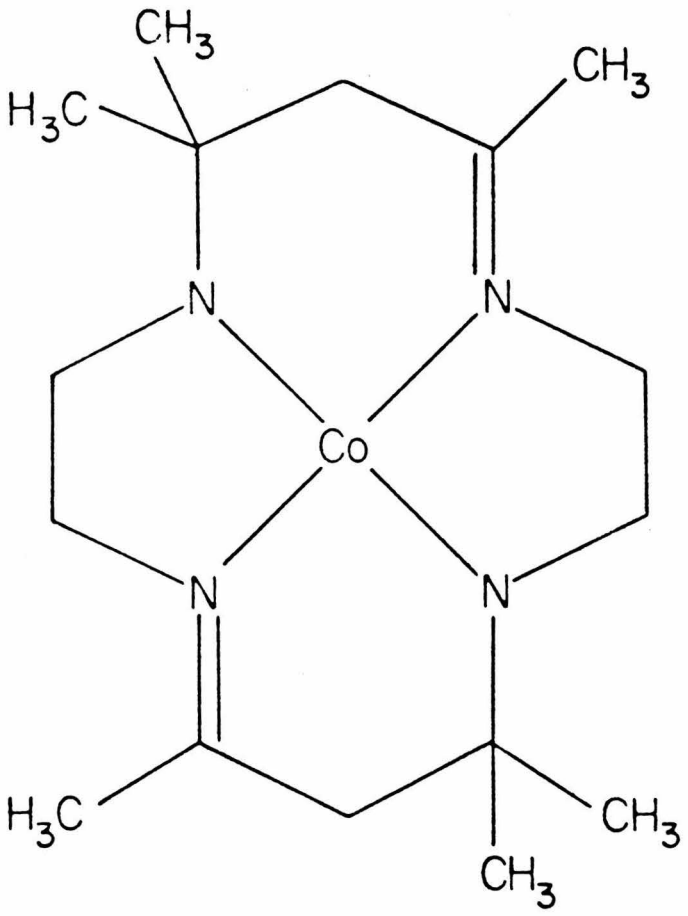
CH3
H3C
CH3
N
N
Co
N
N
H3C
CH3
CH3

porphyrin complexes. The solubility in aprotic media was high and the Co(II/I) reduction potential was sufficiently negative that electrogenerated superoxide could not reduce Co(II). Cyclic voltammetry was used in this investigation. The large affinity of superoxide for cobalt(II) has been demonstrated.

EXPERIMENTAL

The Co(II)Me_6(4,11 diene)N_4 complex was prepared by Dr. M. L. Bowers by a modified literature procedure.[14] Tetraethylammonium perchlorate (TEAP) (Southwestern Analytical) was dried under vacuum for one week prior to use. Dimethylsulfoxide (DMSO) was Burdick and Jackson "Distilled in Glass" grade and was used without further purification. A glassy carbon electrode (Tokai, LTD.) of area 0.071 cm^2 was used after being polished to a glossy finish with 0.3 um alumina (Union Carbide) on a microcloth (Buehler, Ltd.) prior to each scan.

Solutions of electrolyte were 0.1M TEAP in DMSO. Molecular sieves (4Å), which had been heated under vacuum for several days, were added to the solution under an inert atmosphere. These solutions were typically allowed to stand for 1-2 days prior to use.

Cyclic voltammetry was performed with a Princeton Applied Research Model 173/179 potentiostat/digit coulometer along with a Model 175 universal programmer.

Rotating ring-disk voltammetry was performed with a Pine Instrument ASR Rotator and RDE Bipotentiostat. A three electrode cell was used with a platinum counter electrode and Ag/AgCl (saturated KCl) reference electrode. IR compensation was used (from 70% to oscillation).

RESULTS AND DISCUSSION

Figure 2 shows the reversible reduction observed in an oxygen saturated, 0.1M TEAP in DMSO solution at a glassy carbon electrode. The response at -0.9V vs. Ag/AgCl is the diffusion controlled one electron reversible couple observed by Sawyer et. al.[15] (equation 3).

$$O_2 + e^- \rightleftharpoons O_2^{\cdot -} \qquad (3)$$

The cyclic voltammetric behavior for the Co(II) diene complex in the absence of O_2 is shown in Figure 3. An irreversible oxidation at +1.0V is noted as well as an irreversible reduction at 0.0V. The reduction wave results from the product of the oxidation sicne failure to perform the oxidation at +1.0V yields no reduction wave at 0.0V. This very irreversible redox couple may be the Co(II/III) response. The irreversible nature of the Co(II/III) response appears to be due to the solvent, DMSO. Behavior of this type has been observed by other investigators.[16,17] In aqueous media, the Co(II/III) couple exhibits reversible behavior.[18] It is conceivable that DMSO acts as a donating ligand and the difference

Figure 2. Cyclic voltammogram in oxygen saturated (2.1×10^{-3}M) 0.1M TEAP in DMSO at a glassy carbon electrode. Scan rate: 100mV/sec.

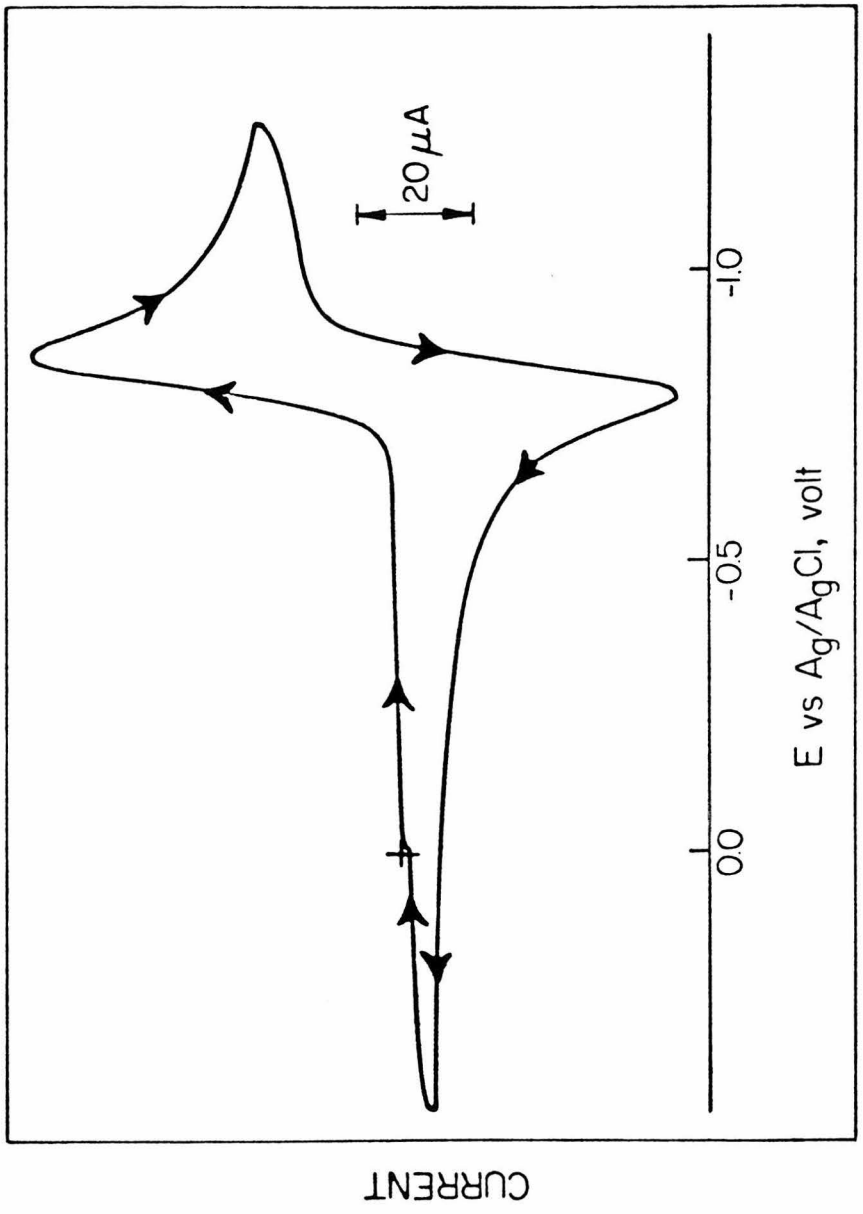
20 μA
0.0
-0.5
-1.0
E vs Ag/AgCl, volt
CURRENT

Figure 3. Cyclic voltammogram of a 2.6mM solution of Co(II)Me_6(4,11 diene)N_4 in argon saturated 0.1M TEAP in DMSO at a glassy carbon electrode. Scan rate: 100mV/sec.

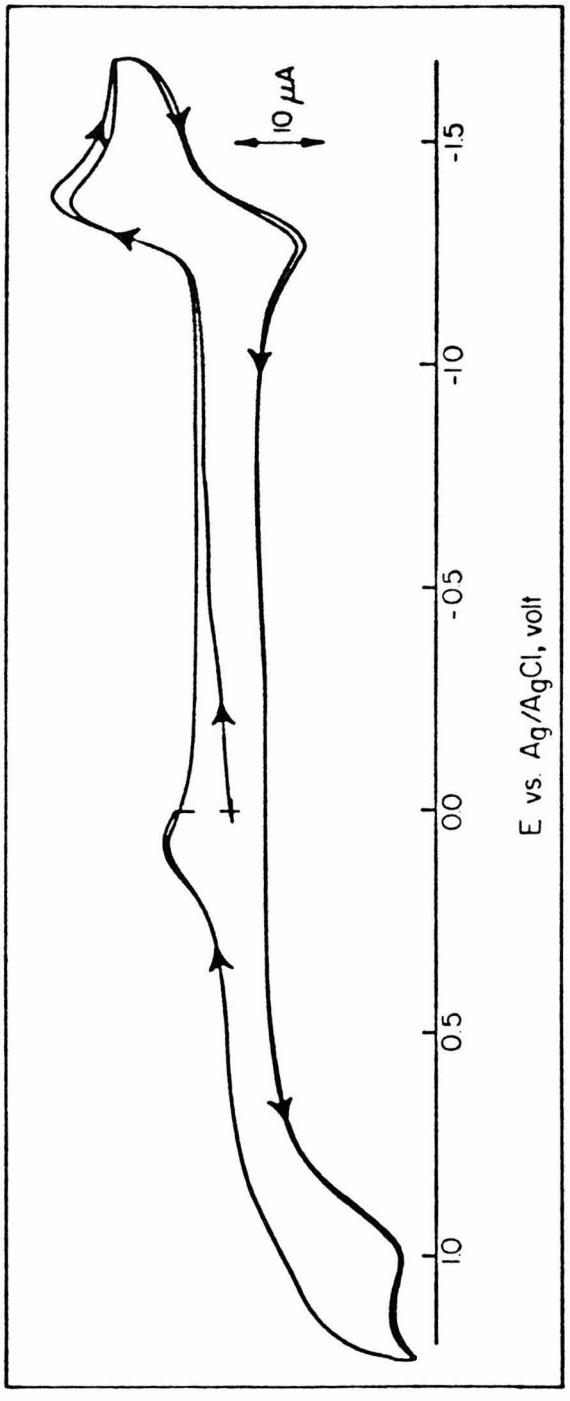
10 μA
1.0
0.5
0.0
-0.5
-1.0
-1.5
E vs. Ag/AgCl, volt
CURRENT

in lability and geometric preference of the two oxidation states account for the large differences in the potential of the oxidation and reduction. The Co(II/I) reduction appears as a reversible wave at -1.3V vs. Ag/AgCl.

Figure 4 shows the cyclic voltammograms of oxygen saturated electrolyte solutions containing 1.1mM and 2.6mM Co(diene). The responses are not the simple composite of the individual components. A prewave develops more positive than the $O_2/O_2^{\cdot-}$ couple and grows as more cobalt complex is added at the expense of the O_2 reduction peak. The oxidation response from the newly generated superoxide diminishes as the concentration of the cobalt complex increases but at a faster rate than does the corresponding reduction peak. The Co(II/I) reduction is distorted by the reaction with O_2, but this reaction was not examined. The Co(II/III) couple does not change in the presence of oxygen. Since the Co(II/III) response is extremely irreversible, the effects of the reaction of oxygen may not necessarily be evident. Finally a new anodic peak is observed at +0.5V which becomes larger with increasing cobalt concentrations. This anodic feature is only observed after cycling over the prewave at -0.4V as shown in Figure 5. The anodic response results from the oxidation of the species formed at the prewave potential. A linear dependence of peak current on the square root of scan rate from 20mV to 500mV/sec. is noted for all peaks observed when both oxygen and the

Figure 4. Cyclic voltammograms of Co(II)Me_6(4,11 diene)N_4 added to oxygen saturated 0.1M TEAMP in DMSO at a glassy carbon electrode. (A) 1.1mM; (B) 2.6mM. Scan Rate: 100mV/sec.

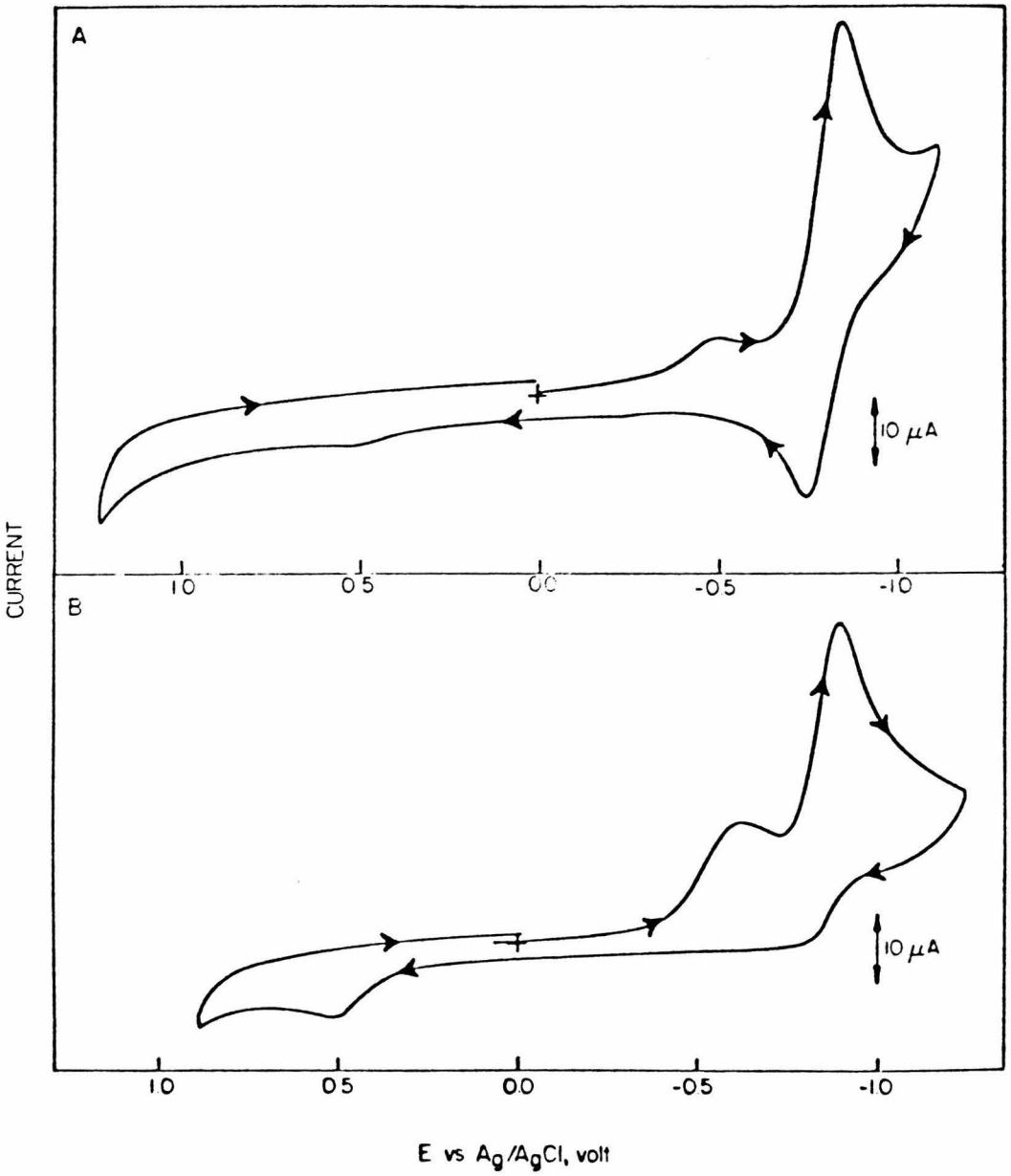
A
10 μA
10
05
00
-05
-10
B
10 μA
10
05
00
-05
-10
CURRENT
E vs Ag/AgCl, volt

cobalt complex are present. This indicates that the responses are diffusion controlled and that equilibrium conditions exist on the timescale of the experiments.

The large positive shift in the O_2 reduction potential produced by the addition of Co(diene) is consistent with $O_2^{-\cdot}$ binding more strongly than O_2. The following scheme is the best description for the electrochemical behavior noted above:

$$O_2 + e^- \rightleftharpoons O_2^{-\cdot} \quad (4)$$

$$O_2^{-\cdot} + Co(II) \longrightarrow Co(II) - O_2^{-\cdot} \quad (5)$$

This scheme suggests that a rapid irreversible chemical step occurs after the electron transfer step. The product of the reaction is the Co(II) - superoxide adduct which can be oxidized at positive potentials. Mechanisms of the type described above are quite common.[19]

The shift in the O_2 reduction potential could be used to estimate the ratio of the binding constants for O_2 and $O_2^{-\cdot}$ if the prewave were nernstian. The greater width of this wave compared to that for the unperturbed $O_2/O_2^{-\cdot}$ couple suggests that slow heterogeneous electron transfer may be affecting the observed current. This is a well recognized phenomenom[20,21] which is encountered when the product of a nominally nernstian electrode reaction is consumed so rapidly by an irreversible chemical step that the electrode potential is shifted to values where the electrode process becomes non-nernstian. The shift to positive potentials

Figure 5. Cyclic voltammogram of Co(II)Me_6(4,11 diene)N_4 (ca. 3mM) in oxygen saturated solution. Initial scan is in positive direction. Scan rate: 100mV/sec.

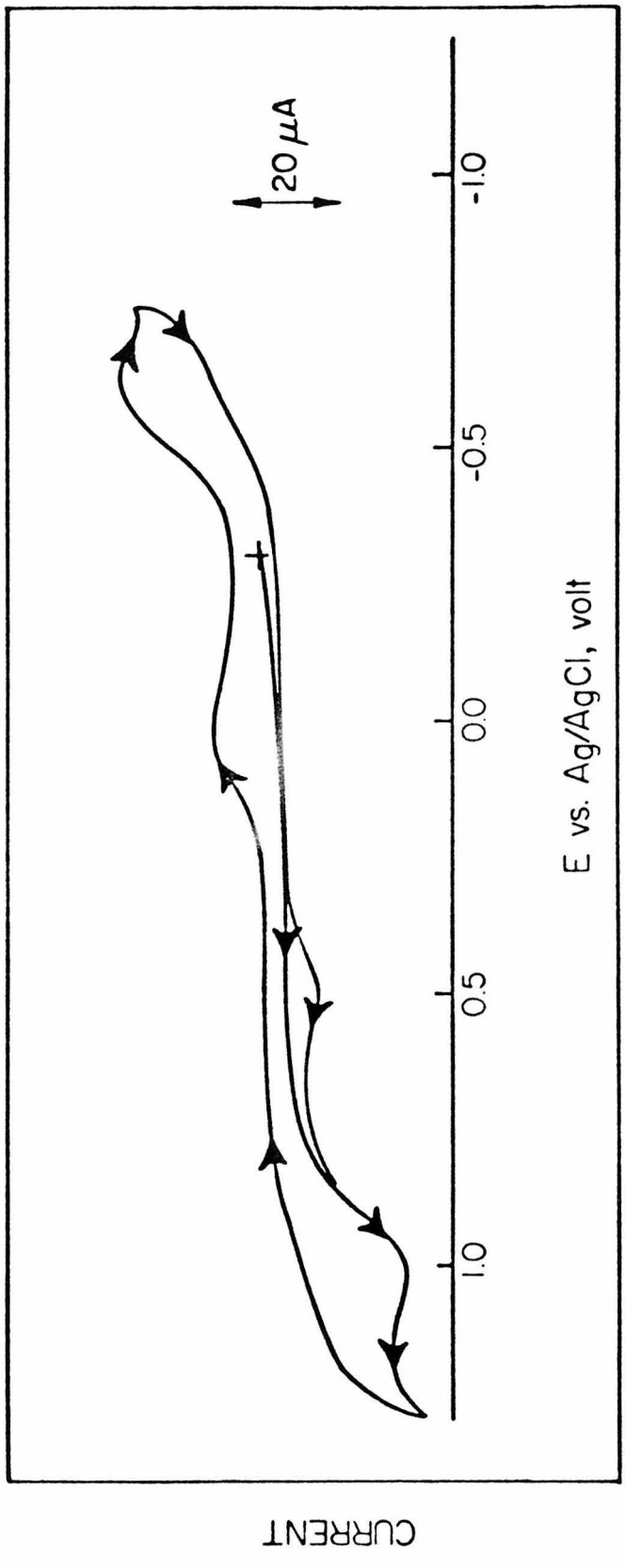
20 μA
-1.0
-0.5
0.0
0.5
1.0
E vs. Ag/AgCl, volt
CURRENT

does clearly argue for stronger binding of $O_2^{-\cdot}$ than O_2. It was not possible to find conditions where the reaction between $O_2^{-\cdot}$ and Co(II) was incomplete enough to obtain an estimate of the binding constants.

Attempts to measure the association constant for the binding of O_2 were unsuccessful. The use of a steady state technique such as rotating disk voltammetry to discern the contributions of O_2 binding to the observed currents would be helpful.

SUMMARY AND CONCLUSIONS

Strong association between a Co(II) complex and superoxide anion has been established, but present results do not permit resolution of the issue of the strength of the interaction. In Chapter 2, it was demonstrated that dioxygen binds too weakly to adsorbed cobalt(II) porphyrins to affect the formal potential of the reversible Co(III/II) responses. If the same is true of related macrocyclic tetra-aza complexes of cobalt(II), their general ability to function as electrocatalysts could be ascribed more to stabilization of superoxide anion formed in the first step of the catalytic reaction than to activation of coordinated dioxygen. It is unclear why cobalt(II) is superior to most other dipositive metal cations in stabilizing superoxide. Further studies of the origin of the strong interaction will be necessary.

REFERENCES AND NOTES

1. D. T. Sawyer and J. S. Valentine, Acc. Chem. Res., 14, 393 (1981) and references cited therein.
2. J. A. Fee and J. S. Valentine in, "Superoxide and Superoxide Dismutases," A. M. Michelson, J. M. McCord, I. Fridovich, eds., Academic Press, New York, p. 19 (1977).
3. J. S. Valentine and A. B. Curtis, J. Am. Chem. Soc., 97, 224 (1975).
4. F. Magno and G. Bontempelli, J. Electroanal. Chem., 68, 337 (1976).
5. D. T. Sawyer, D. T. Richens, E. J. Nanni, Jr., and M. D. Stallings, Dev. Biochem., 11A, 1 (1980).
6. E. J. Nanni, Jr., and D. T. Sawyer, J. Am. Chem. Soc., 102, 7591 (1980).
7. E. A. Mayeda and A. J. Bard, J. Am. Chem. Soc., 95, 6223 (1973).
8. P. F. Knowles, J. F. Gibson, F. M. Pick, F. Brick, and R. C. Bray, Biochem. J., 111, 53 (1969).
9. J. M. McCord and I. Fridovich, J. Biol. Chem., 244, 6049 (1969).
10. J. S. Valentine, Y. Tatsuno, and M. Nappa, J. Am. Chem. Soc., 99, 3522 (1977).
11. M. Nappa, J. S. Valentine, A. R. Miksztal, H. J. Schugar, and S. S. Isied, J. Am. Chem. Soc., 101, 7744 (1979).

REFERENCES AND NOTES

12. M. G. Simic and M. Z. Hoffman, J. Am. Chem. Soc., 99, 2370 (1977).

13. I. B. Afanas'ev and S. V. Prigoda, Koord. Khim., 6, 909 (1980).

14. M. P. Liteplo and J. F. Endicott, Inorg. Chem., 10, 1420 (1971).

15. D. T. Sawyer, G. Chiericato, C. T. Angelis, E. J. Nanni, Jr., and T. Tsuchiya, Anal. Chem., 54, 1720 (1982).

16. J. Vasilevskis and D. C. Olson, Inorg. Chem., 10, 1228 (1971).

17. D. P. Rillema, J. F. Endicott, and E. Papaconstantinou, Inorg. Chem., 10, 1739 (1971).

18. M. L. Bowers, unpublished results.

19. A. J. Bard and L. R. Faulkner, "Electrochemical Methods: Fundamentals and Applications," J. Wiley and Sons, New York, (1980).

20. Ibid, p. 454.

21. L. Nadjo and J. M. Saveant, J. Electroanal. Chem., 48 113 (1973).